ISSN 2227-6920

Research Bulletin SWorld

Modern scientific research and their practical application

Published by:

Kupriyenko Sergiy Vasilyovich *on* ***Project SWorld***

With the support of:

State research and development institute of the merchant marine of Ukraine

Odessa National Maritime University

Ukrainian National Academy of Railway Transport

Volume J21208

June 2012

Please use the following format to cite material from this book (*italics indicate the fields to change to your data*):

Author(s), 'Title of Paper," in Modern scientific research and their practical application, edited by Alexandr G. Shibaev, Sergiy V. Kuprienko, Alexandra D. Fedorova. Vol. J21208 (Kupriyenko Sergiy Vasilyovich, Odessa, 2012) *Article CID Number*.

This volume contains research papers of scientists in the field of TECHNICAL SCIENCES

Published by:

Kupriyenko Sergiy Vasilyovich
on ***Project SWorld***
P.O. Box 38, Odessa, 65001 Ukraine
Telephone: +380667901205
e-mail: orgcom@sworld.com.ua
site: www.sworld.com.ua

Paper Numbering: Papers are published as they are submitted and meet publication criteria. A unique, consistent, permanent citation identifier (CID) number is assigned to each article at the time of the first publication.

CONTENTS

TECHNICAL SCIENCES

CID: J21208-024

UDK: 621.9

Yashkov VA Silin LV

ON THE NEED TO INCREASE SPEED OF FLOW AND PRESSURE COOLANT IN THE GRINDING ZONE.

Муромский институт (филиал) федерального государственного бюджетного образовательного учреждения высшего профессионального образования «Владимирский государственный университет имени Александра Григорьевича и Николая Григорьевича Столетовых»

Keywords: Grinding, mathematical modeling, the temperature.

This work on the hydrodynamic phenomena in internal grinding teams abrasive wheels with radially movable segments.

Ключевые слова: Шлифование, математическое моделирование, температура.

Эта работа о гидродинамических явлениях при внутреннем шлифовании сборными абразивными кругами с радиально подвижными сегментами.

In modern engineering one of the most pressing problems is the high-abrasion holes of machine parts (eg, cylinders), the surface layer which meet high standards.

The processing of the holes with the help of abrasive tools is connected with a number of difficulties arising primarily due to the complexity of supplying coolant technological environment (SOTS) in the cutting zone through a narrow gap between the wheel and the workpiece under the action of strong wind flows generated by a rotating tool. This leads to a decrease in processing performance clue to the danger of the formation of thermal defects in the surface layers of ground parts.

The basic ways of increasing the productivity of the tool for grinding holes are the intensification of the cutting and the increase of the contact area of a circle with the workpiece.

The traditional scheme of internal grinding with the help of the eccentrically positioned relative to a solid billet abrasive wheel does not allow for a qualitative

increase in productivity due to restrictions imposed by the complexity of the supply coolants in the processing area, a small contact area of the circle and the workpiece, the complexity of a substantial intensification of the cutting without grinding born in the processed work pieces and growth of the imbalances of tools reducing the accuracy of processed holes.

Therefore, solving the problem of increasing the productivity of the tool for internal grinding by increasing the contact area of the circle and the workpiece and creating conditions for a reliable income of SOTS in the cutting area is promising.

The analysis of the scientific technical and patent literature led to the conclusion that the most effective way of internal grinding is a method of centrifugal grinding with the help of the tool with prefabricated radial sliding abrasive segments [1] (Fig. 1).

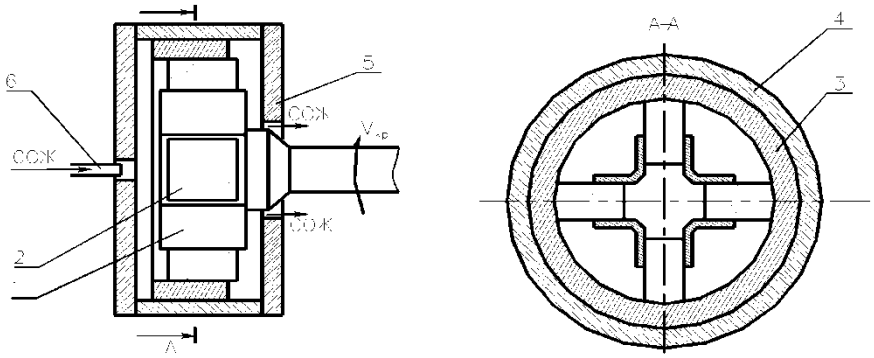

Figure 1 The method of centrifugal grinding with the help of the tool with prefabricated radial sliding abrasive segments

The present method of grinding presupposes that with the help of the precast abrasive tool with a radially movable segments is placed coaxially with two of workpiece 3, flow-organizing capacity of 4.5 for coolants. The liquid is fed through the left hole in lid 6 and discharged through the larger hole on the right side cover of tank five. When you rotate the tool, coolants accelerate and form rotating liquid ring, effectively cooling and washing the workpiece. The well-known works recorded the average pressure coolants in the working area reaching 1.3 MPa.

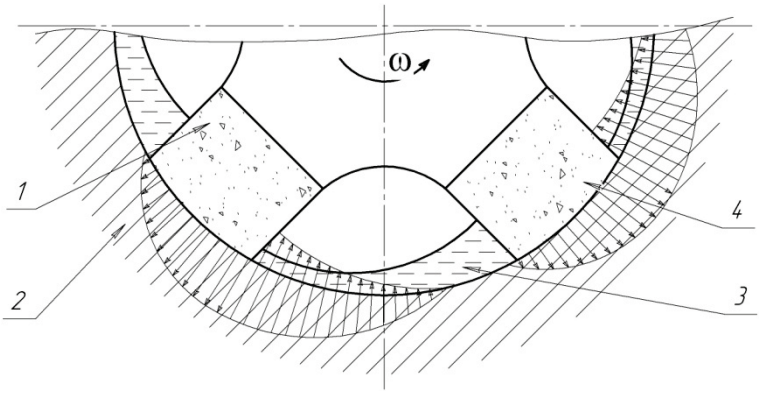

In Fig. 2 – The scheme of heat transfer between the abrasive segments, the workpiece and the cutting fluid

From the viewpoint of heat transfer the scheme of internal grinding with the help of abrasive wheel can be represented in the following diagram (Figure 2): moving one after another abrasive segments 1 and 4 produce heat spreading in the workpiece 3 and 4 SOTS. Because of the Peclet criterion (Pe = 5,38 * 104) abrasive segments 1 and 4 are fast-moving sources of heat spreading beneath them and for them. In this case lowering the temperature of the workpiece in accordance with Newton - Richman is law describes the process of heat exchange between the workpiece and cutting fluids is as follows (1)

$$(T_з - T_{сож}) = \frac{q}{a} \qquad (1)$$

where: q (W/m2) - the heat flux density, α (W/m2K) - heat transfer coefficient defined by the formula (2)

$$\alpha = 6 * 10^4 V^{0,8}_{zh}, \qquad (2)$$

where: Ts - the temperature of the, Tsozh - the temperature of coolants.

As can be seen from the above relationships to accelerate the heat from the workpiece it is necessary to increase the flow velocity of coolants under abrasive segments and for them on the surface of the workpiece.

The flow of the coolant is also dependent on the shape of a segment. Calculations carried out in a software package for FloWorks Solid Works show it vividly.

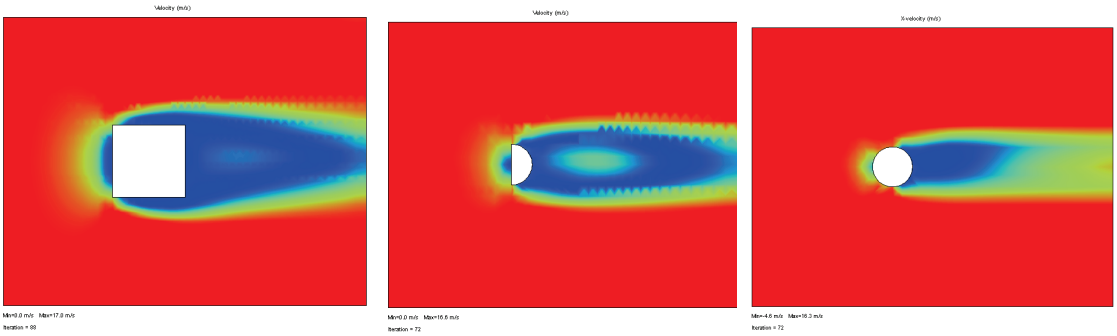

In Fig. 3 The wraping SOTS abrasive segment square, cylindrical and semicylindrical

As can be seen from Fig. 3 the fluid flow in terms of the flow rate is at the best as for cylindrical segment but SOTS transport to the cutting zone is the best on a flat surface

The presence of fast-moving SOTS on the front plane of the segment provides cleaning, lubricating and dispersing property, the generated hydrodynamic wedge with (high pressure) between the treated surface and the abrasive segment provides the flowing of coolants in the pores of the circle, close to the cutting zone, and in front of the segment, providing a heat transfer in SOTS.

The high velocity of the flowing of coolants in the interstellar space segment provides an efficient heat removal from the workpiece and thus bezprizhogovoe, high-speed grinding (high-grinding) without grinding burn.

References:

1. RF patent № 2182531. The method of internal grinding / DR Blurtsyan, VG Gusev, Y. Trifonova, etc. - BI, 2002. - № 14.

2. Yashkov VA Silin LV Technological approaches to Reduced earnings. - Fundamental and applied problems of engineering and technology. 2011. № 4-288. S. 100-103. 0 2

3. Yashkov VA Silin, LV, AJ Albagachiev DEVELOPMENT OF THE MATHEMATICAL MODEL OF HEAT TRANSFER IN TEAMS internal grinding Abrasive wheels - Mechanical engineering and life safety. 2009. Number 6. S. 182-184.

CID: J21208-402

Turgenev D.V.

SIMULATION AND RESEARCH OF ELEVATOR INDUCTION GEARLESS ELECTRICDRIVE WITH SWITCHING CONTROL SYSTEM

National Research Tomsk Polytechnic University

This paper is about functional structure of gearless electric drive based on low-speed induction motor with switching control system. The electric drive simulation model is created. Comparison of simulation and experimental results is done.

Key words: control system, gearless drive, low-speed induction motor.

Introduction

Nowadays special software is used for designing and predicting quality of control system. One of the widely used is Matlab with the means of visual simulation Simulink. This software with library of function blocks and the universal language of object-oriented programming with debugging tools allows creating high-quality simulation models. During the simulation it is possible to observe the processes occurring in the system and to evaluate the changing of various parameters on the quality of its operating. Interesting system characteristics can be presented in numerical and in graphical form.

The paper presents the functional diagram and developed simulation model of gearless electric drive which allow to explore and analyze the characteristics of his operating.

Statement of the problem

Operation of elevator induction gearless electricdrive in a two-speed mode showed that the transition to low-speed may result to resonance phenomena appearance in the elevator mechanics [3, 4] and lead to incorrect operation of control systems and mechanical equipment failure. These problems can be eliminated by setting a servo drive, but in this case the installation of modern control station required. On the basis of economic considerations, the control system which requires no additional costs can be used.

Functional structure of induction gearless drive control system with combined control

Functional structure of induction gearless drive control system with combined control is shown in fig.1.

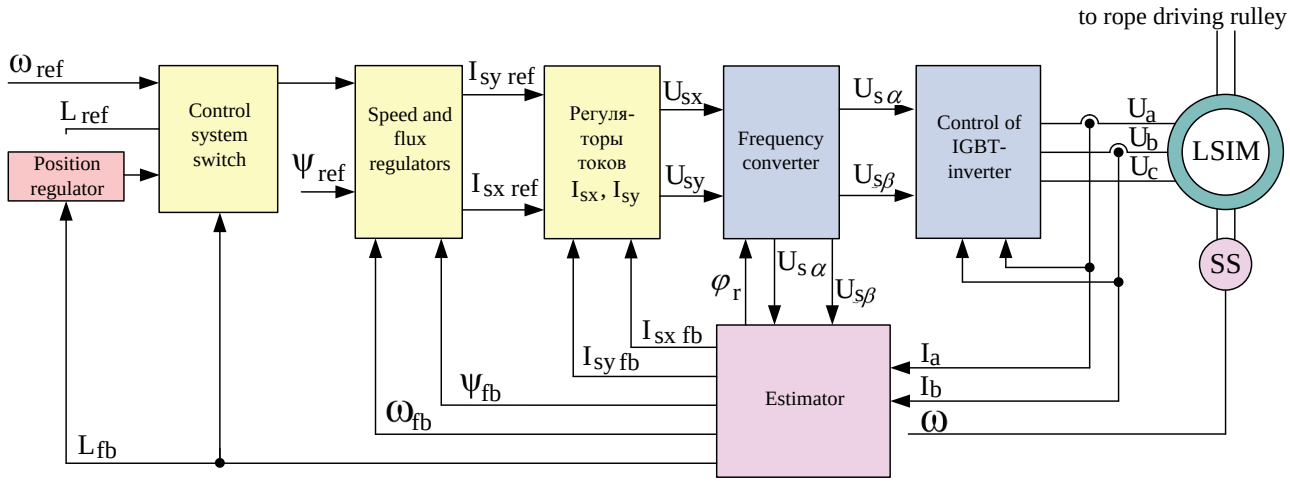

Fig.1. Structure of induction gearless drive control system with combined control

Elevator induction gearless electricdrive control system based on vector control system with speed or position sensor. A distinctive feature of designed control system is a combined control structure realized by means of the switch, which allows organizing the operation of the drive via the following algorithm: the beginning of the cabin movement is carried out on the electricdrive speed control loop with S-shaped ramp. Once the drive receives the signal from preliminary stall detector, control system switches, after that it operates under reference from position control loop and smoothly halt the cabin at floor level. Next movement is carried out on the electric drive speed control loop.

Simulation model of electricdrive

Shown in fig.2 there is a simulation model of elevator induction gearless elecricdrive with combined control based on vector control system created in Simulink Matlab. The marked block are model of low-speed induction motor (LSIM), mechanical part and control system.

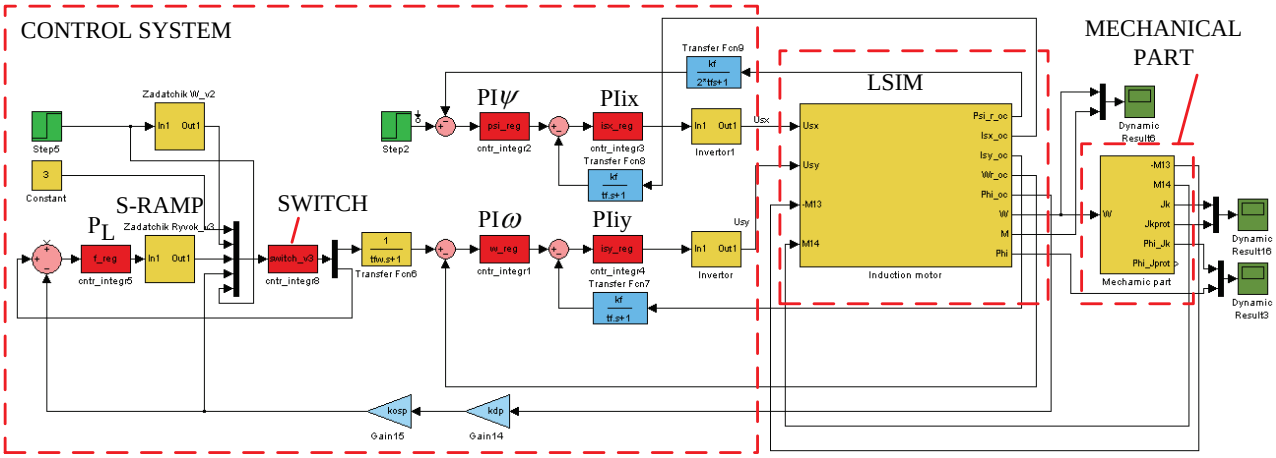

Fig.2. Simulation model of induction gearless electricdrive with switching control system

Based on second Kirchhoff's law, Faraday's law and space vector method there are equations for LSIM in stationary coordinate system were created and realized in simulation model.

The mechanical part is a simulation model of three-mass mechanical system: inertia moments of drive, cabin and counterweight. The mechanical part takes into account the variable inertia moment of cabin (empty or loaded) and changing oscillations frequencies of cabin and counterweight.

Vector control with speed feedback is used to control the electridrive (fig.2): PIix – current regulator for x axes component; PIiy – current regulator for y axes component; PIψ – flux regulator; PIw – speed regulator; PL – position regulator (traveled distance); S-ramp – S-shaped ramp. The results of simulation shown in fig.3a.

Matching of simulation and experiment results

Experiments for gearless induction electricdrive with switching control were done in the laboratory. Experimental assembly consisted of frequency converter ESD-TCL; LSIM – ЧРАД225–8Л ($n_{\text{rated}} = 60\text{rpm}$, $M_{\text{rated}} = 240\text{Hm}$). The results of experiments shown in fig.3b.

Next diagrams shown in fig.3b: $L = f(t)$ – cabin traveled distance ($L = 0.18\text{r.u.} = \text{one floor}$); $w = f(t)$ – LSIM speed $w_{\text{rated}} = 1\text{r.u.} = 6.28\text{rad/s}$); $M = f(t)$ – LSIM moment ($M_{\text{rated}} = 1\text{r.u.} = 240\text{Hm}$).

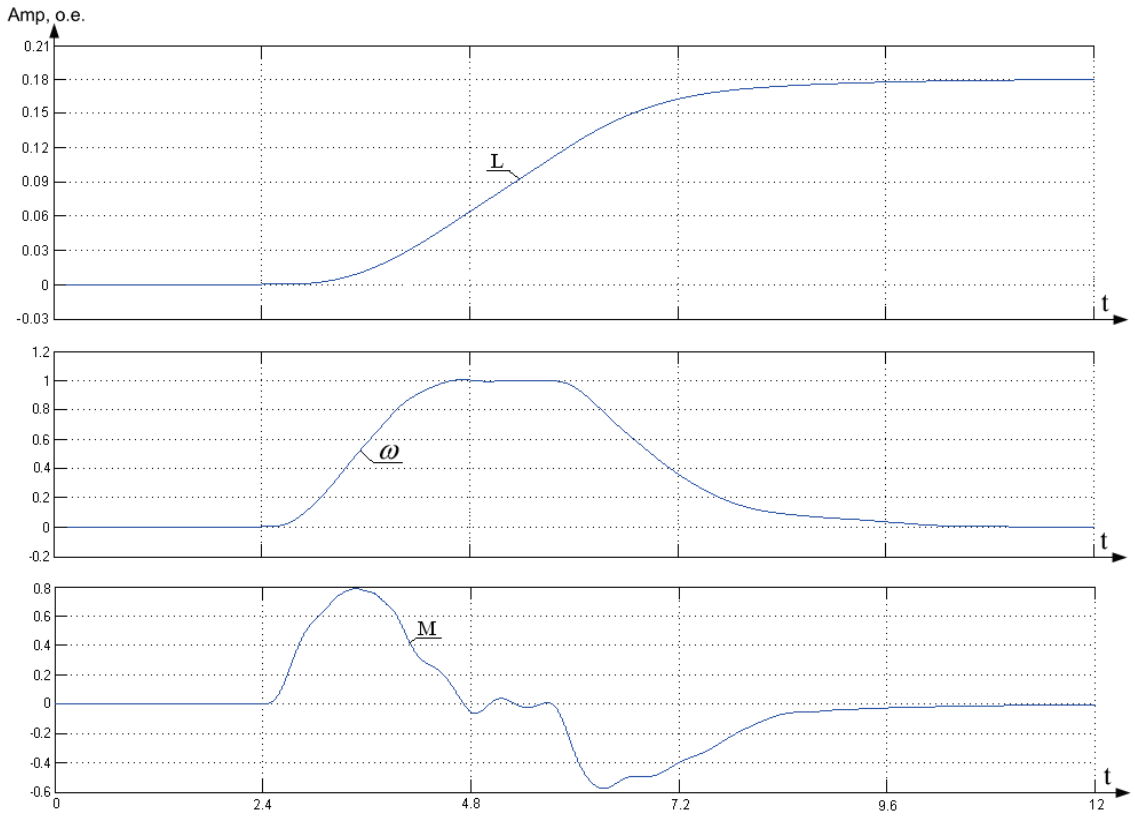

a.

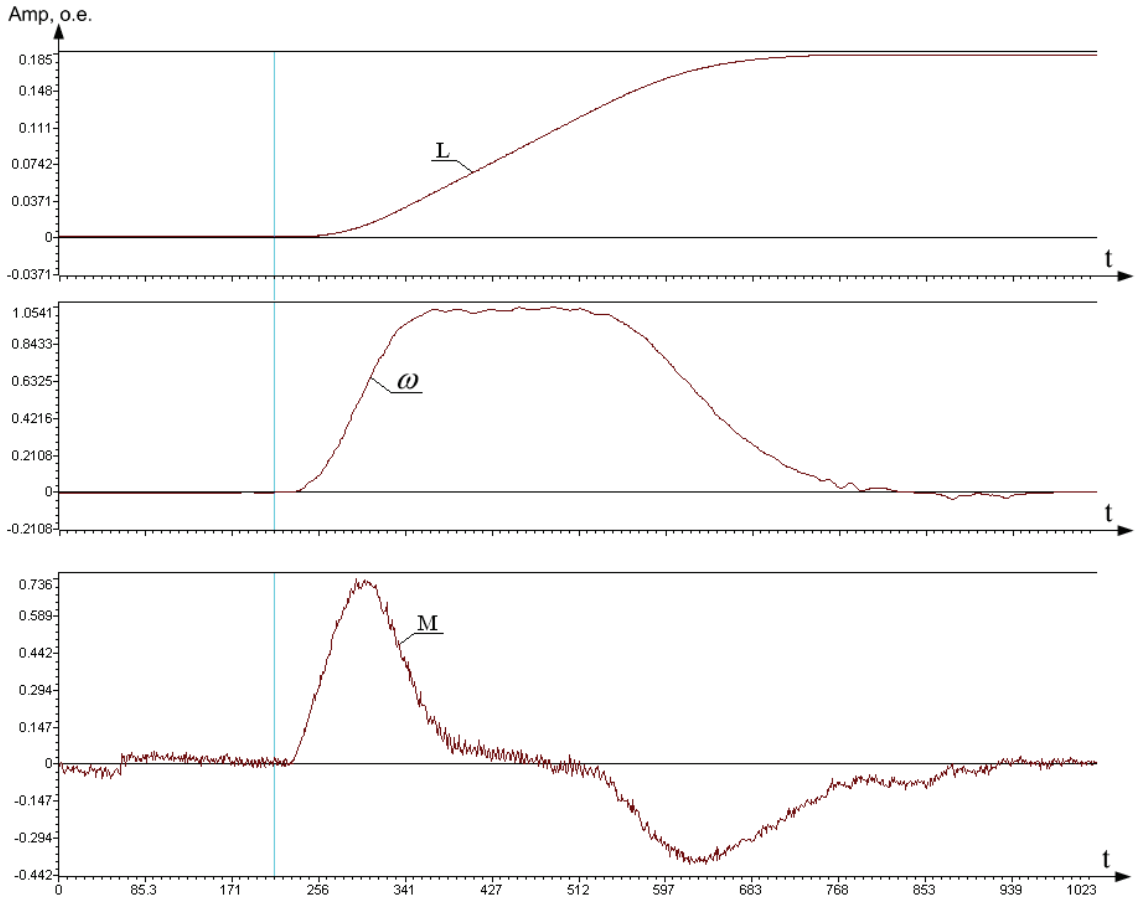

b.

Fig.3. Operation of electricdrive with switching control system

Analysis of the transient ($L = f(t)$, $w = f(t)$, $M = f(t)$) shows a good qualitative and quantitative convergence results of simulation and experimental studies of induction gearless drive.

Conclusion

The proposed control method in the paper is optimal in terms of elevator cabin movement, do not require any additional costs and meet the requirements of "Rules for design and safe operation of elevators" for passenger elevators.

Literature:

1. Kopylov I.P. Matematicheskoe modelirovanie elektricheskikh mashin. – M.: Vysshaya shkola, 2001. – 274s.

2. Olsson G., G. Piani. Tsifrovye sistemy avtomatizatsii i upravleniya. – SPb.: Nevskii Dialekt, 2001. – 557 s.

3. Turgenev D.V., Dementev Y.N., Langraf S.V. Osobennosti mekhaniki liftov s bezreduktornym privodom lebedki // Sbornik trudov mezhdunarodnoĭ nauchno-tekhnicheskoi konferentsii «Elektromekhanicheskie pryeobrazovateli energii 2009», TPU, 2009. – S. 236 – 240.

4. Turgenev D.V., Dementev Y.N., Langraf S.V. Osobennosti protsessov v silovom kanale chastotno-reguliruemogo elektroprivoda bezreduktornoĭ liftovoi lebedki // Sbornik trudov mezhdunarodnoi nauchno-prakticheskoi konferentsii «Energetika i energoeffektivnye tekhnologii 2011», LGTU, 2011.

CID: J21208-527

UDK 621.3.07

Grigoryev A.V.

A LINEARIZATION OF THE MODEL OF THE ELECTRIC MOTOR THAT WORKS IN THE DIRECT TORQUE CONTROL DRIVE

The Kuzbass State Technical University

Results of the research of the linearized induction motor model using in modified direct torque control systems are presented in this report.

Key words: linearized model, induction motor, direct torque control

The direct torque control method of the AC electric motor was proposed relative recently (M. Depenbrock, 1984). So in initial definition this method had a lot of disadvantages. It was proposed many developments of direct torque control method for the purpose to remove its disadvantages [1]. It is necessary to say about some of them: control systems with space vector pulse width modulation (SVPWM) and constant switching frequency; control systems based on the pulse width calculation through fuzzy logic; stator flux vector control systems with feedback of the stator flux and electromagnetic torque.

Some works about direct torque control systems switching frequency calculation also was published [2, 3]. An analysis of different parameters on switching frequency was based on linearization of a motor model on a little control interval (for direct torque control systems it is less than 50 microseconds) [3]. Unfortunately in the article [3] an electromagnetic torque prediction error done such reduction hasn’t researched.

In this report results of the research of the electric motor model linearized on a little control interval was presented. Also a diagram of the electromagnetic torque prediction errors on the ends of control intervals that were result of the linearization was produced.

Theoretic researches and calculation experiments were done on base following AC electric motor model:

$$\frac{dY_{sa}}{dt} = U_{sa} - R_s \frac{1}{L_s'} Y_{sa} + R_s \frac{k_r}{L_s'} Y_{ra},$$

$$\frac{dY_{sb}}{dt} = U_{sb} - R_s \frac{1}{L_s'} Y_{sb} + R_s \frac{k_r}{L_s'} Y_{rb},$$

$$\frac{dY_{ra}}{dt} = - R_r \frac{1}{L_r'} Y_{ra} + R_r \frac{k_s}{L_r'} Y_{sa} - pwY_{rb},$$

$$\frac{dY_{rb}}{dt} = - R_r \frac{1}{L_r'} Y_{rb} + R_r \frac{k_s}{L_r'} Y_{sb} + pwY_{ra},$$

$$M = \frac{3}{2} p \frac{k_r}{L_s'} \left(Y_{sb} Y_{ra} - Y_{sa} Y_{rb} \right),$$

$$Y_{sm} = \sqrt{Y_{sa}^2 + Y_{sb}^2}.$$

where $\Psi_{s\alpha}$, $\Psi_{s\beta}$, $\Psi_{r\alpha}$, $\Psi_{r\beta}$ – stator and rotor fluxes in axes α-β; $U_{s\alpha}$, $U_{s\beta}$ – stator voltages in axes α-β; Ψ_{sm} – a magnitude of the stator flux; p – poles pair; ω – circular frequency of the rotor; R_s, R_r – active resistances of the stator and rotor windings; L_s', L_r' – transient inductances of the stator and rotor windings; k_s, k_r – dissipation coefficients.

From this model an expression for the electromagnetic torque is followed:

$$T_M \frac{dM}{dt} + M = K_M \left(U_{sb} Y_{ra} - U_{sa} Y_{rb} \right) - K_M pw \left(Y_{ra} Y_{sa} + Y_{rb} Y_{sb} \right),$$

where $T_M = \frac{1}{\left(\frac{R_S}{L_S'} + \frac{R_R}{L_R'} \right)}$, $K_M = \frac{1}{\left(\frac{2R_S}{3pk_R} + \frac{2R_R}{3pk_S} \right)}$.

Rewrite this expression to more compact form:

$$\frac{dM}{dt} = C_1 + C_2 + C_3, \tag{1}$$

where $C_1 = - \frac{M}{T_M}$, $C_2 = \frac{K_M}{T_M} \left(U_{sb} Y_{ra} - U_{sa} Y_{rb} \right)$, $C_3 = - \frac{K_M}{T_M} pw \left(Y_{ra} Y_{sa} + Y_{rb} Y_{sb} \right)$.

With purpose to research an influence of all members of the expression (1) to derivative of the induction motor electromagnetic torque the simulation of the electromechanical processes of the induction motor VRP160M4 was done (see fig. 1).

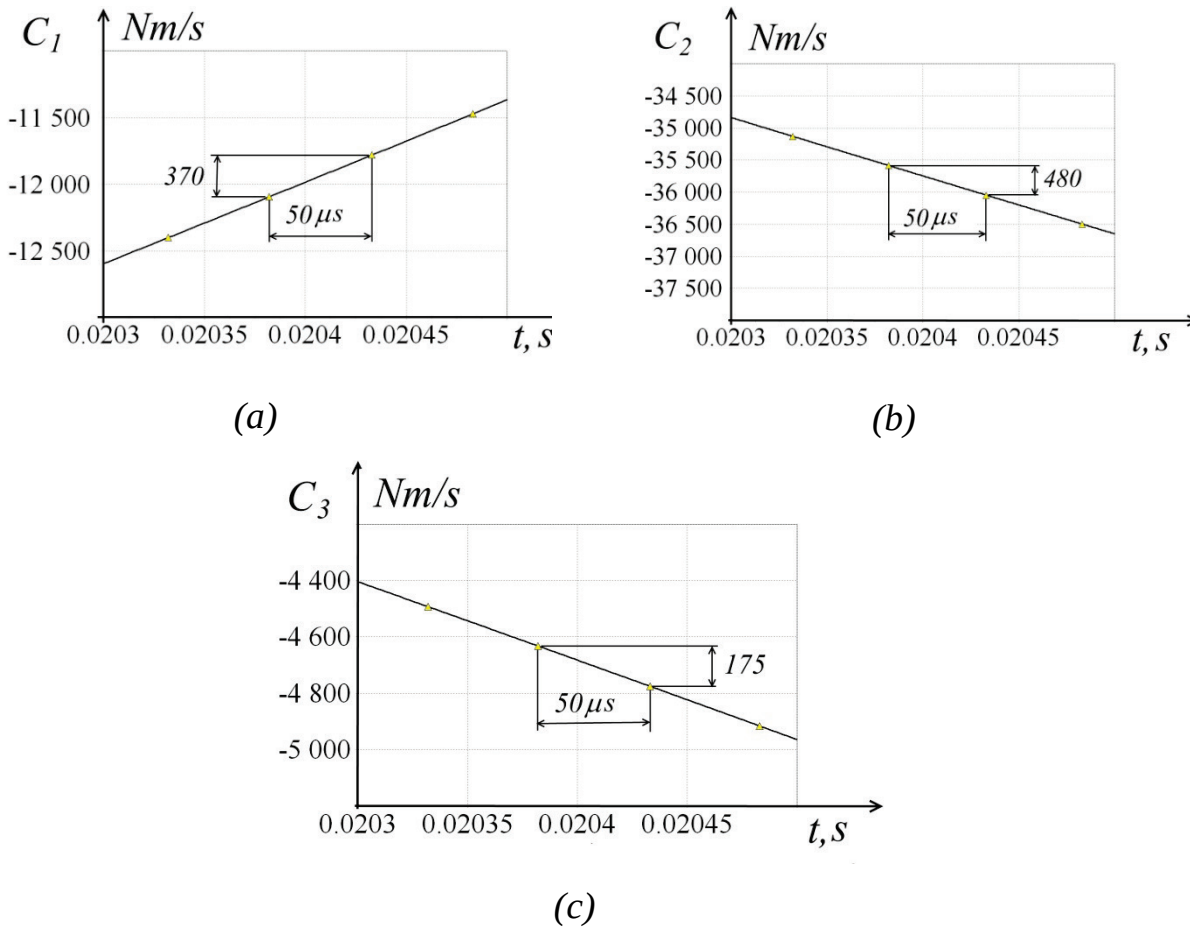

Fig. 1. Members of the expression (1): (a) C_1; (b) C_2; (c) C_3

Results of the simulation have shown that the member C_1 in the expression (1) was too small for taking into account. It simplifies also the model. As the result of this an expression for the induction motor electromagnetic torque may be simplified without some significant error in the electromagnetic torque prediction value:

$$\frac{dM}{dt} = C_2 + C_3 . \tag{2}$$

It is necessary to mark that in the low rotor circular frequency region the influence of member C_3 is also small. It don't do possibility to ignore this member because it grows with the rotor circular frequency and it is equal member C_2 in the rated speed region – in this case the derivative of the electromagnetic torque is equal 0 and a further growth of the electromagnetic torque is not possible.

An influence of members C_2 and C_3 for the control period (in this work, one more time say, the control period is equal 50 microseconds) is negligibly small (see fig. 1). Therefore for the control time values C_2 and C_3 can be accept as constants and

these constants are approximate equal C_2 and C_3 starting values. How much this simplification is true can be shown from the calculation of the electromagnetic torque prediction error on the end of a control period of the direct torque control system.

For the purpose of the electromagnetic torque prediction error definition on the end of the control period the simulation experiment was executed. Results of this experiment (relative values of the electromagnetic torque prediction error) are shown in fig. 2.

It is necessary to mark that the relative error of the electromagnetic torque prediction was calculated on base follow expression:

$$e_m = \frac{\left|\hat{M} - M\right|}{M_Z} \cdot 100, \ [\%]$$

where $\hat{M}$ – predicted from the expression (1) value of the electromagnetic torque; M – actual value of the electromagnetic torque; M_z – reference value of the electromagnetic torque.

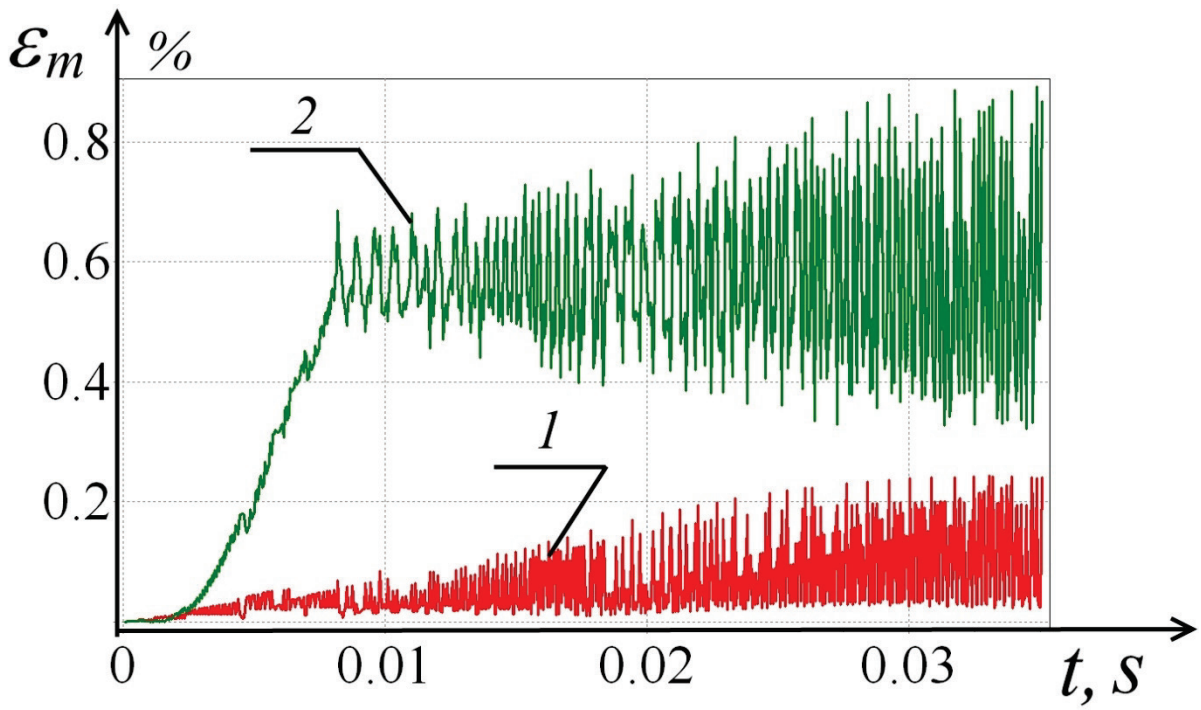

Fig. 2. The electromagnetic torque prediction error on the end of the control period: with taking into account a member C_1; without taking into account a member C_1

Thus the potential possibility of the precise electromagnetic torque value prediction on the end of the control period T_{clk} on base follow expression was shown:

$$\hat{M} = M + \frac{K_M T_{clk}}{T_M}\left(U_{sb}Y_{ra} - U_{sa}Y_{rb}\right) - \frac{K_M T_{clk}}{T_M} pw\left(Y_{ra}Y_{sa} + Y_{rb}Y_{sb}\right),$$

where T_{clk} – the control period of the direct torque control system.

From done simulations it can be concluded that prediction values of the electromagnetic torque are near real values on next step of the control. This fact take a possibility to consider AC electric motor as linear object relatively control (stator voltages) and disturbing (rotor circular frequency) values into a little control period. Though the prediction error done such simplification is exist, so if the synthesis of the control system is made on this model base it is necessary to do special actions to reduce static error in the control loop.

Literature:

1. Buja, G. Review of Direct torque control methods for voltage source inverter-fed induction motors/ G. Buja, M.P. Kazmierkowski// IEEE Industrial electronics society: proceedings of the 29th annual conference of the IEEE. Warsaw, 2003. – Vol. 1. – P. 981-991.

2. Kang, J.-K. New direct torque control of induction motor for minimum torque ripple and constant switching frequency/ J.-K. Kang, S.-K. Sul// IEEE Transactions on industry applications. – 1999. – Vol. 35. – No. 5. – P. 1076-1082.

3. Kang, J.-K. Analysis and prediction of inverter switching frequency in direct torque control of induction machine based on hysteresis bands and machine parameters/ J.-K. Kang, S.-K. Sul// IEEE Transactions on industrial electronics. – 2001. – Vol. 48. – No. 3. – P. 545-553.

CID: J21208-480

Moskalev A. Y., Vetlova S. A., Gushchina I. O.

THE POSSIBILITY OF USING CUDA TECHNOLOGY TO SOLVE FINANCIAL-ECONOMIC PROBLEMS

National Research University "Moscow Power Engineering Institute"

In this report we consider the task of building an integral portfolio Markowitz on maximum profitability with limiting of value portfolio risk. We describe steps of the proposed algorithm for solving this problem, based on branch and bound method and on simplex method. We present results of experiments that are demonstrating the effectiveness of NVIDIA CUDA technology to solving this problem.

Key words: Markowitz model, investment portfolio, CUDA technology, GPU, massive-parallel processing.

Capital market is a fast developing structure of international and, in particular, Russian economy at the present time. It offers different types of investment when performance evaluation of which analysts widely used method and models of forecasting the value of financial assets. Among them it should be note the classic two-criterion model of choice portfolio investment. It's a model of Markowitz [1]. Portfolio theory act on the premise that the implementation of investing activity investors can invest not in one, but in several sites, thus building a kind of collection of investment objects. In process of building investment portfolio there is a problem of choice projects in accordance with given preferences. In the theory of financial assets may be split in the total portfolio investment in shares. In practice, this is unacceptable, because the securities are sold (bought) indivisible lots that, in general, can lead to the formation of an inefficient portfolio [2].

Introducing the integrality restriction on the purchased lots, we can set the following objectives: to formalize the task of building a portfolio, taking into account constraints, suggest an algorithm that allows to obtain solutions for a reasonable time. At the same time as the hardware is proposed to use massively parallel processing based on NVIDIA CUDA technology [3].

We consider the discrete price pattern of capital market. Let us suppose that list of lots n is known, which includes same securities, and their volume is $V_1, V_2, ..., V_n$. Initial cost of each share at time t = 0 and the probability distribution of future stock price of each species at time t = T are known. Let coefficients $в$ $(b_i, i = 1,2,...,n)$ for

each type of financial assets which set a quantitative risk assessment for each type of securities are known. Let the future cost of the i-th asset is given by allocation $g_i^1,...,g_i^m$ with probability $p_1,...,p_m$. Then the expectation of the future cost of the i-th asset is the value:

$$\overline{g_i} = \sum_{j=1}^{m} g_i^j \times p_j \tag{1}$$

In this notation, the interpretation of Markowitz model on maximum profitability with limiting of value portfolio risk R_{cp} can be represented as follows:

$$\sum_{i=1}^{n} V_i y_i (\overline{g_i} - a_i) + F \to \max, \tag{2}$$

$$\sum_{i=1}^{n} V_i y_i a_i \le F, \tag{3}$$

$$\sum_{i=1}^{n} y_i x_i^2 s_i^2 + 2\sum_{i=1}^{n}\sum_{i>j} y_i y_j x_i x_j \operatorname{cov}_{ij} \le R_{cp}, \tag{4}$$

$$y_i \in \{0,1\}, i = 1,2,...,n, \tag{5}$$

where $x_i = \frac{V_i a_i}{F}$ is the share of total investments for the stocks V_i in the portfolio; y_i is unknown quantity, it's equal to 1 if the i - th item is included in the portfolio, and equal to 0 otherwise.

This model affords an opportunity to find solutions that maximize profit from investment project with aspiration level of risk (see Fig. 1).

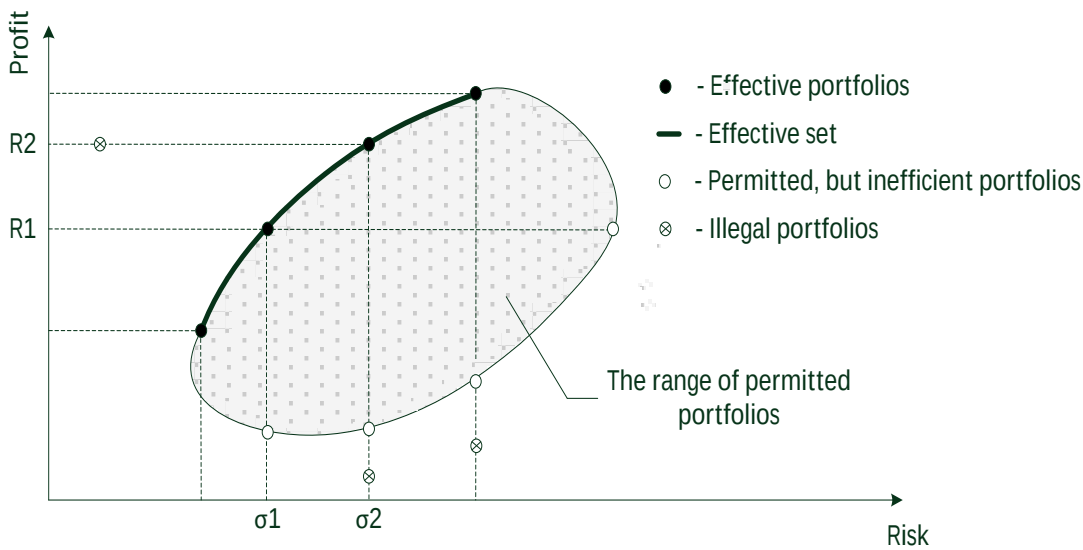

Fig. 1. Kinds of sets from generated portfolios.

Problem (2) - (5) is NP-complete problem. For large values of n solution with

exchaustive search is not possible, because decision tree is growing very rapidly (see Fig. 2).

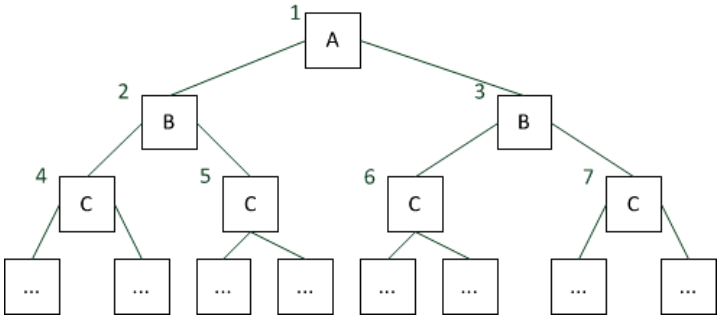

Fig. 2. An example of parallel processing of formed decision tree.

To solve the indicated problem of integer linear programming (2) - (4) we suggest to use the branch and bound method, steps are presented below [4].

Step 1. Calculation of the upper bound of the optimal value of problem (2) - (5).

This bound can be obtained by exception for the restriction (4) and replace (5) to restriction:

$$0 \leq y_i \leq 1, i = 1,...,n \tag{6}$$

Then the problem (2) - (5) becomes a continuous linear programming problem and its optimal solution can be obtained using the simplex method [4]. If, moreover, the obtained solution satisfies the restrictions (4) and (5), it is also a solution of the initial problem. Otherwise, proceed to Step 2.

Step 2. Determination of the lower bound of the optimal value of problem.

Investment resources F can be taken as a lower bound of the initial problem. Substantially, this means that no item is sold, and, consequently, the magnitude of risk is equal to 0.

Step 3. Calculation of the current upper bounds on the optimal value of the objective function during building the portfolio.

Calculation of the current upper bound for partially-formed portfolio, provided that the portfolio has included lots of set K, is as follows:

$$F_в^{тек}(K) = \sum_{i \in K} \overline{g}_i V_i + F_в(N/K), \tag{7}$$

Where $F_в(N/K)$ is the upper bound solution of (2) - (5) in the set of lots N / K and the amount of financial resources $F_к = F - \sum_{i \in K} V_i a_i$.

Building portfolio should satisfy restrictions on the level of risk (i.e. condition (4)). Consequently, after the portfolio included lots of the set K, it must be satisfied the following inequality:

$$\sum_{i \in K} x_i^2 \sigma_i^2 + 2 \sum_{i,j \in K} \sum_{i>j} x_i x_j \operatorname{cov}_{ij} + \min\{0, x_q^2 \sigma_q^2 (n-k) + 2 \operatorname{cov}_{mp} x_m x_p\} < R_{гр}, \quad (8)$$

Where cov_{mp} - is minimal negative covariance of two assets from the set of assets N / K; x_m, x_p - even distribution of the rest in shares of capital stock after purchase the set K; σ_q^2 - is minimum dispersion for a set of assets N / K; n-k - number of lots in a set of assets N / K; $x_q^2 = \left(\frac{F - \sum_{i \in K} V_i a_i}{F(n-k)}\right)^2$ - It's the share of financial assets remaining after purchasing lots of the set K, evenly distributed between assets of the set N / K.

When the value of $F_в^{тек}(K)$ is calculated fulfillment of condition being verified:

$$F_в^{тек}(K) > F_н \quad (9)$$

If conditions (8) and (9) are satisfied, then choice of another purchased lot is going on and investment portfolio is building, which includes a lot lots of $K_1 (K \cap K_1)$. If in the set K_1 condition (8) and (9) are satisfied, the process of building a portfolio is continuing. Otherwise, the portfolio is discarded and a new one is building. When choosing the next purchased lot we should be guided by the following rule. The lots are arranged in descending order of magnitude $\frac{\overline{g_i}}{a_i}$. Another selected item corresponds to the maximum specified value.

If according to the given algorithm was able to form a portfolio for which the following restrictions (8) and (9) are satisfied and the value of the objective function (2) $F^* > F_н$, then we set $F_н = F^*$, and then the next iteration of the algorithm for building portfolio is going on. The algorithm terminates when after the next adjustment of $F_н$, we obtain $F_н = F_в$, or when all variants of building portfolio are considered.

As the optimal portfolio is chosen the one that corresponds to the largest value

of $F_н$.

A modern graphic accelerator with support of CUDA technology contains more than 100 cores. At the same time their cost, sizes and power consumption are much lower than in computer systems based on x86 and / or x64 processors architecture [4]. The steps of this algorithm can be independently calculated for each branch of solutions that will maximize the potential of multi-core GPU. For example, in Figure 2, there is the top of the decision tree and there can be independently calculate the portfolio variants 1-2-4 - (...) 1-2-5 - (...) 1-3-6 - (...) and 1-3-7 - (...) on 4-core graphic accelerator .

Experimental results on test data.

We consider the model (2) - (5). We simulate a set of input data: the number of available lots and their dimensions, the initial price for each stock in the lot, a set of random variables with a given deviation from the initial price for the calculation of prices for the time T (we assume that the distribution of prices is normal), risk coefficients for each paper and generate a covariance matrix. Limiting parameters are the size of the resources of the investor and the total allowable portfolio risk.

The result of the experiments is shown in the following graphs

Fig. 3. The time of formation of the optimal portfolio with different input data.

As can be seen from the graphs presented in Figure 3, the use of massively parallel calculators based on NVIDIA CUDA technology provides a significant gain in speed of formation for an effective set of portfolios that allow for quick correction

of the portfolio structure when preferences and basic conditions are changing. In the future, using more than one GPU, the problem (2) - (5) can be solved in real time.

References:

1. Касимов, Ю. Введение в теорию оптимального портфеля ценных бумаг. / Ю. Ф. Касимов. – М.: Анкил, 2005. – 144 с.

2. Мищенко, А. Модельный подход к анализу целочисленных инвестиционно-финансовых активов. / А.В. Мищенко, Е.В. Виноградова, Л.С. Хайрулина. – Прикладная информатика. - 2007, № 3(9).– с. 128-139.

3. Боресков, А. Основы работы с технологией CUDA. / А.В. Боресков, А.А. Харламов. – М.: ДМК Пресс, 2010. – 232 с.

4. Амосов, А. Вычислительные методы: учебное пособие. 3-е изд., перераб. и доп. / А.А. Амосов, Ю. А. Дубинский, Н.В. Копченова. – М.: Издательский дом МЭИ, 2008. – 672 с.

CID: J21208-352

UDK:621.778.08:669-408 .3

Danenko V.F., Ponkratova G.V.,

Tsyutsyura V.YU.

THE INFLUENCE OF TECHNOLOGICAL FACTORS ON THE LEVEL OF HETEROGENEITY OF THE DEFORMATION IN THE TRANSITION ZONE OF BIMETAL STEEL 45+12H18N10T IN THE SUBSEQUENT HIGH-TEMPERATURE LOADING

Volgograd state technical university

Diffusion processes, developing near the surface section of the layers in the production of bimetals carbon steel + 12H18N10T hot rolling [1,2], determine the peculiarities of the structure of the transition zone of bimetal. When cooling after rolling heating in a layer of steel 12X18H10T is formed over-saturated austenite, the degree of over-saturation depends of conditions of cooling and distribution of carbon.

The repeated heating up to 500-700 ^{0}C causes allocation of carbides on the grain boundaries [3]. Chemical and structural heterogeneity of the transition zone of bimetal changes the level of heterogeneity of the deformation of microvolumes transition zone in comparison with the basic layers, this fact affects the nature of the origin and development of micro-cracks.

Bimetallic samples of steel 45+12X18H10T (cladding layer) had been tested after: a) rolling; b) the following patenting. The temperature modes are given at [2]. Analysis of deformation of microvolumes transition zone of bimetallic sample in creep flow conditions at a temperature of 700 ^{0}C was conducted at a facility MERI-9-66 by the method of reference points with the base of 20 microns. Measuring of micro hardness was carried out at room temperature (the load on the indenter composition-was around 1 N).

To quantify the degree of heterogeneity of the deformation of microvolumes was used the coefficient of variation of micro deformations, where is the standard deviation of micro deformations, ε_i - relative deformation of the i-th microvolume, the average deformation; n - the number of microvolumes in each row.

Diffusion redistribution of carbon between plating and the basis during hot rolling resulted in a significant difference of values of hardness of microvolumes of transition zone of bimetal (curve 1 in fig. 1,a). Patenting changed the ratio of the formed after rolling values of micro hardness (curve 2 in fig. 1,a). In close vicinity of the surface of layer section the comparison index of micro hardness values after a) rolling was i_c=3,1 and after (b) patting it was i_c=2,0.

The set difference of the values of the i_c is mainly connected with the diffusion processes in the boundary layer for steel 12X18H10T. Slow down cooling after rolling in comparison with patenting causes allocation of carbides, which increases the hardness of the layer.

In fig. 1,b is given shows the change in the level of heterogeneity of deformation microvolumes of transition zone of bimetallic sample tested at a temperature of 700 ^{0}C (left and right of the graph show the values for the main layers). The compatibility condition of deformation of microvolumes which directly adjacent to

the surface of section implies the equality of the levels of heterogeneity of the deformation of these microvolumes. Ensuring the mentioned conditions is accompanied by the increasing complexity of the stress state in the border areas.

For bimetal in condition after rolling levels of heterogeneity deformation of microvolumes in border zones for of steels 12X18H10T and 45 differ almost in 2 times (curve 1). This is due to embitterment of carburized layer of steel 12X18H10T because of the allocation of carbides on the limits of the grains of austenite in the process of deformation. The lower the plasticity of the metal, the more heterogeneity of its deformation. This increases the probability of brittle cracks: in carburized zone after deformation at a temperature of 700 ^{0}C were recorded lacerations between grains.

Fig.1. Distribution of micro hardness (a) and changing the level of heterogeneity K_ε of strain during creep at 700 ^{0}C, $\dot{\varepsilon}$ =4% (b) microvolumes of the transition zone of bimetal after: 1 - rolling 2 - patenting

The decline of microvolumes of transition zone of bimetal after patenting (curve 2 in fig. 1,b) particularly true for the border zone of steel 12X18H10T and is associated with an increase of plasticity of carburizing layer. During metallographic study in decarburized zone were recorded micro cracks, the formation of which was explained by the allocation of carbides on the limits of the ferrite grains, connected with the diffusion of chromium, and had into-grained character.

Analysis of metallographic transition zone of bimetal after patenting shows that the development of cracks in the process of deformation is hampered by on the one hand plots, adjacent directly to the surface of the section, and on the other - the main layers of bimetal, where the level of heterogeneity of the deformation is lower. Decrease of the values in the main layer after patenting is due to the favorable terms of the common deformation of microvolumes structure of sorbitol, which enhance the strength and plastic properties of bimetallic sample, compared to the samples after rolling.

Thus, decrease of probability of formation and development of micro-cracks in the transition zone with the following processing and the improvement of the

properties of the investigated bimetal can be achieved by the choice of the technological process, thermal-power mode of which ensure a minimum level of heterogeneity of the deformation of microvolumes of the transition zone.

Literature:

1. Prediction of the strength characteristics of bi-metallic corrosion-resistant wire / YU.P.Trykov, V.F. Danenko, L.M.Gurevich, A.S.Sergienko // Production of rolled products. - 2009. - № 9. - C. 29-33.

2. The effects of structural and chemical heterogeneity of bimetallic steel bars on the formation of their properties / VF. Danenko, YU.P.Trykov, L.M.Gurevich, V.YU. Tsyutsyura // Scientific research and their practical in-application. Modern state and ways of development '2011 : sb. nauch. tr. SWorld : mater. of the international scientific.-prakt. konf. (04-15 oct. 2011.). T. 5. Technical science / RDI marine fleet of Ukraine [and others.]. - Odessa, 2011. - WITH. 61-64.

3. Metallurgy / A.P. Gulyaev. - M.: Metallurgy, 1986. - 544c.

CID: J21208-010

Lvova J.S.

THE DECISION-MAKING PROCESS BASED ON THE ONTOLOGICAL APPROACH UNDER CONDITIONS OF UNCERTAINTY OF INITIAL INFORMATION

Volgograd State Technical University

The questions of using the ontological approach to the knowledge integration in tasks of supporting the decision-making under conditions of uncertainty have been contemplated. The approaches to the construction of structured conclusions containing the recommendations of the using mechanisms for the interpretation of the fuzzy information have been defined.

Key words: Ontology, support in decision-making, information support,

semantic network

The core question of the improvement in quality of the complex systems' control is to enhance the effectiveness of decision making in problem situations. In the process of knowledge formalization during the situation modelling it should be borne in mind that the fundamental properties of the described processes may change during development, which could lead to a qualitative change of behaviour and modes of operation. A definition of a method and degree of an influence on each other, a display of qualitative transitions of elements and system from one state to another, transient processes, the identification of the operation mode represents a significant challenge.

The problem of multi-selection with the use of fuzzy models, which is providing information about the relationship between the criteria and methods for calculating the integral estimates, can't be considered less difficult. Methods based on different approaches give different results.

In this regard, the aim of this work is to develop the concept of information support in decision-making process, which is based on the ontological analysis of the effective measures in case of the uncertainty of the initial information.

The main tasks that must be implemented in the formation process of decision-making support model can be defined as the following [1]:

- representation of the information as semantic relations between domain objects;
- modelling operations and methods of processing knowledge to develop recommendations for decision-making.

During the construction of a process model of support decision-making, the set of initial structures of preferences are defined and the choice's process of method which is processing the initial structure of a methods' class is analyzed. The variation of the various structures of classification's models is based on the properties, which are determined on the assumption of the content of expert information: a preference among alternatives, the consequences of its choices, the kind of information about preferences (fig. 1). [2]

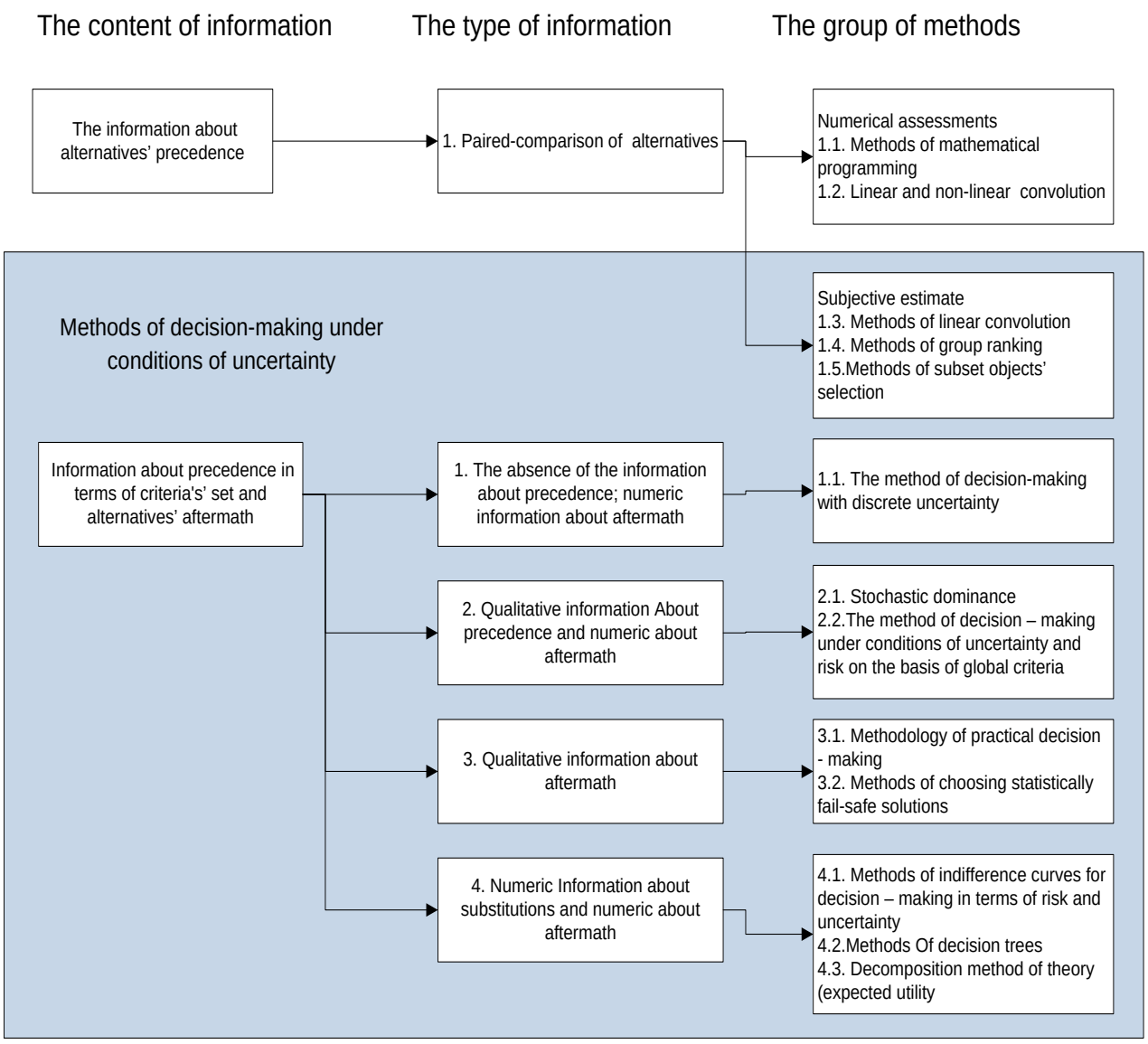

Fig. 1. The classification of methods of decision - making based on the content of expert information

This methods' classification was the basis for the ontology creation, and allowed to form the basic concepts, such as properties, relations, constraints, axioms and statements needed to describe the tasks of the chosen subject area.

For the example of visualizing the concept of building decision models, there is the initial stages of developing ontology for the method of decision trees.

The ontology creation consists of series of sub-processes of intermediate representations. Sub-processes are not performed consistently, and are determined by the completeness and accuracy of accumulated knowledge. First of all, a glossary of

terms is constructed, then classification trees of concepts and diagrams of binary relations, and then the rest of the intermediate representation.

The glossary includes terms that can be semantically classified into three groups [3]: the structure of (tree nodes, links), data filling task (Scale, method comparisons, paired comparison, terms of decomposition), and the results of calculations (Vector priorities, Index consistency, relative consistency) (table 1).

Table 1

The fragment of the glossary of Terms

Term	A definition of the item
Tree	Unite grouped nodes of hierarchy into levels (objectives, criteria or factors, alternative)
Node of the tree	May be a target, factor or an alternative. Located on one of the levels of the hierarchy. Can be included in a cluster as its top element or element with the distribution of links between nodes, as well as be an internal node of the tree, the check node
Target	Is a node in the hierarchy. Is the vertex of the cluster after the distribution of links between nodes
Factor	Is a node in the hierarchy. Can be included in a cluster as its vertex or a cluster member after the distribution of links between nodes
Attribute	Criteria, the independent variable that specifies the method of comparison for objects, alternatives, and determines the factors ‘ meaning factors
Class label	The dependent variable, the sign determining the class of the object
Object	An example, a template, an observation, an alternative belonging to a definite class and occupying a certain level of the hierarchy
Leaf	The end node of a tree, node of a solution
Test	A condition in a node

After building the terms’ glossary the classification trees of concepts were generated. At that time, relationships such as “subclass-of” were used. Thus, the major taxonomies of the data domain were identified. The basic taxonomy of the ontology regarding the methods of decision trees - is a node of the hierarchy (Figure 2).

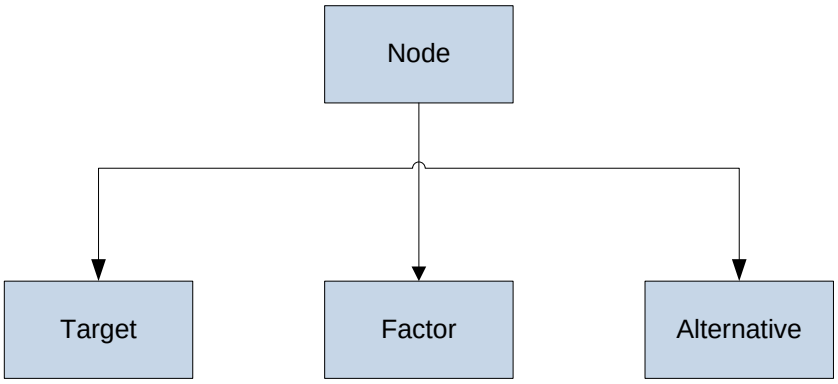

Fig. 2. The fragment of the taxonomy within the ontology

The next step is to create diagrams of binary relations (Figure 3). During this phase the relationship between concepts of the ontology are determined.

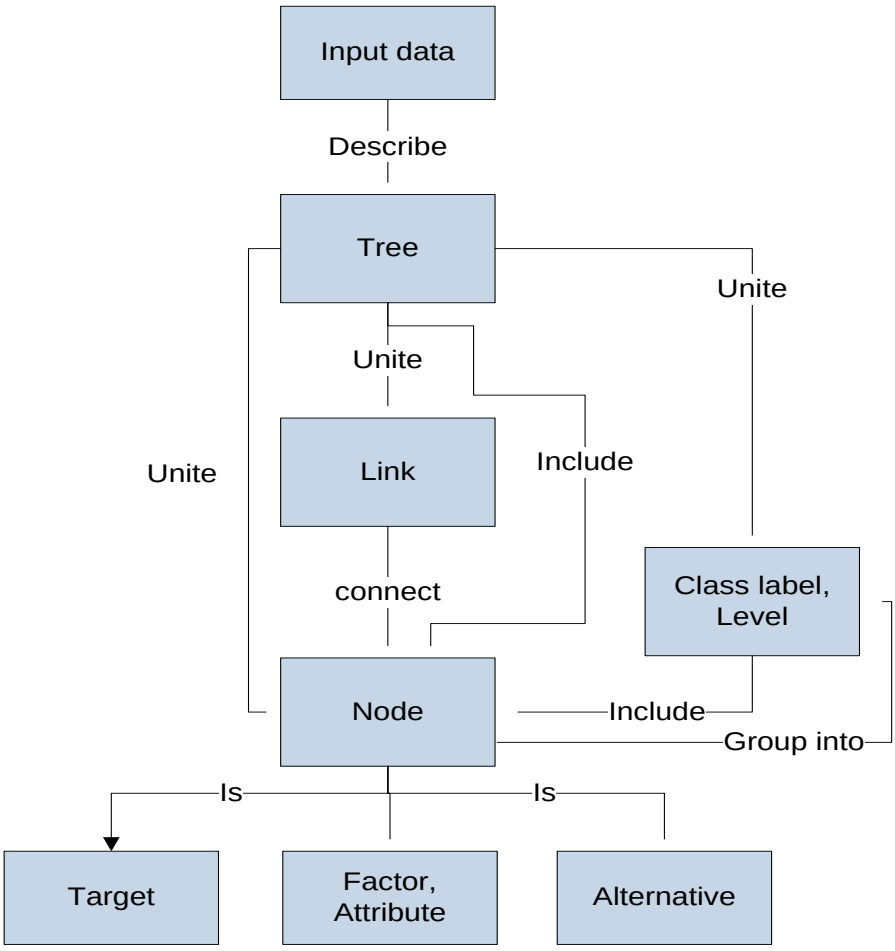

Fig. 3. The fragment of the binary relations within the ontology

For each classification tree the following items tree are constructed [3]:

- dictionary of the concepts;

- table of the binary relations;
- the table of the attributes for each instance of the concepts' dictionary;
- the table of class attributes for each class of the concepts' dictionary;
- the table of logical axioms that defines concepts via logical expressions which are always true;
- the table of constants;
- the table of formulas for each formula included into the attribute table of an instance;
- classification trees of the attributes;
- the table of instances for each entry in the concepts' dictionary.

In this case, the purpose of the ontology' creation is the definition of concepts and axioms defining the basic (initial) conditions for the applicability of decision-making support which are taking into account the uncertainty in the formalization and processing. As the result, the system of constraints of concepts' interpretation forming the basis of these methods should be constructed and recommendations on the choice mechanism for solving problems are given.

Thus, the proposed modelling technique allows describing complex processes of decision support from different points of view. As these complex processes contain many elements and connections, the technique gives the opportunity to reduce the time required for their development, to improve the quality of decisions.

On the basis of this approach algorithms for constructing structured conclusions can be developed. These conclusions contain recommendations on the use of mechanisms of fuzzy sets to solve tasks regarding decision-making support under uncertainty.

References:

1. Sadovnikova N.P., Lvova J.S, Sanjapov B. The conceptual model of the decision – making process based on the ontological approach under conditions of uncertainty of initial information // Public education №2 (88). Ch.2, 2011. P.185-187.

2. Blumin, S.L. Models and methods of decision-making under uncertainty / SL

Blumin, IA Shuykova. - Lipetsk: ЛЭГИ, 2001. – 138с.;

3. The ontology of method of the Satie hierarchy's' analysis / A. Grechko // Artificial Intelligence, 2005 [electronic resource] : the electron. scientific. jounal. Kiev: UDC 681.3:519, 2005. (iai.dn.ua/public/JournalAI_2005_3/Razdel9/07_Grechko.pdf).

CID: J21208-821

Zaitseva T., Igrunova S., Nesterova E.,

Pusnaya O., Putivzeva N.

DEVELOPMENT AND BUILDING EXPERT SYSTEM FOR CHOICE OF TYPE SERVICE IT-INFRASTRUCTURE

Belgorod National Research University

Virtually every enterprise, regardless of the scope of activities and organizational-economic characteristics, has a specific IT infrastructure. Its operation plays an important role in the organization, so you must keep it in order and to troubleshoot the problem in time. In addition, having learned to save money on the crisis in the IT, business today does not seek to increase their expenditure on computerization dramatically. On the contrary, more and more attention is paid to optimize the capabilities of the IT infrastructure. The task is complicated - you need time to provide the development and stay within the budget. Thus, it is important to choose the right kind of service company to support IT infrastructure.

Subject area for this expert system is to serve the IT infrastructure. Often the head of the organization faces a difficult task of choosing this type of service on its own, without the help of experts, etc. Alongside it is necessary to take into account many different criteria and parameters of the company. In order to simplify this task an expert system which allows you to take into account all necessary factors and opportunities of the enterprise, was developed reducing the time spent by the head and reducing the risks when making decisions.

Expert systems are the bright and rapidly progressive direction in the field of

artificial intelligence. The reason for the increased interest is the possibility of their application to solving problems from various areas of human activity.

It is the quality of the expert system which is determined by the size and quality of the knowledge base (rules or heuristics). The system operates in the following cyclic mode: select (query) data or test results, observation, interpretation of results, the assimilation of new information, the creating with the rules of temporary hypotheses and then choosing the next piece of data or test results. This process continues as long as the sufficient information to enable a final conclusion is received.

At any given time there are three types of knowledge in the system:

1. Structured knowledge - knowledge about the static field. Once these skills are identified, they are not changeable.

2. Dynamic knowledge - variable knowledge about the subject. They are updated while the new information as to identified.

3. Working knowledge - skills used to solve a specific problem or for consultation.

Thus, the main challenge in developing an expert system was the choice of subject area.

Subject area at a time can be represented as a set of entities, concepts and situations. The selected set of entities, concepts and situations is called of the subject area its state. Since the concepts differ with each other with the help of the signs state the of the subject area can be set if the values of all attributes of the concepts used to describe subject area are known. The concept is a generalization of a class of objects according to their specific characteristics.

To understand the chosen subject area one should be aware of the value of the following concepts:

1. IT infrastructure through the concept of infrastructure

2. Software – licensed free

3. Local Area Network hardware as a software complex

4. Information resources through the property of information "importance"

5. IT outsourcing through the concept of outsourcing

6. IT Manager - full-time employee, a representative of an IT company, freelancer

The next step was to determine the relationships between concepts and the selection of the conceptual component of the field of knowledge. The formation of the conceptual component of the field of knowledge is based on the identification of the conceptual structure of the subject area, since this structure contains concepts and models the basic functional relationships (or relationships between concepts). These relationships reflect the model or strategy for making decisions in the selected subject area.

The functional component of the field of knowledge was further highlighted. Determination of decision strategies, ie, the identification of chains of reasoning, connects all the previously formed concepts and relationships in a dynamic system of the field of knowledge. That strategy gives the activity to the knowledge, they sort out the model of the subject area and conduct a search from the conditions to the target. Conceptual and functional components complement and refine each other.

Further, the expert system using shell EsWin was developed. Tool software ESWin is used to create and exploit the advising expert systems for solving various problems, leading to the decision-making tasks (diagnosis, configuration, identification, etc.). The software is designed on the base of the technology of hybrid expert systems represents the knowledge in the form of frames, rules, products and linguistic variables, which allows to develop and launch special programs in the form of exe-files, but also in the process of solving problems it allows to use the data from the database access which is carried out using SQL-queries generated automatically.

The selected software supports the solution of problems by the method of reverse fuzzy inference. In this case the facts are taken from the dialogue with the user and stored in the database of facts. Subject area and dialogue with the user are described in the form of frames. The dialogue can be used to explain the graphics format GIF, BMP, JPEG, HTML, PNG, as well as text files in TXT. Progress in the solution is explained by the trace, reflecting the sequence of rules-products and

derived facts.

The results of the test system show that the proposed expert system has been successfully operating in the area of decision-making concerning the choice of a particular type of service company for IT infrastructure.

The system can not only help in choosing the type of service, but also to pinpoint the bottlenecks of his enterprise to the head.

The main advantages of this expert system are the opportunities to accumulate knowledge and to adjust it to a specific company with the minimum time spent. In this regard, as a further development of the expert system it is supposed to broaden the base of knowledge, clarifying certain rules, as well as to improve the inference mechanism in order to improve ergonomics expert system.

CID: J21208-378

UDK 004.021

Reyzlin V.I., Tartakovsky E.A.

THE PARALLEL ALGORITHMS BASED ON THE CUDA TECHNOLOGY FOR SOLVING ADAPTIVE OPTICS PROBLEMS

Tomsk Polytechnic University

In this paper we consider the possibility of using NVIDIA CUDA technology for the construction of parallel algorithms for solving problems of adaptive optics.

Keywords: parallel computing, computing on graphics processors, the technology NVIDIA CUDA, adaptive optics.

Currently, all the more urgent becomes parallel computing. Many scientific problems and problems of mathematical modeling for calculating a reasonable time require more computing resources than able to provide a central processor (CPU) of PC sequential calculations. When parallelizing calculations for modern CPU, with up to six cores in Intel Core i7-980X, calculation speed increases proportionally to the number of nuclei. If you do not optimize the program further, the rate of increase in the number of times, how many kernels parallelized computation.

In addition to the CPU for parallel processing at the present time, there is the possibility of computing on graphics processors (GPU). To date, there are several technologies that allow programming the GPU for non-graphics calculations. One of them, NVIDIA CUDA, in the opinion of the authors is the most elaborated. The platform includes the CUDA library of parallel algorithms for linear algebra, fast Fourier transform, and, in the latest version of the random number generator, and algorithms to work with sparse matrices [1].

The main advantages of GPU vs CPU, from the perspective of parallel computing are as follows:

• The number of cores – NVIDIA GPUs to date, have up to 480 cores (NVIDIA GeForce GTX480), each of which handles blocks of 768 threads.

• The number of threads – the modern GPU can process hundreds of thousands of flows. Time required creating a flow comparable to the cost of the computation of mathematical operations. This amount and lightness of flow allows parallelization of tasks to refine the calculated matrix element [2].

In addition to the advantages of GPU's computations there are shortcomings, rather strongly restrict the range of problems in which the possible gain in speed with respect to parallel computing on the CPU. These disadvantages are the low rate of information transfer in the GPU memory and the low velocity of circulation of the global memory. Copying from the CPU to the GPU is about 10–15 times slower than one within the GPU (Fig. 1). If the time to access the shared memory from kernel-function is 4 clock cycles, while recourse to the global memory – 400-600 cycles [3–4].

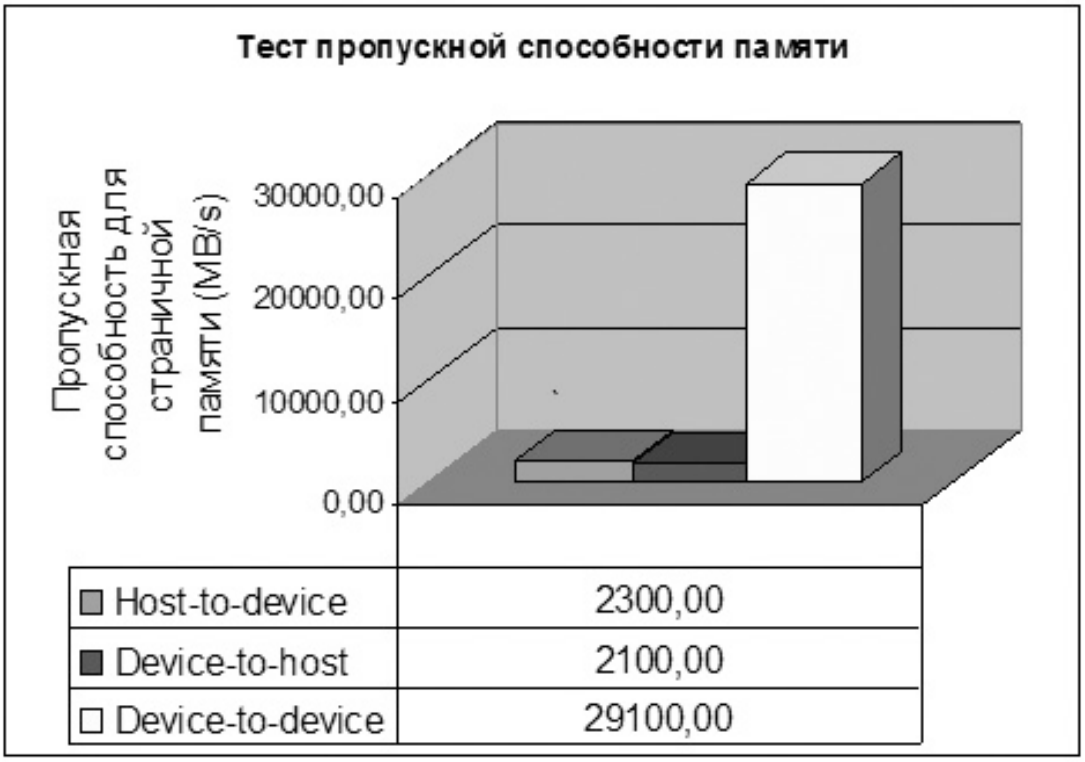

Fig. 1. Comparison of the rates of copying data between the CPU and GPU, as well as inside the GPU

Given the above advantages and disadvantages can be said that the GPU is best suitable for a large number of calculations on a large number of rare incoming data. The modeling of adaptive optics is just such a task.

The formulation and implementation of the task

In optics, the wave equation describes the propagation of coherent laser beam in free space. Software implementation of the solution of this equation involves the following steps: the calculation of the signal's matrix, calculation of the signal's matrix spectrum using the Fourier transform, the multiplication of the signal and filter, obtaining a matrix signal using the inverse Fourier transform.

Let the matrix signal and filter functions are calculated in advance and at the time of start of the algorithm are known. Then the software solution of the equation is reduced to the use of algorithms for multiplication of complex matrices, and Fourier transform. Fast Fourier transform algorithm for CUDA is implemented in the library CUFFT, delivered the platform. Matrix multiplication is performed element by element according to the rule of multiplication of complex numbers:

re = ac - bd; im = ad + bc,

where re, a, c – the real part of the result and multiply numbers; im, b, d – the imaginary parts. Calculations are made as follows [5-6].

The task is divided into blocks of the same type that are calculated in parallel on different cores:

```
#define BLOCK_SIZE 16;
dim3 dimBlock (BLOCK_SIZE, BLOCK_SIZE);
```

Find the block size. In this case, there are 16 to 16 elements. Find the size of the grid blocks needed to cover the matrix:

```
dim3 dimGrid (sze/dimBlock.x, sze/dimBlock.y);
```

Each block's element corresponds its flow, the blocks are evenly distributed over the nuclei. To start the calculations necessary to allocate memory for GPU:

```
cufftComplex * pDeviceMemA;
cudaMalloc ((void **)&pDeviceMemA, sze * sze * sizeof (cufftComplex));
```

After that, you should copy the required data in memory, specify the size of the grid and the block and cause a kernel-function:

```
MxMcomplex_dot_kernel <<< dimGrid,
dimBlock >>> (pDeviceMemA, pDeviceMemB, sze);
```

After completing the calculation result is copied back into main memory, the GPU’s memory is released.

```
cudaMemcpy((void *)pA, pDeviceMemA, sze * sze *
sizeof(cufftComplex), cudaMemcpyDeviceToHost);
cudaFree(pDeviceMemA);
```

Kernel-function is a function that is called parallel to each core. As part of the stream function are the indices in the block, the block in the grid, the dimension of the block and grid blocks:

```
int bx = blockIdx.x;
int by = blockIdx.y;
int tx = threadIdx.x;
int ty = threadIdx.y;
int bdx = blockDim.x;
```

```
int bdy = blockDim.y;
int gdx = gridDim.x;
int gdy = gridDim.y;
```

With the calculation of these indices is realized only one block in each kernel-function. The calculated by the core block is copied into the shared memory when the kernel to provide high speed access to the elements of the matrix:

```
__shared__ cufftComplex
As[BLOCK_SIZE][BLOCK_SIZE];
int elemnum = BLOCK_SIZE * by + sze * bdx * bx + tx * sze + ty;
As[ty][tx] = A[elemnum];
```

Comparison of results of algorithms by the CPU and GPU

For the parallel version of the algorithm for solving the wave equation has been measured the acceleration of computing by NVIDIA GeForce GT240 graphics cards and NVIDIA GeForce GTX285. Computing speed was measured in hertz, and then calculated the ratio of the rate calculations to the GPU to speed computations on CPU (Fig. 2).

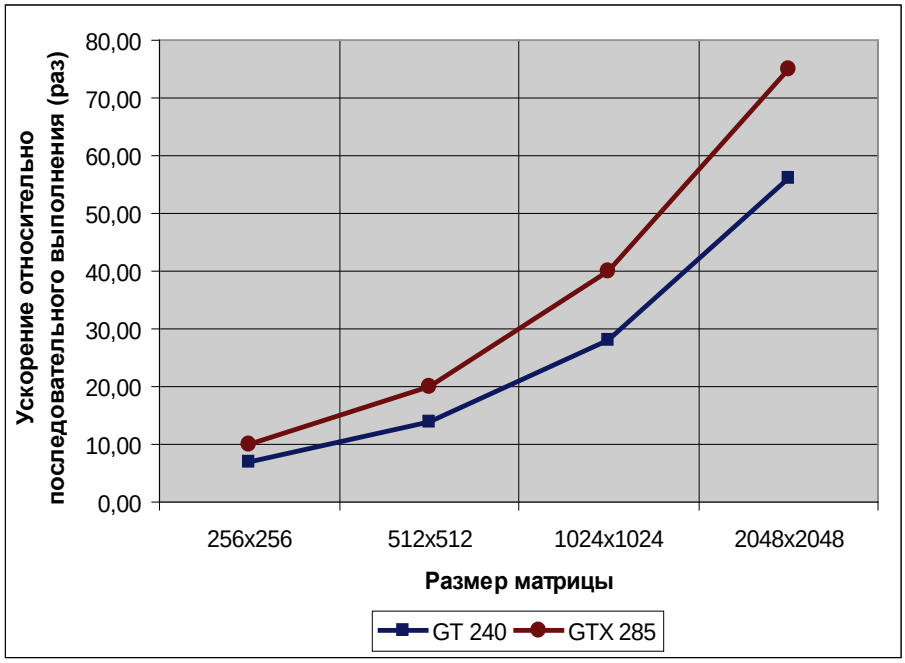

Fig. 2. The acceleration algorithm for solving the wave equation in CUDA relatively consistent calculations

Calculations were performed on the CPU on a single core CPU Intel Core i7 860

2.8 GHz.

Note that the acceleration of computations in the dozens of times not only saves time but also to move to an entirely different level of problem solving.

This work performed within the state grant of R & D.

References:

1. NVIDIA CUDA: The Beginning. // [Electronic resource]. – Mode of access: http://habrahabr.ru/blogs/CUDA/54330/, free.

2. NVIDIA CUDA: How does the GPU. // [Electronic resource]. – Mode of access: http://habrahabr.ru/blogs/CUDA/54707/, free.

3. NVIDIA CUDA: Working with memory. Part 1. // [Electronic resource]. – Mode of access: http://habrahabr.ru/blogs/CUDA/55461/, free.

4. NVIDIA CUDA: Working with memory. Part 2. // [Electronic resource]. – Mode of access: http://habrahabr.ru/blogs/CUDA/56514/, free.

5. NVIDIA CUDA C Programming Best Practices Guide. CUDA Toolkit 2.3. // 2009.

6. NVIDIA CUDA Programming Guide. Version 2.3. // 2009.

CID: J21208-820

Zaitseva N.O.

ON THE NEED FOR A NEW DESCRIPTION AND PERFORMANCE STANDARD BUSINESS PROCESSES

National Research University "Belgorod State University"

This article raises the question of the need for a new standard for the description and execution of business processes.

Keywords: business process, business process model, visualization model.

By the beginning of 2012 the industry's business process automation, mainly abroad, was formed firm understanding of the basic tenets of description languages and execution of business processes. Despite all the debate and open competition among software vendors and suppliers of automation possible problems of parallel

development of the majority of protocols and standards that describe the same domain, largely avoided. And the whole interest was centered around three standards: BPMN, XPDL and BPEL. However, this prompted the organization to join the big secret conflict with each other, which led to inconsistencies in some cases, a notation on the other, and, therefore, to the obvious problems of visualization of the same business process model in various standards [1].

The application of each of the different standards: BPMN model helps to interpret the graph, XPDL allows you to store its semantics and be an intermediary between the other standards, and describes the interaction of BPEL processes. But the analysis of standards can not be certain that they are too different. Thus, for each pair of standard BPMN - XPDL, XPDL - BPEL, BPMN - BPEL has its own specific difficulties. This may be a problem vzaimovizualizatsii, preserving the integrity of the model and some other problems.But for now the solution of such problems is shifted to software developers and systems, and the user has the choice of software provider.Identify weaknesses and strengths of this or that standard suggests that there is a situation that forced them to improve existing or develop new standard for describing business processes [2].

Thus, we are faced with the purpose to develop a new standard for the description and execution of business processes, realizing the benefits and shortcomings of the existing ones. This problem should be solved in the near future.

Literature

1. A. Michael Hammer. Reengineering the corporation. The manifesto of the revolution in business. / Michael Hammer, James Champy. - M. Mann, Ivanov and Ferber, 2007 - 288 pages

2. Two. Some of the most well-known standards for describing business processes / [electronic resource] / M. Romanov, 2009 / /

CID: J21208-628

Saenko I.B., Nizhegorodov A.V.,
Kabanov A.S.

The need for a unified system to control access to information resources in automated systems

St. Petersburg Institute for Informatics and Automation of RAS

The article discusses the need for a unified system to control access to information resources in automated systems. Various aspects of uniform access control system using are considered. The analysis of various information security threats for automated systems is performed.

Keywords: access control system, information resource, automated system, unauthorized access.

In today's society the information becomes one of the most important resources for analysis, forecasting and decision making. The availability of information is a key element in which the actors who have the right of access, can implement these rights without hindrance, in real time, with a degree of protection from unauthorized access (UAA). The availability of information is one of the three main components of information security in addition to its confidentiality and integrity.

Increasing information security threats for automated systems (AS) stemmed from the growing volume of information flows, circulating in them, availability of information technologies, and their openness and widespread. The urgency of the problem are not left without attention to a number of leading countries of the world. In the United States, Canada and the UK in 2009, cyber-command centers have been set up. These units are responsible for the security of critical information systems of the State. In 2010, a similar unit was established in China. The ruling circles and a number of other States are of the view that in future wars control over information flows will be a decisive factor in achieving victory [1]. These units are the implementation of a real-time assessment of information networks, followed by immediate measures in response to violations of information security and the

possibility of adequate against aggressors. It should be noted that Russia is also included in the list of countries that threaten the United States in the security information area, in addition to China, India and Iran.

In addition, there is a real risk of software attacks on vital public installations by various terrorist organizations. Purpose of these organizations is to provide access to information resources in the AS or the provision of the destructive impact on these resources and AS as a whole. Terrorists actively use cutting edge information technologies [2]. Such a situation does not remain without attention from the power structures in Russia, but requires an integrated approach to her studies with respect to the above threats.

The essential problem of improvement and development of information security is the creation of a uniform system to control access to information resources. Uniform system to control access to information resources should be an information space with a high degree of freedom from malicious attacks and provide ongoing monitoring of the situation.

The lack of detailed methodical ware of access control process, in turn, makes it necessary to focus in this study the main efforts on preventing breaches of the availability of information, assess the quality of your access schemes and their impact on security against UAA of information systems as a whole. Existing access control systems are suitable for use in individual organizations, and they do not have the ability to integrate into larger systems, centralized at the national level. Generally, the developers of these systems are based on the use of software products of foreign manufacturers with closed source code that may have a negative impact on their use in critical infrastructures.

The problem of establishing a uniform system of access control to information resources of AS is related to theory framework for access control, developing approaches and methods for the design, construction, operation and future development of that system. This approach should be carried out with the full analysis of subsystems of management. Solution of the above problems is of great importance to society, government, law enforcement, industry and academia.

The literature:

1. China created "digital special troops"//Open technologies / an access Mode: http://www. ruvr.ru (accessed February 21, 2012).

2. S.Supichenko Internet extremism and terrorism / S.Supichenko – information analytical magazine TSATU: Dissymetric threats and conflicts of low intensity. – № 5. – 2008.

CID: J21208-288

UDK 004.896:528.721.22

Uryvskiy E., Smirnov U.

METHODS AND ALGORITHMS, USED IN IMAGE-BASED 3D MODEL ... SYSTEM

Ukhta State Technical University

169300, Komi republic,sity the Ukhta, Pervomaiskaya st., 13

New algorithm of automatic 3d modeling of real objects is suggested. An estimate and justification of the algorithm is given. The report examines the well-known approaches to quality improvement and optimization of 3d models creating methods taking into account the peculiarities of human vision. The practical significance of the study is to show the relationship of speed and quality of the image processing to reconstruct 3d scene and the character of its optimization, taking into account the individual characteristics of the algorithm.

Key words: Reconstruction, system, image processing, computer vision, automation.

In modern conditions the need of artificial intelligence and computer vision arises in various fields of human activity, which is why pattern recognition and computer vision has the increased interest and intensive development of the theory now. Automation tasks associated with processing the data obtained from routine and time-consuming process, which was not originally adapted computer, such as, for example, viewing records from a large number of cameras to search for stolen

vehicles, a set of multiple handwritten text in a text editor , the search for potentially dangerous objects on the photo and video materials of public lands are highly relevant. To date, the application of the theory is limited to addressing issues of identification and retrieval of objects, at the same time, relatively recently begun to develop a direction associated with the automation of the process of creating 3d models of objects, their recovery by some well-known properties. Recognition of 2d images are widely developed and used effectively in practice, while at the same time, the algorithms of 3d "vision" far from perfect, have significant drawbacks and need further development.

The task of reconstruction of 3d model of the environment scene is to determine the spatial coordinates of points on the surface of objects from images in the pictures. Images containing necessary for the reconstruction objects from different angles (or videostream) used as the initial data. From such images you can extract the spatial characteristics of objects. As a result of processing raw data generated 3d model of the scene, which is refined and adjusted for the receipt and processing of new data.

The most popular algorithm of this system consists of the following steps:

1. Finding the camera calibration;
2. Finding features in the images (projections of a point in space);
3. Comparison of features for the spatial coordinates of the point;
4. Reconstruction of the model on a set of points and model texturing.

This algorithm, despite its speed (due to the small number of stages of the system and its simplicity) is working very unstable since a large number of errors and mistakes (which arise due to non-standardized and raw input data, the errors of each method at each stage of work, lack of control over the quality of reconstruction, etc.) and used in systems where necessary to indicate at least once a 3d model, or know in advance what specific data will be necessary to reconstruct.

In any other case, processing of raw data is required, the complexity of methods and algorithms in general, the optimization of the data obtained on the basis of new, cross-checked by different methods, and more. Developed an automatic 3d modeling of surrounding objects also requires real-time and, accordingly, the organization of

multi-threading applications, and a good optimization software implementations of the methods used.

An algorithm for improved accuracy of the system, compared to the above, which consists of the following steps is developed:

1. Preprocessing, normalization and sorting images package (a package consists of 25-30 frames, ie, a second of video);
2. Segmentation of images;
3. Calibration and rectification of images;
4. Determination and comparison of features, camera tracking (tracking);
5. Construction of vertex models;
6. Building and texturing models;
7. Optimization of results;
8. Output processes (updating data in the database, the output of the reconstructed scene, convert the output to external systems, histograms, and logs).

Consider the algorithm in more detail.

1. Preprocessing, normalization and sorting images package (a package consists of 25-30 frames, ie, a second of video).

Pretreatment imaging is performed using the appropriate noise reduction filters (median filter) and contrast sharpener (contrast filters).

With the normalization of images, they are reduced to a single size and histogram equalization is processed (if necessary).

Sorting is based on optimizing the stereobase (ie, the distance between the points of taking pictures). Selects a package of 3 images and store data about the sequence - the order of the handle. Analysis of the depth of the scene in one image, in principle, impossible without clarification and specification stage. Reconstruction of the two images is called the stereo. The algorithm selected 3 images from the package to find and compare features on the later stages with stereo algorithms with refinement results third image. Finding features in the third image clarifies find features on the first two images. In this case, the quality of matching features increased significantly since there are a large number of emissions (points, which are

features not initially, but fall into them because of the distortion of images, features scenes and other reasons).

With this step reduces the number of errors related to image quality, reduces time and increases accuracy of the model building by selecting the best three shots, image processing time is reduced at the following stages of standardization, etc.

2. Segmentation of images.

At the stage of segmentation, the image is divided into objects with respect to the depth of the stage and location of the object in it (disparity), the properties of pixels (such as brightness, color, etc.) or on the basis of detectors boundaries (Algorithm Kenni, Sobel filter, the filter Prewitt). Data on the segmentation is stored in the form of dynamic resolution panoramic image and transferred to the stage of camera calibration to match the results. Due to the segmentation of images significantly increases the accuracy of camera calibration and calibration errors affect the quality of recognition the most. Also, segmentation simplifies the process of breaking points found in the space of the respective models.

3. Calibration and rectification of images.

Camera calibration is an automatic way, with the support of the subject. The camera is fixed on the subject, and the relative sizes of a given coordinate system, and, respectively, are determined by calibrating the camera, as the internal (focus cameras) and external (displacement and rotation of the camera). On the basis of previously determined by the method of least squares and found the faces of the object (algorithm Kenny) defined the vanishing point (vanishing points), which is constructed on the basis of the coordinate system relative to which the camera calibration and are in the form of the fundamental matrix. At this stage, work is going on with the database and specifies the fundamental matrix with each new cycle of the system, if the difference in the data below a certain threshold.

After finding the camera calibration image rectifies (the image plane are in one straight line), thus simplifies subsequent work with them. Also, there is gomography conversion of one image to another coordinate system. The obtained camera calibration allows you to work with images on, and the rectification of images

reduces the matching of features (especially in the two images lie on a straight line, which follows from the epipolar constraints).

4. Find and compare features, tracking camera.

There are many ways of finding and comparing features. The most used method for the representation of feature points and their neighborhoods is the Harris detector, which works on the change in the gradient. If the displacement of the considered windows to either side brightness of the pixels varies greatly, so the angle, if the brightness varies by only 2 out of 4, it is bound, if the practice does not change in any direction that is the surface of the object. Are key features (the most precise angles in the images) and then compiled a pair of these features with respect to the similarity of their neighborhoods.

To test this algorithm is also used tracking, ie, tracking chamber (Lucas–Kanade algorithm). Memorable features of previous cycles (stored in the database) are compared with the current, and thus approximated the line of camera movement, and, therefore, extrapolated values of the features in the next frame based on the spline. In agreeing on the results of these two methods are specified. All results for future work are stored in the database. With this agreement the results of different methods of comparing the quality of the features in the images is significantly improved. The result of this phase is to complement the universal segmented image resolution and dynamic descriptions of pairs of features, keeping the coordinates of a pair of points and the average brightness of a point in space.

5. Construction of vertex models.

From the universal descriptors of segmented images models are made. Based on epipolar geometry and handles pairs of points are projections of points in space - handles point models. The division of points into groups with respect to their membership of the objects is based on the models and generic descriptors of segmented images. With these descriptors, and models built by Universal segmented image building models takes much less time due to decrease in the number of iterations of the algorithm RANSAC stage of construction and texturing models.

6. Building and texturing models.

Finding the texture coordinates, sifting the false points and the construction of models on the found points (RANSAC) is at this stage. Simulation may be due to selection of voxel representation of geometric primitives, or, as in this case, the models are constructed using polygons. Construction of a polygonal model method significantly reduces the simulation time in comparison with other methods (the construction of voxels, the selection of primitives and splines), due to ease of implementation and operation of the method.

7. Results optimization.

In the optimization phase of constructed objects are specified descriptors models and vertex models, optimized scene is calculated estimates of the accuracy of the reconstructed scene changes and the universal segmented image. Also at this stage, if necessary, make changes to user settings. Due to the fact that a lot of data stored in databases, the quality and speed of the proposed algorithm in general is much higher, and many others, including the above distributed algorithm.

8. The output processes (output of the reconstructed scene, convert the output to external systems, histograms, and logs).

At this stage of the work an interactive 3d scene with the system settings and the ability to control the scene itself (control of the camera within the scene, pointing at an object, accurate results, etc.) and viewing of all the important time series data of each phase of the system with the ability to editing is available to the user. Reconstructed scene can be exported to other systems, working with 3d scenes (Autodesk Maya, 3D Studio MAX).

As a result, for the first cycle of a second video stream is processed by the three best shots and all variables are initialized and the appropriate descriptors. For all subsequent cycles of the system is optimized and the results of the construction of 3dscenes reconstructed in real-time environment.

This algorithm is certainly much more accurate and more stable than previously indicated one to harmonizing the results of different methods and to optimize the results of using the database and threading the input data.

Many algorithms, such as the construction of disparity maps based on a

comparison of graphs [1] or camera tracking using voxel representation of models [2] require a large number of calculations and, consequently, time operation. Building a disparity map takes about 20 seconds per image 300x400, a voxel representation of the usual cylindrical cans takes 3-4 seconds. There are ways in which the ratio of the speed / quality is much higher, and given the validation and harmonization of almost every stage of the system, you must select the fastest of them.

The set of data stored in databases, which reduces the time of the system when required recalculations. Many of the calculations can be moved from CPU (Central Processing Unit) on the GPU (graphics processor). Some steps are parallel, and in such cases, application of multiple streams of data. These threads can run simultaneously and have the order in time. Multithreading is applied during the transition from one cycle to another (as long as the scene is built you can start to process a new set of images). All of the above can repeatedly reduce processing time and makes it possible to develop this system.

As a result, we obtain an algorithm of high accuracy, running at high speed. This algorithm can be used for any reconstruction of the scene environment, creating 3d scene from the apartment amateur footage, reconstruction of the environment of the films, both artistic and documentary or any other recording or photographs.

Literature

1. A. Agarkov A. Building a disparity map based on a comparison of graphs / / Artificial Intelligence. - 2003. - № 1. - S. 126-136.

2. Sato, T., Kanbara, M. 3-D modeling of an outdoor scene by multi-baseline stereo using a long sequence of images. Pattern Recognition // Proceedings 16th International Conference.– 2002. – V.3.– P. 581-584.

CID: J21208-888

UDK 539.389.3/669.018.8

Sukhenko V.J.

DEPENDENCE DISLOCATION STRUCTURE DEFORMED ZONE ON THE CONDITIONS AND LOADING MODE FRICTION SURFACES IN CORROSION-ACTIVE MEDIA

National University of Life and Environmental Sciences of Ukraine

In this scenario report the problem of destruction of solids, which is reflected in the different fields of knowledge - mechanics, solid state physics, metalphysics, materials, physical-chemical mechanics of materials, electrochemistry, engineering.

Key words: solid, friction, wear, dislocation theory, the frictional contact.

Review of the problem of destruction of solids occurs at the intersection of several research areas, caused by the fact that this problem includes macro-, micro- and submicroscopic aspects of the mechanisms of destruction. How Notes IV Krahelskyy, now can not be challenges to consider friction and wear, not including physical and physico-chemical processes occurring in atomic-molecular level in a thin surface layer [1]. In this regard, it is vital to the study of friction and wear in terms of dislocation theory, which explains the atomic mechanism of plastic deformation, the structure of grain boundaries and mosaic blocks, the process of diffusion, destruction, etc. [2,3,4,5,6,7,8]. In Ukraine work in this direction and started developing B.I. Kostets'ky and his school, N.V.Nazarenko co-workers, E. Yevdokimov.

B.I. Kostetskyy with co-authors showed the features of the restructuring of the surface layer of metal by friction with a lubricant in the presence of surfactants [9], the role of structure and orientation of crystals in the formation process of external friction [10], fracture of metals due to the type of crystal lattice [11] and the dislocation model of the processes of setting and oxidation of metals during friction [12,13]. In the doctoral thesis D.V. Nazarenko defined deformation plastic springand structural changes in the processes of external friction [14]. Influence of reverse

sliding friction on the working surface submicrostructure dedicated work V.D.Yevdokymova [15]. At the same time, the result of deformation and fracture of metallic sliding friction in microvolumes and on the atomic-molecular level can not yet explain many phenomena in this region is the accumulation of experimental data. Thus, the corrosion-mechanical wear of metals not studied the impact of dislocation structure of deformed zone of the chemical composition and pH of active liquid media, the properties of metals, such as their crystal lattice and tension in them, modes of electrochemical polarization, the magnitude and direction of current that passes through frictional contact, conditions of load connected surfaces and the like.

Physical and electrochemical mechanical frictional contact, in fact, at the present stage of development of theory about not disclosed [16]. The value of this theory to explain the mechanism of corrosion-mechanical wear of metals in food processing environments and methods to increase their durability is obvious that it is necessary to continue research in this direction.

Literature:

1. Крагельский И.В. Некоторые задачи науки о трении, В об. "Проблемы трения и изнашивания", К., «Техніка», 1971, вып. I, с. 11-17.

2. Костецкий Б.И. Трение, смазка и износ в машинах. К., "Техніка", 1970, 895 о. с ил.

3. Крагельский И.В. Трение и износ. М., "Машиностроение", 1968, 480 с. с ил.

4. Ребиндер П.А., Щукин В.Д. Поверхностные явления в твердых телах в процессах их деформации и разрушения. "Успехи физических наук", 1972, т.108, вып.1, с.32-42.

5. Регель В.Р., Слуцкер А.И. Кинетическая природа прочности. В сб. "Физика сегодня и завтра", Л., "Наука", 1973, с. 90-176.

6. Уэрт Чм Томсон Р, Физика твердого тела. М», "Мир", 1969, 558 с. с ил.

7. Френкель Я.И. Введение в теорию металлов. Л.: "Наука", 1972» 424 с.

8. Фридель I, Дислокации. М.:, "Мир”, 1967, 643 с. с ил.

9. Костецкий Б.И., Колесниченко Н.Ф. Качество поверхности и трение в машинах. К.:, «Техніка», 1969. 215 о. с ил.

9. Костецкий Б.И., Бармашенко А.И., Славинская Л.В. Роль структуры и ориентации монокристаллов в формировании процесса внешнего трения. В сб. «Металлофизика», К.: «Наукова думка», 1972, вып.40, с. 24-37.

10. Костецкий Б.И., Дяченко Ю.П., Артемьев Ю.И. Разрушение металлов при трении скольжения в связи с типом их кристаллической решетки. В сб. "Проблемы трения и изнашивания", К:, «Техніка»,1973, вып. 4, с. 64-66.

11. Костецкий Б.И., Лозовский В.Н. Факторы, определяющие вероятность возникновения схватывания и окисления металлов при трении. ФХШ, 1968, т. 4, Л 5, с. 54-57.

12. Костецкий Б.Й., Шульга О.В. Электросопротивление поверхностных слоёв металлов и механизм схватывания. ДАН СССР, 1969, т. 188, № I, с, 80-82.

13. Костецкий Б.И., Носовский И.Г. Процесс схватывания металлов и критерии оценки его интенсивности. В сб. "Проблемы трения и изнашивания", К., «Тежніка», 1972, вып. 2, с.74-77.

14. Назаренко П.В. Исследование влияния упруго-пластических дефоруаций и структурных изменений на процессы внешнего трения и износостойкость. Автореферат докторской диссертации. К.: КНИГА, 1973, 49 с. с ил.

15. Евдокимов В.Д., Семенов Ю.И. Экзоэлектронная эмиссия при трении. "Наука", 1973, 182 с. с ил.

16. Крагельский И.В. Износ и безизносность. В сб. «Избирательный перенос при трении и его экономическая эффективность», М., МДНТП, 1972, с. 15-21.

CID: J21208-045

UDK 534:62-13

O.V. Lomakina, V.I Galaev

ANALYTICAL METHOD OF DEFINING EQUIVALENT RIGIDITY OF THE SYSTEM “ROTOR-BEARING WITH GAPS”

FGBOU VPO "Tambov State Technical University»

The calculating dependence of the equivalents stiffness characteristics in both horizontal and vertical directions of the node references with the clearances of the rotor under the action of technological stress. The results are making possible to conduct a qualitative investigation the some of tasks of nonlinear dynamics of rotor systems.

Key words: amplitude oscillations, the reference node, the radial gap, the resonance and the skeletal surface, rotary machine, the frequency, the equivalent stiffness.

Development and construction of rotary machine design should take account of requirements to provide an acceptable level of vibration, which is a testament to its excellence and serves as a guarantee of durability and reliability, as work flow machines and vibration generated by it what’s are closely linked and interdependent. Rotary machine is a multi-parameter dynamic system containing nonlinear relationships and under the influence of loads, differing both in nature and intensity of action.

The main working body of the machines of this type is a rotor, rotating in the elastic supports. It should be noted that the motion of the rotor in horizontal and vertical planes are interconnected, because of the gyroscopic member as differential equations of motion of the rotor, and the presence of radial gaps in its support, formed due to wear pins and bearings of the rotor.

Need to study the vertical oscillations of the rotor is predetermined by the problem of calculating dynamic forces transmitted to the body of the car by the rotor [1]. Vibrations of the rotor in the horizontal plane is determined for certain types of

rotating machinery quality and precision manufacturing operation. Examples of such machines are planning in leather processing, intended for semi-finished leather required thickness and a smooth clean its surface finish.

The problem of determining the equivalent linear stiffness characteristics of reference sites with gaps loaded rotor, whose use makes it possible to conduct some studies of dynamic processes based on linear differential equations, taking into account the qualitative features of nonlinear system "rotor - elastic supports with a clearance."

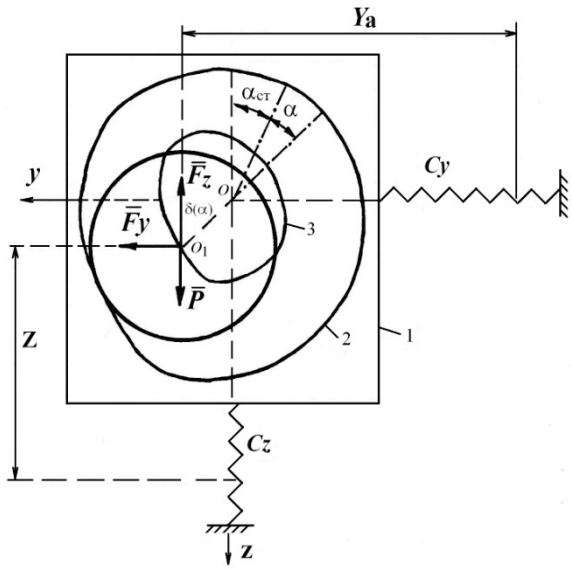

Fig.1 A dynamic scheme of the investigated mechanical system: *1- bearing rotor, 2- line contact pins of the rotor based, 3- trajectory of the relative motion of the center pin of the rotor.*

Dynamic model of the rotor, rotating in the elastic supports with gaps, is shown in Fig. 1. Denote: m, C_y, C_z - mass of rotor, overall rigidity of the shell reference nodes in the horizontal and vertical directions respectively, $d(a)$- radial clearance in the bearings of the rotor as a function of the angle of deviation of its pins from the vertical direction, a_{st} - static deflection angle due to the influence of the technological burden on the rotor, a - dynamic angle of the rotor pins, $f = \frac{F_z}{F_y}$ - the ratio between vertical and horizontal components of the technological burden, y_{st}, z_{st} - static

displacements of the center of mass of the rotor in horizontal and vertical directions, respectively, due to deformation of the support units, y_a, z_a - absolute dynamic displacement of the center of mass of the rotor in that direction.

The potential energy of the system "rotor - an elastic support with a gap" is:

$$\Pi = \frac{1}{2} C_y [y_a + y_{st} - d(a + a_{st}) \sin(a + a_{st}) + d(a_{st}) \sin a_{st}]^2 +$$
$$+ \frac{1}{2} C_z [z_a + z_{st} - d(a + a_{st}) \cos(a + a_{st}) + d(a_{st}) \cos a_{st}]^2 -$$
$$- mg[z_a + z_{st} + d(a_{st}) \cos a_{st}]$$

The kinetic energy of the rotor:

$$T = \frac{1}{2} m(\dot{y}_a^2 + \dot{z}_a^2) + \frac{1}{2} A w^2,$$

where A - polar moment of inertia rotor, w - its angular velocity.

Generalized forces corresponding to no potential forces and coordinates, y_a, z_a and a, for the considered mechanical system have the form:

$$Q_{y_a} = F_y, \; Q_{z_a} = - F_z,$$

$$Q_a = F_y \left\{ [d(a + a_{st}) \cos(a + a_{st}) + d'(a + a_{st}) \sin(a + a_{st})] + f[d(a + a_{st}) \sin(a + a_{st}) - d'(a + a_{st}) \cos(a + a_{st})] \right\},$$

where $d'(a + a_{st})$ - derivative of the radial clearance on the corner a.

Equations for the dynamics of the system have the form:

$$\begin{cases} m\ddot{y}_a + C_y \times y_a - C_y d(a + a_{st}) \sin(a + a_{st}) + C_y d(a_{st}) \sin a_{st} = 0, \\ m\ddot{z}_a + C_z \times z_a - C_z d(a + a_{st}) \cos(a + a_{st}) + C_z d(a_{st}) \cos a_{st} = 0, \\ mg[d(a + a_{st}) \sin(a + a_{st}) - d'(a + a_{st}) \cos(a + a_{st})] - \\ - C_y [y_a - d(a + a_{st}) \sin(a + a_{st}) + d(a_{st}) \sin a_{st}] \times \\ \times [d'(a + a_{st}) \sin(a + a_{st}) + d(a + a_{st}) \cos(a + a_{st})] + \\ + C_z [z_a - d(a + a_{st}) \cos(a + a_{st}) + d(a_{st}) \cos a_{st}] \times \\ \times [d(a + a_{st}) \sin(a + a_{st}) - d'(a + a_{st}) \cos(a + a_{st})] = \\ = F_y \left\{ [d(a + a_{st}) \cos(a + a_{st}) + d'(a + a_{st}) \sin(a + a_{st})] + f[d(a + a_{st}) \sin(a + a_{st}) - d'(a + a_{st}) \cos(a + a_{st})] \right\}. \end{cases} \quad (1)$$

The equation for determining the angle a_{st} obtained from the third equation (1), if it take $a = 0$. The linearizing equation of this system, we get:

$$\begin{aligned} m\ddot{y}_a + C_{\text{экв}}^{y} \times y_a + C_{\text{экв}}^{yz} \times z_a = 0, \\ m\ddot{z}_a + C_{\text{экв}}^{z} \times z_a + C_{\text{экв}}^{zy} \times y_a = 0. \end{aligned} \quad (2)$$

From equations (2) that the elastic supports with a clearance in the first approximation can be regarded as a support to the following linear elastic characteristics in the horizontal and vertical directions:

$$F_y = C_{\text{equ}}^{y} \times y_{\text{a}} + C_{\text{equ}}^{yz} \times z_{\text{a}}, \quad F_z = C_{\text{equ}}^{z} \times z_{\text{a}} + C_{\text{equ}}^{zy} \times y_{\text{a}},$$

where $C_{\text{equ}}^{y} = \dfrac{C_y \left[mg \times r + \cos^3 \alpha_{\text{st}} \left(\varphi + f \times z \times z^2 \times C_z \right) \right]}{D}$,

$$C_{\text{equ}}^{z} = \frac{C_z \left[mg \times r + \cos^3 \alpha_{\text{st}} \left(\varphi + f \times z \times \varphi^2 \times C_y \right) \right]}{D}, \quad C_{\text{equ}}^{yz} = C_{\text{equ}}^{zy} = \frac{C_y C_z \cos^3 \alpha_{\text{st}} \times \varphi \times z (\varphi + f \times z)}{D},$$

$$r = \delta^2 (\alpha_{\text{st}}) + 2\delta\text{¢}(\alpha_{\text{st}})^2 - \delta(\alpha_{\text{st}}) \times \delta\text{¢}(\alpha_{\text{st}}), \quad \varphi = \delta(\alpha_{\text{st}}) + \delta\text{¢}(\alpha_{\text{st}}) \times tg\alpha_{\text{st}}, \quad z = \delta(\alpha_{\text{st}}) \times tg\alpha_{\text{st}} - \delta\text{¢}(\alpha_{\text{st}}),$$

$$D = mg \times r + \cos^3 \alpha_{\text{st}} (\varphi + f \times z) \times \left(C_z \times z^2 + C_y \times \varphi^2 \right).$$

Quantities $C_{\text{equ}}^{y}, C_{\text{equ}}^{z}$, C_{equ}^{yz} are equivalent stiffness characteristics of the support with a gap, and the stiffness reflects the relationship between the movements of the rotor in horizontal and vertical planes. Thus, in the first approximation is possible the study of the dynamics of the rotor is not as linear elastic supports with the above characteristics.

Equation (2) will not be linked, if $C_{\text{equ}}^{yz} = 0$, and then it is possible in the following cases:

1) radial clearance in the bearings is equal to zero, while $C_{\text{equ}}^{y} = C_y$, $C_{\text{equ}}^{z} = C_z$,

2) radial clearance and the constant angle $\alpha_{\text{st}} = 0$, that corresponds to the idle mode of the rotor (radial displacement of the rotor in a vertical direction relative to the support in this case a small quantity of higher order than its movement in the horizontal direction), while $C_{\text{equ}}^{z} = C_z$,

3) radial clearance and constant angle $\alpha_{\text{st}} = 90^0$, which corresponds to the work of the rotor at the selected technological load gaps (radial movement of the rotor in the horizontal direction, a small quantity of higher order than in the vertical), while $C_{\text{equ}}^{y} = C_y$,

4) value $z = 0$, that corresponds to the radial displacement of the rotor with respect to the support in the neighborhood of the point at which the tangent to the

trajectory of the relative motion of the center pin is horizontal (a generalization of Case 2), while $C_{\text{equ}}^{z} = C_z$,

5) value $\varphi = 0$, the radial displacement of the rotor occurs in the neighborhood in which a specified in Section 4 the tangent is vertical (a generalization of Case 3), while $C_{\text{equ}}^{y} = C_y$,

6) value $\varphi + f \times z = 0$, which corresponds to a radial displacement of the rotor relative to the support in the neighborhood in which the normal to the trajectory of the relative motion of the center pin of the rotor is directed along the line of action of resultant forces F_r и F_b (specified displacement of the rotor with respect to the support is much less than its movement with the support). It should be noted that in this case $C_{\text{equ}}^{y} = C_y$ and $C_{\text{equ}}^{z} = C_z$, was expected.

It is known that the frequency of free oscillations, and hence the equivalent stiffness characteristics of nonlinear mechanical systems depends on the amplitude of oscillations [2]. To obtain these dependencies in the expansion of trigonometric functions in the equations of system (1) take into account higher order terms with respect to the angle α.

Accepted $y_a = A_y \times \sin \omega_1 t$, $z_a = B_z \times \cos \omega_1 t$, where A_y and B_z - the absolute amplitude of vibration of the rotor in horizontal and vertical directions ω_1 - the oscillation frequency. Assumption that absolute motion trajectory of the center of mass of the rotor is close to elliptical, confirmed by the practice of exploitation of rotors and theoretical studies of their dynamics [1].

Equivalent stiffness of the support nodes of the rotor is determined in accordance with the formulas:

$$C_{\text{экв}}^{y} = \frac{\omega_1}{\pi A_y} \int_0^{\frac{2\pi}{\omega_1}} \Phi_y(y_a, z_a) \sin \omega_1 t dt,$$
$$C_{\text{экв}}^{z} = \frac{\omega_1}{\pi B_z} \int_0^{\frac{2\pi}{\omega_1}} \Phi_z(y_a, z_a) \cos \omega_1 t dt, \quad (3)$$

where $\Phi_y(y_a, z_a)$, $\Phi_z(y_a, z_a)$ - coordinate functions y_a, z_a determined from the system of differential equations (1).

The results of integration in (3) allow us to obtain the specified hardness as:

$$C_{\text{экв}}^{y} = \frac{C_y\left(mgr + C_z \cos\alpha_{\text{ст}} \times b \times z^2\right)}{D} + \frac{C_y^2 \cos\alpha_{\text{ст}} \times y \times q \times b^3\left(C_y^2 \times q^2 \times A_y^2 + C_z^2 \times z^2 \times B_z^2\right)}{8D^3},$$
$$C_{\text{экв}}^{z} = \frac{C_z\left(mgr + C_y \cos\alpha_{\text{ст}} \times b \times q^2\right)}{D} + \frac{C_z^2 \cos\alpha_{\text{ст}} \times y \times z \times b^3\left(C_y^2 \times q^2 \times A_y^2 + C_z^2 \times z^2 \times B_z^2\right)}{8D^3}, \quad (4)$$

where $b = \cos^2 \alpha_{st}(q + f \times z)$, $y = d(\alpha_{st}) + 3d\text{¢}(\alpha_{st})tg\alpha_{st} - 3d\text{¢}(\alpha_{st}) - d\text{¢¢}(\alpha_{st})tg\alpha_{st}$,

$$x = d(\alpha_{st})tg\alpha_{st} - 3d\text{¢}(\alpha_{st}) - 3d\text{¢¢}(\alpha_{st})tg\alpha_{st} + d\text{¢¢¢}(\alpha_{st}).$$

Analysis of (4) allows us to formulate conclusions similar to those previously considered special cases of the formulas of the first approximation for the equivalent stiffness of the rotor bearing assemblies.

From these relations it follows that equivalent stiffness are interrelated not only through the stiffness C_y, C_z corps support units of the rotor, but also by the amplitude A_y, B_z of its absolute radial oscillations.

An example of using the results could be the problem of forced oscillations of the rotor poles with gaps, arising from its static unbalance. Considering the rotor as a linear elastic supports, which are equal to the rigidity C_{equ}^{y}, C_{equ}^{z}, we write the wave equation in the form:

$$\begin{cases} m\ddot{y}_a + C_{\text{экв}}^{y} \times y_a = m \times e \times w^2 \sin wt \\ m\ddot{z}_a + C_{\text{экв}}^{z} \times z_a = m \times e \times w^2 \cos wt \end{cases}, \quad (5)$$

where e - eccentricity of the rotor, w- angular velocity of rotor.

For the amplitudes of the oscillations of the system (5) we obtain:

$$A_y = \frac{m \times e \times w^2}{C_{\text{equ}}^{y} - m \times w^2}, \quad B_z = \frac{m \times e \times w^2}{C_{\text{equ}}^{z} - m \times w^2}. \quad (6)$$

In (6) values C_{equ}^{y}, C_{equ}^{z} depend on the amplitudes A_y, B_z, so they should be regarded as a system of equations for these amplitudes.

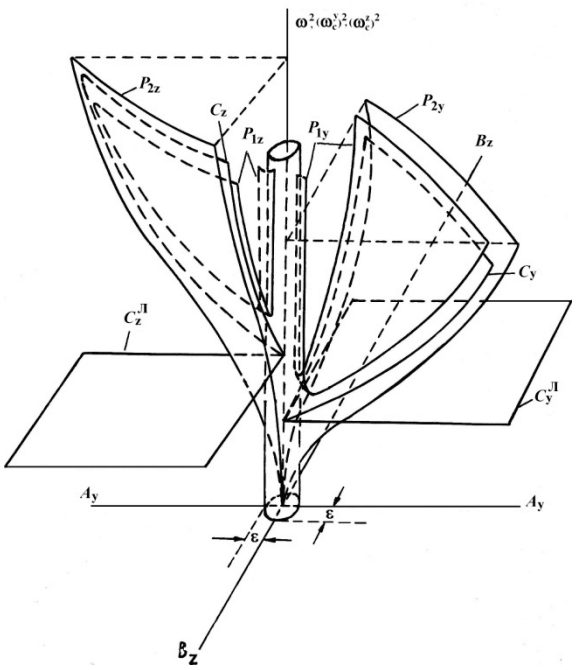

Fig. 2 Graphical representation of the dynamic characteristics of the absolute vibration of the rotor in the bearings with clearances.

Resonant, P_{1y}, P_{2y}, P_{1z}, P_{2z} and C_y, C_z the skeleton, the surface of the system, built on the assumption of independent changes in amplitudes A_y and B_z in accordance with (6) and relations $C_{\text{equ}}^y = m\left(\mathrm{w}_c^y\right)^2$, $C_{\text{equ}}^z = m\left(\mathrm{w}_c^z\right)^2$, are shown in Figure 2. The values w_c^y, w_c^z are the frequencies of free oscillations of the system. Skeletal surfaces are elliptic paraboloid.

Resonance and the skeletal surface, corresponding to vibrations of the rotor in horizontal and vertical planes, built in different coordinate octant. This figure also built the plane $C_y^Л$, $C_z^Л$, which are skeletal surfaces of the linear system, when in terms of equivalent rigidities are taken into account only the first terms, and shows that the frequency of free vibrations of a linear system does not depend on the oscillation amplitudes.

Since the amplitude of forced vibration A_y, B_z are interrelated, in order to establish their value, corresponding to a given frequency of disturbing forces w_0, we must build the plane $\mathrm{w}^2 = \mathrm{w}_0^2$ and on the lines of intersection of this plane with the surface P_{1y}, P_{2y} и P_{1z}, P_{2z} , and find relevant points with the same coordinates, which

will be the vibration amplitudes of the rotor . t is possible that the same frequency will correspond to several of these points and in this case in the system can be several modes of vibration, while some may be unstable, and with a sustainable mode of motion, the system can switch to another as a result of random addition of external influences. Such is the characteristics of nonlinear systems [3].

The growth of operating speeds of rotary machines, the requirements of the stability of their vibration characteristics and dynamic functioning stipulate the importance of research objectives and to reduce fluctuations in nonlinear mechanical systems of these machines.

Literature:

1. Kelzon A.S. Rotors dynamic in elastics bearings / A.S. Kelzon, Yu.P. Tsimansky, V.I.Yakovlev. - Moscow: science, 1982–page 280.

2. Wolfson I.I. Nonlinear tasks of the machines dynamic / I.I. Wolfson, M.Z. Kolovskiy. - Leningrad: mechanical engineering, 1968–page 284.

3. Vibrations in technique. Directory in the 6-th V.: mechanical engineering, 1979-V.2. Oscillations of nonlinear mechanicals system. Edited by Blekhman I.I. 1979–page 351.

CID: J21208-490

UDK 621.01

Balakin P.D., Shamutdinov A.H.

SCHEMATIC MEHANISM OF SPATIAL ROCKER

Omsk State Technical University

In this report we describe the schematic spatial manipulator of general type with six independent partial motions.

Keywords: arm, mobility, driving the partial movements.

1. The urgency of the problem

As is well known [1-3] for the automation of certain manufacturing operations,

the empowerment process equipment, and other widely used mechanisms of spatial manipulators with advanced drive system. Recently, these manipulators have a digital motion control system of executive that gives any kind of movement and change its characteristics. However, the complexity of the control system is largely dependent on the circuitry of the manipulator, since the partial motion of the individual drives are connected. In this context, the problem of finding manipulator circuitry of the general form of independent partial motions, in order to simplify the management executive movement, is urgent.

2. A spatial mechanism

It is proposed schematic of the manipulator in a spatial mechanism with mobility equal to six (**Fig. 1**).

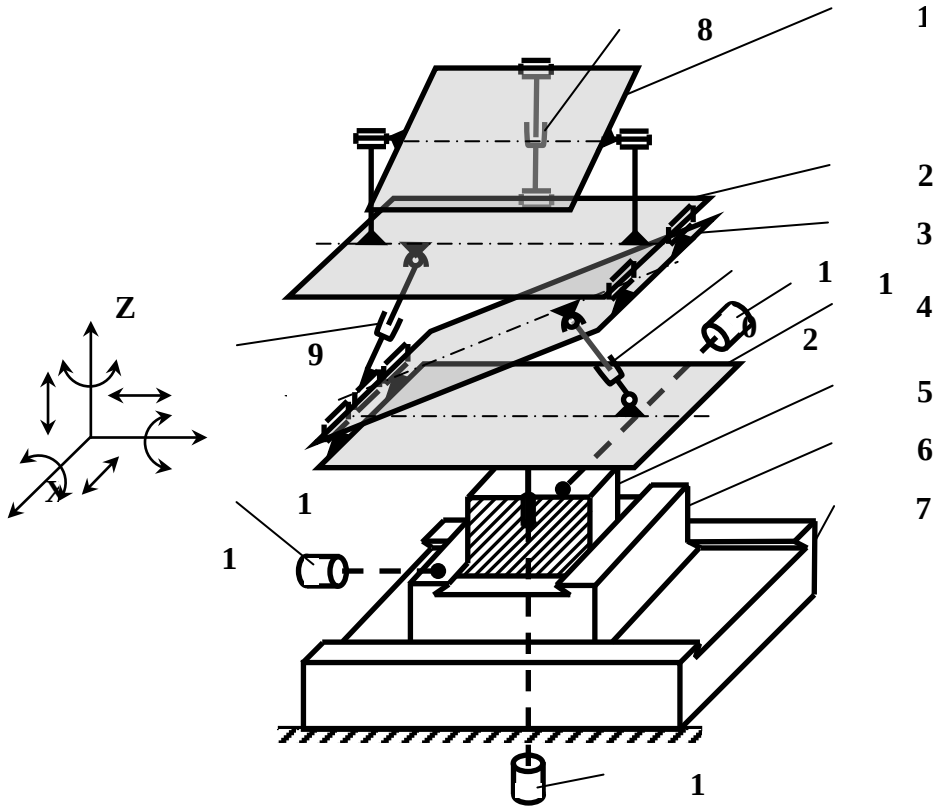

Fig. 1. A spatial mechanism

Positions in Fig. A.:

1-link setup (desktop), 2-support-rotating device;

3-inclined platform, and 4-povortny table; 5 transverse carriage, the carriage longitudinal 6-and 7-bed (base), 8, 9 and 10 drives the progressive movement, as a rule of hydro-and electro-motors, 11, 12 and 13 electro-motors translational motion

and rotation of the table 4.

The mobility of the mechanism defined by the formula Somov-Malyshev [4]:

$$W = 6n - 5p_5 - 4p_4 - 3p_3 - 2p_2 - p_1, \qquad (1)$$

where n-number of moving parts, pi - the number of kinematic, respectively, the i-th class. From **Fig. 1** we see that n = 6, p5 = 6, p4 = p3 = p2 = p1 = 0. Then the mobility of the mechanism of the formula (1) will be: $W = 6 \cdot 6 - 6 \cdot 5 = 6$

Feature of the circuitry is to achieve forward movement along the Z axis by adding the two opposing rotations of units 2 and 3 [5], whereas the separation of the angular motion of these residues leads to the rotation of the executive body of the axis X.

3. The elements of the kinematics of the translational motion of the proposed drive mechanism

With the unification of all drives forward movement, the design scheme of the kinematic characteristics of the transformation of motion reduces to modeling relationships in a mutable "triangle", one side of which changes its size and structurally executed, for example, a hydraulic cylinder with a rod (**Fig. 2**). Of interest are the two characteristics of motion, namely: 1) a change in α and $\dot{a}$ for l = var, and $\frac{dl}{dt} = const$ 2) change of z and $\dot{z}$ for the addition of two counter-rotation at $\frac{dl}{dt} = const$, where α and $\dot{a}$ −, respectively, the angle of rotation, and the rate of change of this angle with time inclined platform 3, l − length of the rod 10, z and $\dot{z}$ − respectively, the vertical coordinate of the point to the platform 3 and the rate of change of the point.

From **Fig. 2** well-known theorem we have:

$$l^2 = a^2 + b^2 - 2a \cdot b \cdot \cos\alpha,$$

hence,

$$a = \arccos\left(\frac{a^2 + b^2 - l^2}{2ab}\right) \qquad (2)$$

with $a = const$, $b = const$.

Assuming that $l = V \cdot t$, ie change in the total length l of hydraulic cylinder piston rod is at a constant rate, ie $V = const$, expression (1) can be written:

or in generalized form $\alpha = arcos\ (m - n \cdot t^2)$, (3)

where $m = \left(\frac{a}{2b} + \frac{b}{2a}\right)$ and $n = \frac{V^2}{2ab}$

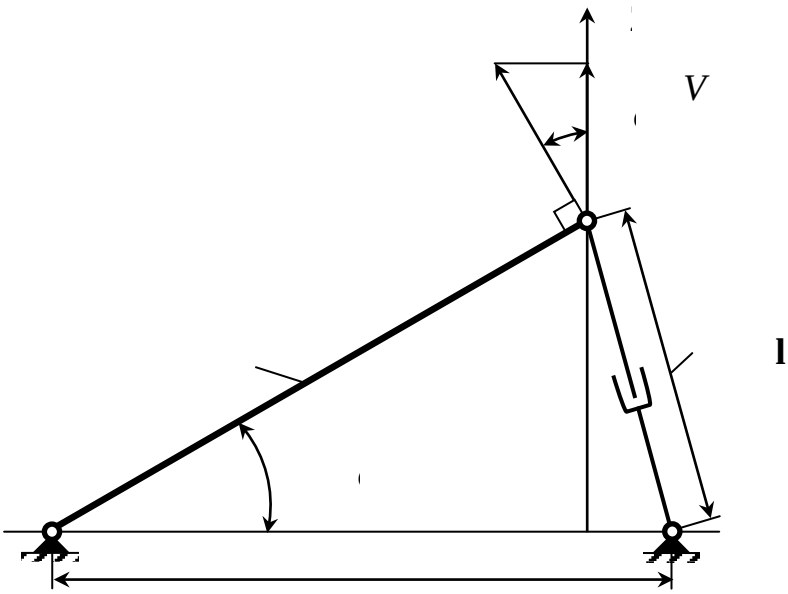

Fig. 2. Design model of a variable triangle mechanism for l = var

Choosing the design parameters so that $a = b$, expression (3) becomes:

$$\alpha\ (n, t) = arccos\ (1 - n \cdot t^2) \quad (4)$$

Denote the $w = \frac{da}{dt}$ − angular velocity of the inclined platform 3 (**Fig. 1**) or OK (**Fig. 2**). Differentiating (3) in time t we find:

$$\frac{da}{dt} = \frac{d\left(\arccos\left(1 - n \times t^2\right)\right)}{dt} = -\frac{-2n \times t}{\sqrt{1 - \left(1 - n \times t^2\right)^2}} = \frac{2n \times t}{\sqrt{2nt^2 - n^2 \times t^4}} = \frac{2n}{\sqrt{2n - n^2 \times t^2}}$$

or $$w(n,t) = \frac{2n}{\sqrt{2n - n^2 \times t^2}} \quad (5)$$

Using the software package MathCAD 14, give the dependence of the expressions (4) and (5), which are presented in **Fig. 3** and **Fig. 4**.

In analyzing these schedules, depending on the parameter n and time t is clear that:

1. with increasing n, and, consequently, increasing the rotation speed V platform is faster;
2. dependence of $\alpha\ (n, t) = arccos\ (1 - n \cdot t^2)$ with $n = 0{,}01 - 0{,}05\ sec^{-2}$ and $t \leq 5{,}4$ sec, almost linear;
3. in the operating range of variation of the angle $\alpha = 0\ ° - 45\ °$ and the angular velocity of the inclined platform 3 is changed slightly.

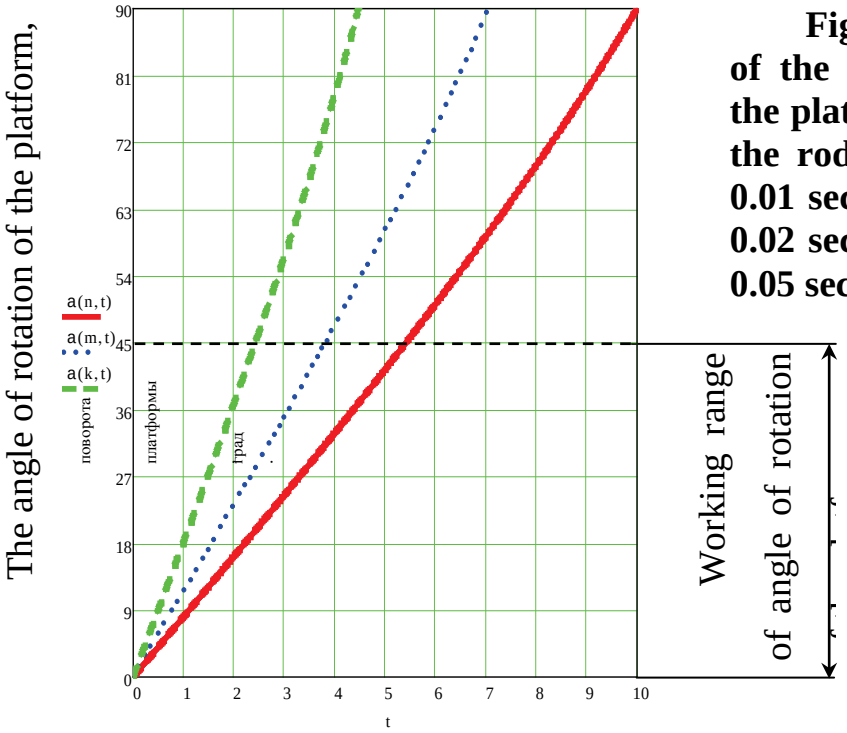

Fig. 3. The dependence of the angle of rotation of the platform and then move the rod: curve 1, with n = 0.01 sec^{-2}, curve 2, with n = 0.02 sec^{-2}, curve 3, with n = 0.05 sec^{-2}

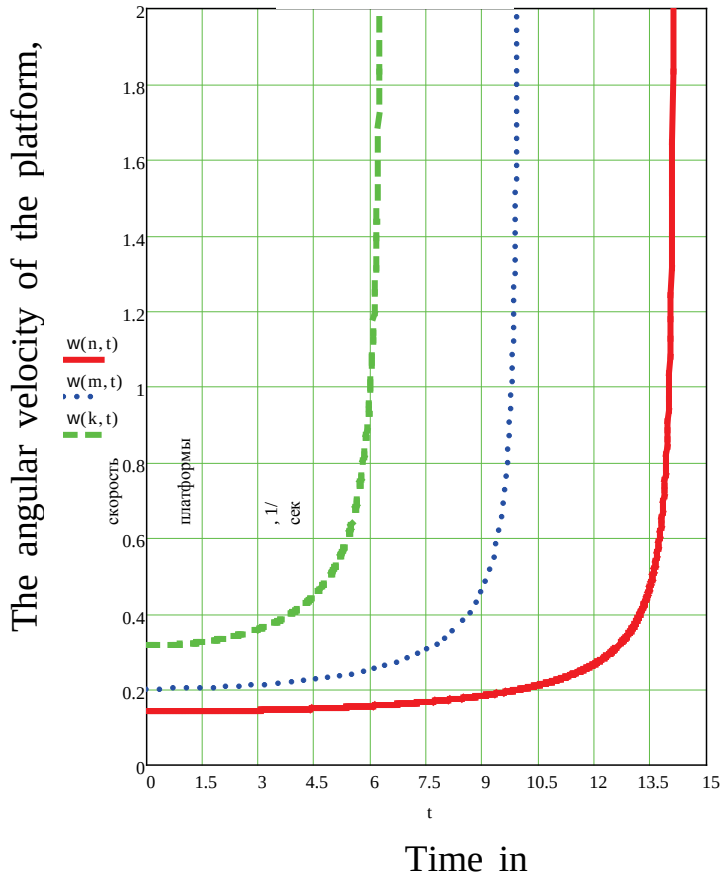

Fig. 4. The dependence of the angular velocity of the platform and then move the rod: curve 1, with n = 0.01 sec^{-2}, curve 2, with n = 0.02 sec^{-2}, curve 3, with n = 0.05 sec^{-2}

Conclusions:

1) Proposed schematic mechanism extends the capabilities of the device manipulated in

space, by providing a degree of mobility of the six coordinates on the basis of kinematic decoupling;

2) Provides a schematic of the executive's independence movement, including the independence of the partial sequence of execution of movements.
3) At a constant velocity of the rod hydraulic platform rotation angle of incline, the operating range, varies almost linearly in time, i.e. angular velocity of the platform is practically constant.
4) This scheme allows the robot arm mechanism for maximum unification of communications links and drives partial movements.

References:

1. Manipulation of robots / A.I. Korendyasev [and others]; under Society. Ed. A.I. Korendyaseva. - Moscow: Mashinostroenie, 1989. - S. 472.
2. Glazunov, V.A. Spatial Parallel Mechanisms / V.A. Glazunov, A.S. Koliskor, A.F. Krainev. - Moscow: Nauka, 1991. - S. 95.
3. Alvan, H.M. On the spatial motion control platform with multiple degrees of mobility / H.M. Alvan, A.V. Sloushch // Theory of mechanisms and machines. - St. Univ. St. Petersburg State University. In 2003. - № 1. - S. 63-69.
4. Artobolevsky, I.I. Theory of mechanisms and machines / I.I. Artobolevsky. - Moscow: Nauka, 1975. - S. 638.
5. Lyukshin, V.S. Theory of helical surfaces in the design of cutting tools / V.S. Lyukshin. - Moscow: Mashinostroenie, 1967. - S. 372.

CID: J21208-616

UDK 621.883

Krasovskij S.S., Borisenko A.V., Kovalyova N.I.

CALCULATION OF THE EFFORTS AND THE MOMENTS OF THE INHALING PROVIDING THE DENSITY OF JOINTS OF FLANGED CONNECTIONS

The Donbass state engineering academy

In given article the analysis of the processes occurring at the inhaling of flanged carving connections is considered. Settlement parameters of carving connections are specified.

Keywords: carving connections, connection of flanges, effort of an inhaling, the inhaling moment.

Calculation of optimum efforts of the inhaling providing density of a joint of knot of consolidation, is a difficult task and depends on many factors, such as the design of knot of consolidation, a lining material, diameter of a flange etc. [1].

The purpose of the given work is the analysis of the processes occurring in the collected package at the inhaling of the flanged carving connections and the specification of their settlement parameters.

The effort of the inhaling should be appointed such that at the set external loading the joint remained dense [2]. Taking into account the condition of the undisclosed joint the settlement dependence of the full effort operating on a bolt (hairpin), is defined under the formula:

$$Q = Q_0 + Q_t + cN, \tag{1}$$

where Q_0 - effort of an inhaling;

Q_t - temperature effort (in the presence of temperature deformation);

N - the external loading operating on a bolt;

χ - factor of the basic loading.

In the presence of temperature deformation Δt at the expense of linear expansion of the intermediate details and a bolt there is a temperature effort

$$Q = \frac{D_t}{l_б + l_д}, \tag{2}$$

where $\lambda_б$ - factor of a pliability of a bolt;

$\lambda_д$ - factor of a pliability of pulled together details.

External loading N causes additional lengthening of a bolt on size $\Delta\ell$ and the effort increases in a bolt on size

$$N_б = \frac{D\ell}{\ell_б}, \quad (3)$$

and the force operating on intermediate details, decreases for size

$$N_д = \frac{D\ell}{\ell_д}. \quad (4)$$

Therefore the additional effort to a bolt will be equal

$$N_б = \frac{\ell_б \times \ell_д}{\ell_б + \ell_д} \times N = cN. \quad (5)$$

In all responsible carving connections it is necessary to supervise the size of the effort (pressure) of an inhaling [2].

In mechanical engineering the method most precisely supervising effort of an inhaling, based on gauging of lengthening of a bolt (hairpin) is extended.

The effort of an inhaling defines on a difference of size of base of measurement before and after an inhaling $\Delta\ell$:

$$D_з = \frac{D\ell}{\ell_б}, \quad (6)$$

For a bolt of a constant section the value $\lambda_б$ is defined under the formula [1]:

$$\ell_б = \frac{\ell_б}{E_б \times F_б}, \quad (7)$$

and for bolts of a variable section - under the formula

$$\ell_б = \frac{1}{E_б} \sum_{i=1}^{n} \frac{\ell_{б_i}}{F_{б_i}}, \quad (8)$$

where $\ell_б$ and $F_б$ - settlement length and the area of cross-section section of a bolt of constant section;

$\ell_{б_i}$ and $F_{б_i}$ - accordingly the length and the area of cross-section section i-th site of a bolt of variable section;

$E_б$ - the module of elasticity of a material of a bolt.

For short bolts (ℓ <6d) the pliability factor should be calculated taking into account a pliability of a carving within connection and a pliability of a head of a bolt

$$\lambda_б = \frac{1}{E_б}\sum_{i=1}^{n}\frac{l_{б_i}}{F_{б_i}} + \lambda_р + \lambda_г, \qquad (9)$$

Where the carving pliability $\lambda_р$ can be calculated under formulas

At $\frac{d}{p} = 6 \div 10$ $\lambda_р \approx (0{,}95 \div 0{,}80)\frac{1}{dF}$

At $\frac{d}{p} = 10 \div 20$ $\lambda_р \approx (0{,}80 \div 0{,}70)\frac{1}{dF}$ (10)

(here p - a carving step);

The factor of a pliability of a head of a bolt in height h is defined

$$\lambda_г = \frac{0{,}15}{E_б h}. \qquad (11)$$

The factor of a pliability of pulled together details of any thickness is defined under the formula

$$\lambda_д = \frac{1}{Ed_0}\lambda^*_д, \qquad (12)$$

where d_0 - diameter of an aperture under a bolt;

$\lambda^*_д$ - dimensionless factor.

The effort of tightening of the flanged bolts, providing the tightness of the connection with flat linings (fig. 1) is recommended to conduct under the formula

$$Q_з \geq K\left[(1-\chi)\frac{pD_{ср.п}}{4}P + P_{уп}\right], \qquad (13)$$

where К=1,0 … 1,4 - the factor, which great values are accepted for metal linings and for the linings which are exposed to frequent influence of repeated loadings at raised temperatures; for rubber linings К=1;

χ - the factor of the basic loading showing, what part of external loading is perceived by fixing details;

$D_{ср.п}$ - Average diameter of a lining;

P - pressure of environment, Н/мм2;

$P_{уп}$ - effort to a lining, necessary for maintenance of density of a joint.

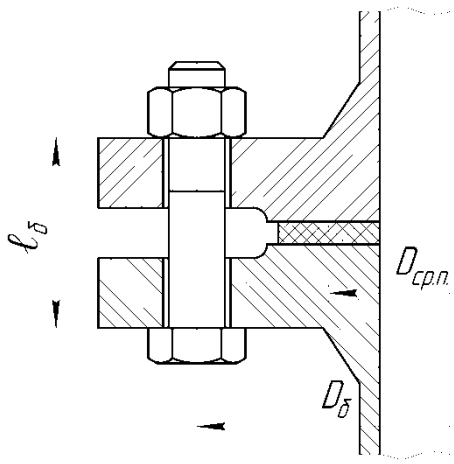

Fig. 1. Connection with flat linings

The effort of consolidation of a lining is defined under the formula

$$P_{уп} = pD_{ср.п} \times b \times q_0, \quad (14)$$

where b - width of a lining, $b = \frac{S}{4}$, where S - width of a ring groove;

q_0 - pressure upon contact surfaces of a lining.

Pressure of an inhaling of fixing details, provides density of a joint taking into account (13) and (14) is defined under the formula

$$s_з = \frac{KD_{ср.п}}{z \times d_1^2}\left[(1 - c) \times D_{ср.п} \times P + Sq_0\right], \quad (15)$$

where z - quantity of bolts;

d_1 - internal diameter of a carving of a bolt.

The inhaling moment is the basic settlement size necessary for the designing of hydraulic screwdrivers which can be defined under the approached formula [3, 4]

$$M_{кл} = K_{кл} \times d \times Q, \quad (16)$$

where $M_{кл}$ - the inhaling moment on a key;

Q - effort of an inhaling;

d - diameter of a carving;

$K_{кл}$ - the factor depending on a condition of a surface of a carving of a bolt and a nut.

Value of factor $K_{кл}$ has been defined by carrying out of experiments on natural

samples of flanged connections. As a result of processing of experimental data values for the carving connections having a satisfactory condition of a carving are received.

So at unbolting $К_{кл}$=0,22, at inhaling $К_{кл}$=0,11.

Conclusions:

The analysis of experimental data shows, that dependence (16) is not a steady one. In this connection at calculation of the moment of an inhaling usually the formula is accepted

$$M_{кл} = h \times K_{кл} \times d \times Q, \quad (17)$$

where η - the factor of a stock equal 1,3.

Literature:

1. Красовский С. С. Механизация сборки резьбовых соединений в машиностроении: теория, исследования, технология, конструкции: монография / Красовский С. С. – Краматорск: ДГМА, 2011. – 148 с. ISBN 978-966-379-515-7.

2. А. Н. Биргер, Б. Ф. Шорр, Г. Б. Иосилевич. Расчет на прочность деталей машин. Справочник. – М.: Машиностроение, 1979.

3. Красовский С. С. Анализ методов механизации сборки крупных резьбовых соединений металлургического оборудования / С. С. Красовский, В. В. Хорошайло, С. А. Бабенко // Восточно-Европейский журнал передовых технологий. 6/7 (54) 2011. С. 14-16.

4. А. с. 1618615 (СССР). Рычажный гайковерт для затяжки резьбовых соединений / Бузунов В. Н., Красовский С. С., Славутский Г. Д. – Опубл. в Б.И. – 1991. – № 1

CID: J21208-722

UDK 621.002.2 + 621:681.3

Visogorets Y.V.

OPTIMUM POINTS OF CROSS-SECTIONS QUANTITY SEARCH AT ACCURACY FORM AND THE RELATIVE POSITIONING OF THE SURFACE PARAMETERS CALCULATION

Russia, South Ural State University, Branch in Miass city

This report describes questions of the optimum search: 1) numbers of details cross-sections points at determination of a form and a relative positioning of surfaces accuracy parameters, such as nonroundness, radial palpation and others, 2) a method of accuracy parameters calculation.

Keywords: accuracy of a form, accuracy of a relative positioning, nonroundness, radial palpation, control.

When high-quality details «solid of revolution» type are supervised usually considered not only the linear/diametrical sizes, but also a form and relative positioning of surfaces accuracy parameters, for example: nonroundness, non-axiality, radial and face palpation, etc.

Ways of form and relative positioning parameters determination with universal devices, such as a calliper, a micrometer, a nutromer with use of information on small quantity of points of sections are inexact (fig. 1) [1]. For example: the method of "triangle" used at definition of nonroundness; the method of cylinder- deviation on three cross-sections definition, etc.

There are also some opposite practicians: when in cross-sections thousands of points (control with CMM and accompanying software) are considered.

During some digital, software and natural experiments (fig. 1, 2) [1] was defined that the methodical error component for diameters 10-100 mm doesn't exceed 0,001 mm at quantity of cross-section points 60-80, thus, by consideration of 100 points this component it will be guaranteed essential less than 0,001 mm.

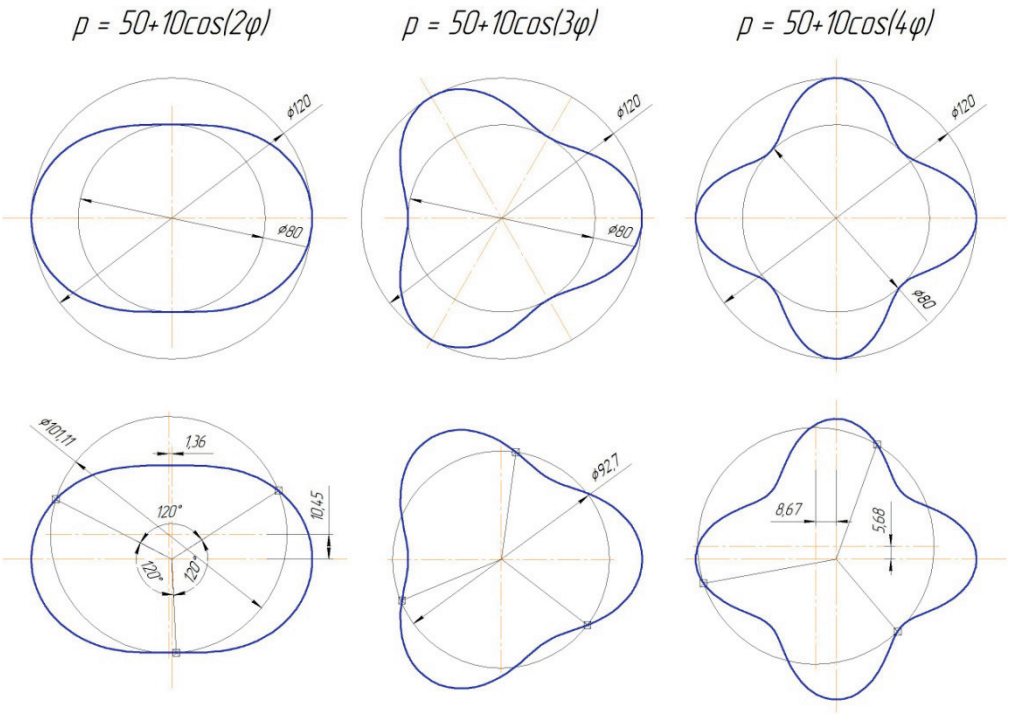

Fig. 1. Search in three casually chosen points of a contour

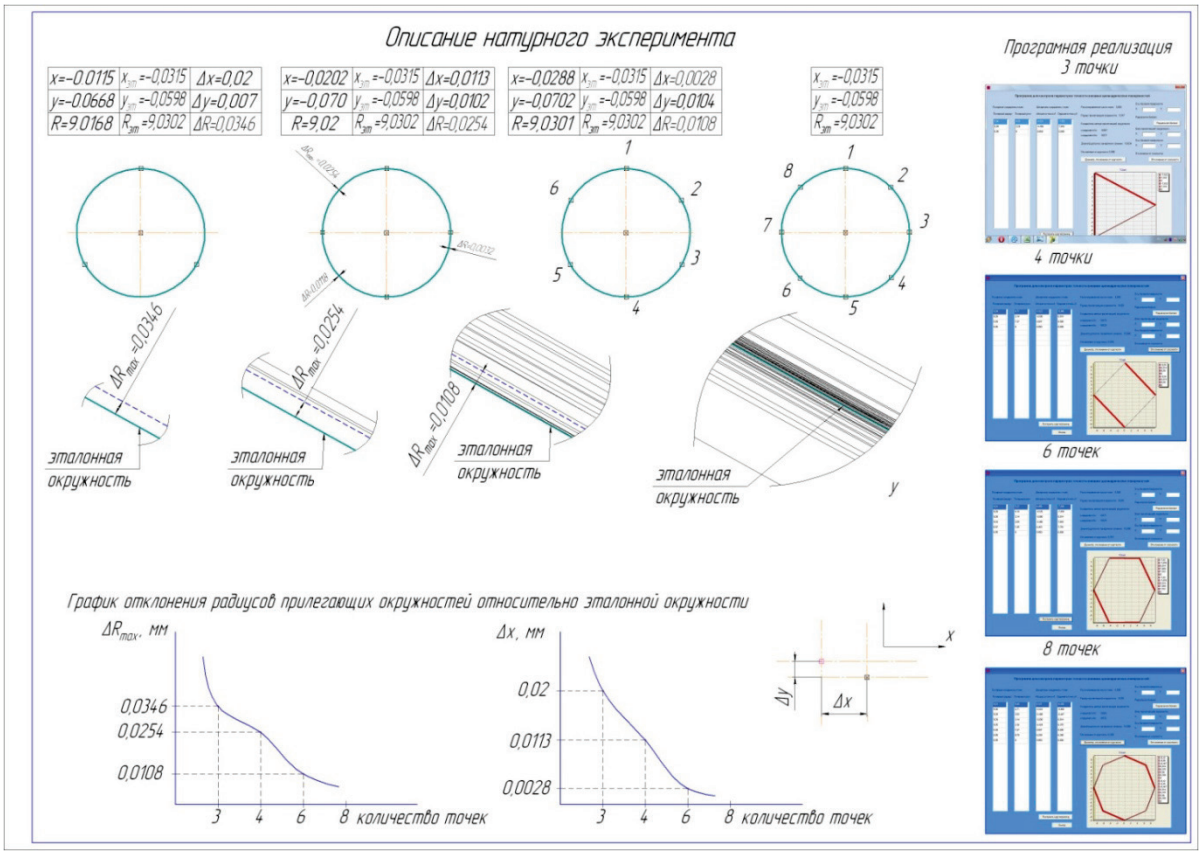

Fig. 2. Software and natural experiments results

When large number of points is considered it is very important what method is applying to search the results. CMM mainly using alignment of curves and surfaces

methods (fig.3), what contradicts to metrology theory. Metrology is using extreme (adjacent) curves and surfaces to determination of a form and a relative positioning of surfaces accuracy parameters [2]. This discrepancy is reason of additional methodic error component appearance.

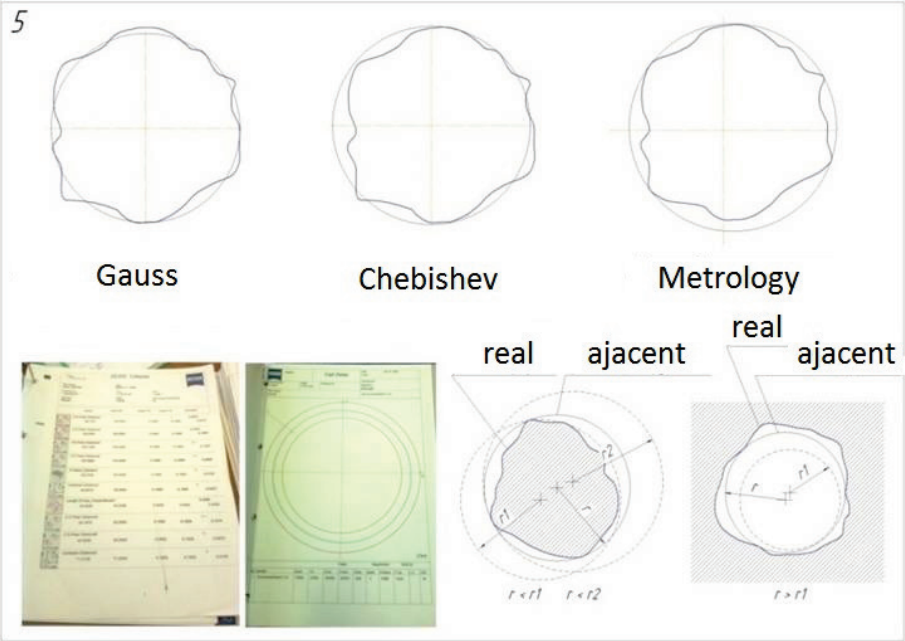

Fig. 3. Methods of curves determination for nonroundness calculation

On the basis of the carried-out researches at control of details of quality 6-7, recommended number of points in sections — 100, a recommended technique — determination of accuracy parameters in according with metrology theory, i.e. on the basis of adjacent curves/surfaces data [1, 2].

References:

1. Visogorets Y.V. Group precision parameters of cylindrical and butt surfaces details control methodic / Y.V. Vysogorets, N.A. Chemborisov // Irkutsk State Technical University messenger №12 (59), 2011 (ISSN 1814-3520). – P.20-26.
2. Machine-building. The encyclopedia in 40 t. / Edition council: K.V.Frolov, etc. Measurements, control, tests and diagnostics. III-7 / V.V. Klyuyev, F.R.Sosnin, V.N.Filinov, etc.; under general V.V.Klyuev's edition, – the 2nd prod., reslave and additional. Moscow: Mechanical engineering, 2001. – 464 p.

CID: J21208-325

Reshetnikova O.P., Korolev A.V.

THE PROGRESSIVE TECHNOLOGY OF GRINDING OF TOROIDAL SURFACES

Saratov state technical university, Saratov, Russia

The perspective technology of grinding of toroidal surfaces by the grinding wheel is considered. In machining by such method the wheel dressing can be fabricated after several parts cutting. The given method raises considerably the productivity of the released products.

Key words: grinding, toroidal surfaces.

The most widespread mode of definitive handling of exact details, type of bearing rings of is grinding. It, first of all, speaks that it is possible to ensure with an abrasive tool the highest exactitude and a minimum roughness of details surfaces from different alloys. The efficiency of the use of abrasive grains in a wheel is rather low. The fraction of grains deleted by the dressing can reach 90 % and more from total in a working stratum. The necessity for a wheel dressing arises because of the loss of working capacity of a working surface of the wheel. In modern manufacture it is possible to update the whole working surface by the wheel dressing, deleting a considerable part of turned out abrasive grains.

Special complexity is represented by the grind of face contours. Usually such surfaces are grounded by periphery of a grind in term of a disk (fig. 1).

For the demanded accuracy of handling, the grinding of these surfaces is carried out with a circle of a small diameter that leads to its increased wear, the necessity of the correction after each finished part and to the frequent substitution of the wheel. It reduces sharply the production efficiency.

On the department of the “Mechanical engineering” of the Saratov state technical university the perspective technology of contoured surfaces grinding like roller ways of rings of axial bearings by the cup grinding wheel back is developed (fig. 2).

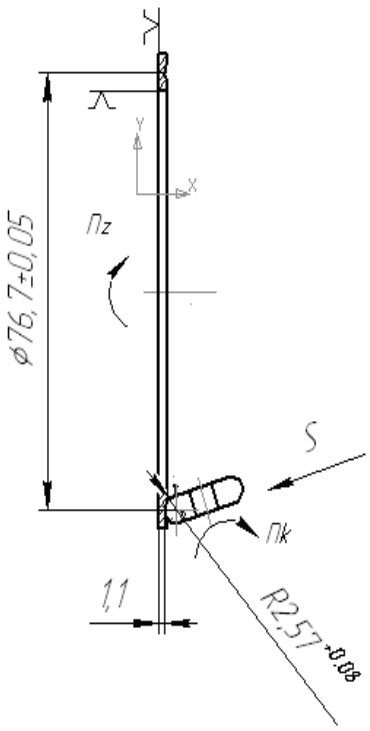

Fig. 1. The traditional scheme of the grinding of the bearing races by the grinding wheel face in the form of a disk

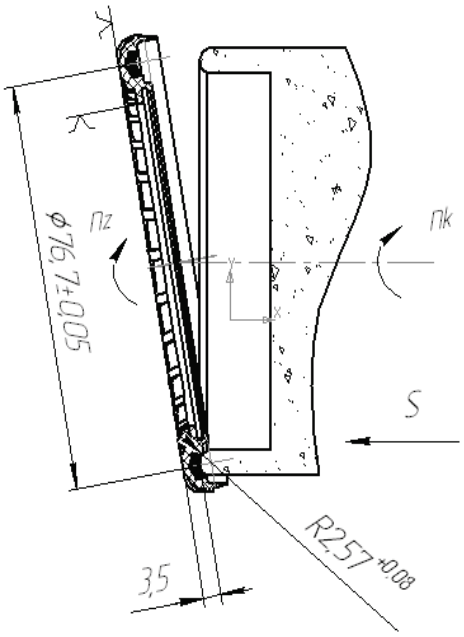

Fig. 2. The perspective technology of contoured surfaces grinding like roller ways of rings of axial bearings by the cup grinding wheel back.

In comparison with a disk grinding wheel cup grinding wheel has the bigger size of a working surface therefore its wear decreases and there is a possibility of the

wheel dressing of a circle after several part cutting. The wheel works long time without substitution. For the improvement of chip removal conditions, temperature lowering in the grinding area, reduction of the work pieces deformation, surface tempering when operated a circle block are artificially reduced the contact zone of the wheel with the work piece by leaning materials.

Experimental researches of the grinding were conducted on the scientific and manufacturing enterprise «Non-standard products of machine building», SSTU.

For deriving of the mathematical model of the process of grinding of bearing races of axial bearers the method of complete multifactor experiment was used. For optimization parameters were accepted the radius of the bearing races R and the depth of bearing rings h, and for factors were taken the grindstone supply *s*, the dwelling period of a grindstone *t*, the work rotational speed *n* at handling of bearing rings. In the research techniques interpolational models were taken, which express power dependence of output parameters on adjusting factors of the process.

Grinding of bearings races was conducted on the modernised internal bore grinder TPK-125. Refrigeration was carried out with 5 %' solute of NGL-25 in the water.

After handling of the results we have received the following mathematical models:

for the radius of the bearing race *R*:

$$R(S,t,n) := 1.26 \times S^{-0.026} \times n^{0.089} \times t^{0.268-0.039 \times \ln(n)} \quad (1)$$

for the dept of the ring *h*:

$$h(S,t,n) := 4.3 \times S^{0.402-0.057 \times \ln(n)} \times t^{0.135+0.0069 \times \ln(S)} \times n^{-0.031-0.016 \times \ln(t)} \quad (2)$$

On the ground of the received correspondences graphs have been constructed. Let's exemplity some of them.

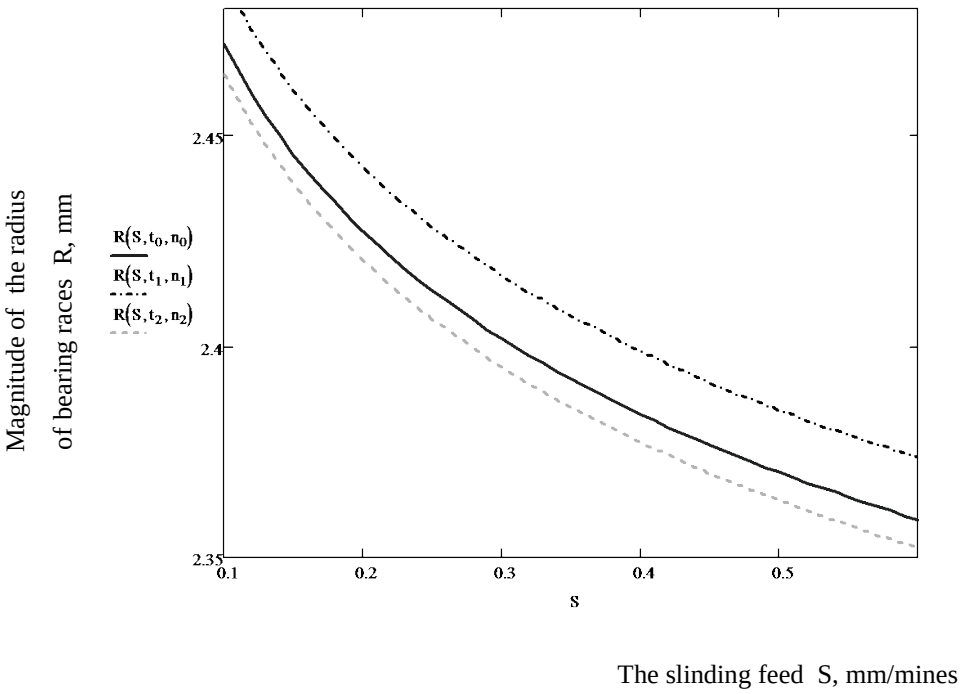

Fig. 3. Dependence of the radius of the bearings race as result of the at change of the sliding feed S at the fixed values *t, n*.

The reason is that by increasing the feed the load on the practical of the grinding stone grows, the grinding stone starts to degrade intensively on the periphery, which reduces the radius of the bearing race. Uneven wear on the grinding stone is due to uneven distribution of allowance along the profile of the bearing race. On the periphery of the bearing race pattern the bulk is greater and therefore the wear of the grinding stone is more intense on the periphery of the pattern of races.

On the ground the aforesaid it is possible to draw a conclusion that the offered method of grinding of tracks of bearing races is perspective. On the given method an application for a patent was filed. Mathematical models pieces of the dependence of geometrics on the machining conditions were offered.

CID: J21208-006

S. Krasovskii, V. Khoroshailo, V. Kovaljova, E. Ladyga

THE ANALYSIS OF EXISTING OF PERCUSSIV-IMPACT MECHANISM

Donbass State Engineering Academy

The analysis of the existing of percussive-impact mechanism due to the different criteria has been carried out. A new classification, which systematizes the shock-impulse mechanism, permitting to choose the optimal construction of a screw-driver has been proposed. The constructions of screwdrivers realizing different schemes of percussive-impact mechanism have been considered and the recommendations for their use have been given.

Key words: screwdriver, percussive-impact mechanism, hammer ram, anvil, construcyion, tightening, draving gear.

As the criterion of division of mechanisms into classes various factors are being chosen such as: a drive type, a kind of movement of the drummer, a sort of energy accumulated by the drummer, the force providing gearing of the drummer with an anvil, a way of management of a blow etc.

Taking into account the way of management of the blow, all designs of the-percussive-impact mechanisms are divided into five groups. Such classification allows to estimate qualitatively the designs of the percussive-impact mechanisms of each group and to choose the optimal scheme of the screwdriver with percussive-rotary action for assemblage of large carving connections.

The most simple ones are the percussive-impact mechanisms of the first group in which there is no feedback of the speed and of the relative position.

In mechanisms of the second group the feedback of the speed is carried out by means of a blow control.

However the designs of these srewdrivers do not exclude the edged blows of the drummer on an anvil that demands the reduction of a relative speed of the impact for the purpose of increasing of the the term of their service.

The widest use in modern screwdrivers of the impulse-rotary action was received by the mechanisms of the third group which have a feedback between the drummer and an anvil by relative position. This group of mechanisms, as well as previous, consists of a control mean of the speed of an impact, the drummer and an anvil. Besides, designs of this group have the device tracing the position of the drummer and anvils at their impact. A design of the impuct-rotary mechanisms of the third group is various, the core, that unites them, is a kinematic communication between the drummer and an anvil.

Unreliability and fragility of kinematics limits the application of the mechanisms of the third group of screwdrivers for the assemblage of large carving connections. For large carving connections it is possible to consider as the most effective ones the mechanisms of the fourth group which have a feedback of a relative position and a speed and intermediate elements of impact. Presence of intermediate elements at impact of the drummer and an anvil allows to avoid eged blows in mechanisms of the fourth group, raises their reliability.

Results of researches of the impulse-rotary screwdrivers on durability show, that all of them fail through 10 … 20 thousand cycles due to the rupture.of a striking group. The reason - their direct shock interaction. Taking into account this circumstance, the design of a percussive-impact mechanism has been developed, allowing to exclude a shock interaction of the drummer on an anvil, that, in its turn, considerably raises the service life of a srewdriver. It is a percussive-impact mechanism of the fifth group. In this group of mechanisms the impulse from the drummer to an anvil is transferred by means of the liquid environment. Except all other advantages these designs allow to raise considerably the power characteristics of a srewdriver, owing to the absence of direct contact of the drummer and an anvil that allows not to limit speed of dispersal of the drummer.

CID: J21208-655

UDK: 669.162

Petelin A.L., Mikhalina E.S., Novikov A.A., Apyhtina I.V.

PENETRATION KINETICS OF LIQUID METAL IN SOLID POLYCRISTALLINE METAL

National University of Science and Technology "MISIS" (MISIS)

This work is about penetration kinetics of Bismuth Melt into Copper Polycrystalline Structure.

Keywords: Bismuth, Polycrystalline Structure, kinetics

Introduction. The problem of solid-liquid metal phases interaction described in several tens of theoretical and experimental researches [1,2].

It is well known that liquid-metal grooves formation occurs on the liquid-solid interface at the exiting places of grain boundaries (GBs). This effect can lead to the solid metal embrittlement. The samples destruction along GBs was observed on copper (solid) - bismuth (liquid) system [3].

In polycrystalline samples the wetting GBs transformation is a complex process, which occurs in the area near the wetting temperature – T_w. The triple junctions (TJs) as a GBs are subject to wetting transformation. The spread velocity of the liquid phase along TJs is more than along grain boundaries [4].

Co-wetting of GBs and TJs in polycrystalline metal samples leads to formation and growth of a continuous liquid-metal channel net. The appearance of the liquid phase channels net was observed by GB wetting investigations of liquid bismuth interaction with polycrystalline copper samples [5]. However, until now there were not experimentally obtained kinetic characteristics of molten bismuth penetration into polycrystalline copper structure near the wetting temperature. The aim of present work is the experimentally research of the kinetics of liquid bismuth penetration into polycrystalline copper in the T_w temperature area.

Experimental part. For the experiments there were used high purity metallic materials, copper - 99.995 wt.% and bismuth - 99.999 wt.%. Copper samples were

the plates which were made on electro erosion machine ARTA 200-2. Plate's thickness was from 150 to 500 microns. The average grain size of copper samples was about 40 microns. It was achieved by pre-deformation and following heat treatment of cooper plates. Deformation of copper was carried out by upsetting (30 – 40 %) after which the samples had two-step recrystallization annealing. Annealing includes exposure for 15 min. at T_1=900 ºC and then holding for 120 min. at T_2=650 ºC. Isothermal exposures of copper samples in contact with liquid bismuth were carried out in the temperature range from 560 ºC to 590 ºC. The experiments were performed in the heating micro-furnace in thermal cell TS1500. This device is accommodated for observations of high-temperature processes in situ, i.e. directly during the heating. This method is used for the analysis the process of metal melt penetration along GBs in solid metal matrix for the first time.

All treatments were carried out in inert atmosphere - there was used Ar of high purity.

Bismuth appearance on copper's free surface was observed using a continuous visual microscopic analysis of the surface (using an optical microscopes LEICA-DMILM, LEICA-L2). After experiments copper samples were investigated by scanning electron microscope HitachiS-800, including using electron microprobe analysis. These results were confirmed the observation data of optical microscopy. The appearing points of bismuth on the free surface of the copper plates correspond to TJs in which there was happened through-penetration. This was confirmed by following chemical etching of the free surface. This fact indicates that the TJs are the fastest ways of the liquid phase penetration through a polycrystalline sample, as previously was noted in [6].

The appearance time of series of bismuth point's on the free cooper surface was fixed during the observation of bismuth penetration process through copper plates at each temperature. Such time was named through-penetration time (t) for definite experimental conditions.

Results. The experimental results for all temperatures conditions - through-penetration times t and the total average lengths of liquid bismuth channels h_1 which

were determined by measuring of the copper plate's thicknesses h with account of copper polycrystalline structure – are present in Table 1.

Under the assumption that the rate-limiting stage of channels formation has the diffusion nature there were made the estimations of the effective diffusion coefficients *D** by the correlation $h_1 \approx \sqrt{D^* \cdot t}$. The estimations of D* were made for all experimental temperatures (see Table 1). The base equation of the diffusion coefficient temperature dependence $D^* = D_0^* \exp\left(-\frac{E^*}{RT}\right)$, where E* - is the effective activation energy, D_0^* - is the effective pre-exponential factor, allows to estimate the E* with the help of graphic dependence $\ln D^*, \frac{1}{T}$ (Fig.1).

Table 1

The experimental results of liquid Bi spreading into polycrystalline copper structure

T, °C	h_1, μm	t, min	D^*, m^2/s
550	261	13	$8{,}7 \cdot 10^{-11}$
560	304,5	13	$1{,}2 \cdot 10^{-10}$
570	246,5	9	$1{,}1 \cdot 10^{-10}$
580	246,5	7	$1{,}5 \cdot 10^{-10}$
590	251	6	$1{,}9 \cdot 10^{-10}$

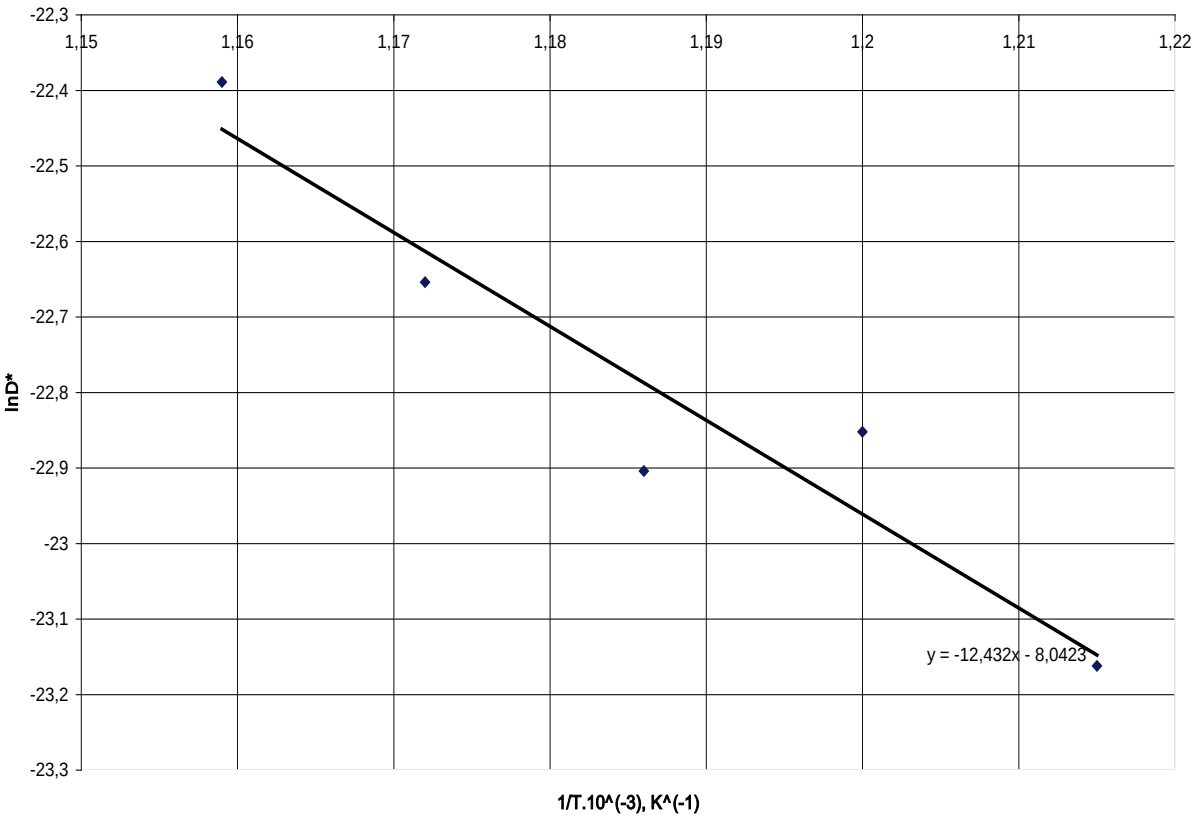

Fig 1. Estimation of E* with the help of linear temperature diffusion coefficient dependence

The effective activation energy (E*) was defined from the slope of the linear dependence. It's significant is equal 103 kJ/mol.

This value correlates with the activation energy of GB Bi-Cu hetero diffusion - 156.2 kJ/mol [7]. But obtained experimental data of activation energy is less than the activation energy of GB diffusion of bismuth in copper. This may be connecting with the contribution of the TJs bismuth diffusion in the copper polycrystalline samples.

References

[1] B.B. Straumal, Grain boundary phase transitions, Nauka publishers, Moscow, 2003.

[2] B.S. Bokstein, N.A. Dolgopolov, A.L. Petelin et al., Izvestiya vuzov tsvetnaya metallurgiya 6 (2006) p.42.

[3] Apykhtina I.V., Gulevskii S.A., Dolgopolov N.A., et al., Defect and Diffusion Forum. Vols. 237240 (2005). P.855.

[4] Gulevskii S.A., Emelina N.B., Petelin A.L., Russian Journall of Non-Ferrous Metals, Vol. 47, № 4 (2006) P.38.

[5] B.S. Bokstein, N.B. Emelina at al., Materiallovedenie, №8 (2007) P.13.

[6] S.A. Gulevskii, L.M. Klinger, A.L. Petelin, Tekhnologiya metallov, №8 (2007) P.13.

[7] Divinski S.V., Lohmann M., Herzig Chr., et al, Phys. Rev. B., Vol. 71 (2005). P. 104.

CID: J21208-654

UDK: 669.162

Mikhalina E.S., Petelin A.L.

INFLUENCE OF INDIUM ON PHASE TRANSFORMATIONS IN ALLOYS ON AN IRON BASIS

National University of Science and Technology "MISIS" (MISIS)

This work is about In influence on structure and phase transformation in alloys on Fe basis.

Keywords: Indium, phase transformation

Introduction. The sphere of practical use of In constantly extends last some tens years. As a result, the quantity of the secondary materials containing In, which can be processed by metallurgical methods, increases. As a microimpurity In gets to metal materials on an iron basis. At the same time, influence of In on structure and properties of such materials as steels, cast iron, etc. iron-containing alloys, still remains not studied.

Object, methods and results. In this work as object of research gray pig-iron has been chosen. Samples of alloys containing from 0,1 % to 10 % of In have been melted in the high-temperature vertical tubular electric furnace intended for carrying out of reactions of heterogeneous synthesis in the gas environment (in the given work

- in the environment of argon), using gray pig-iron.

Microscopic studying of structure of metal depending on quantity of In was spent. On fig. 1 and 2 the microphotos received at the content of In of 0,1 % (1) and 6 % (2) are presented. Increasing of In content in an alloy makes considerable impact on its structure, in particular the form of graphite inclusions is exposed to change. Micro XRF and the phase analysis of samples has shown that introduction of In in an alloy in amount up to 10 % in alloy doesn't lead to formation of an independent In phase, In passes in a firm solution.

Conclusions. The assumption of influence of diffusive mobility of In in volume and on borders of grains on a parity of structural components in the received samples is discussed.

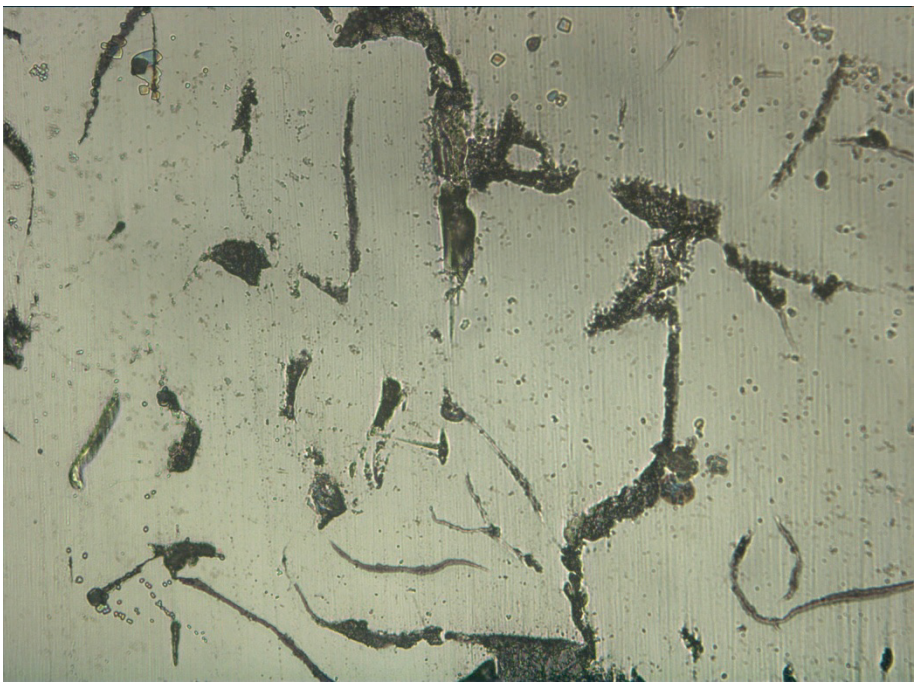

Fig 1. Microstructure of an alloy on the basis of the gray pig-iron containing 0,1% (weight) In

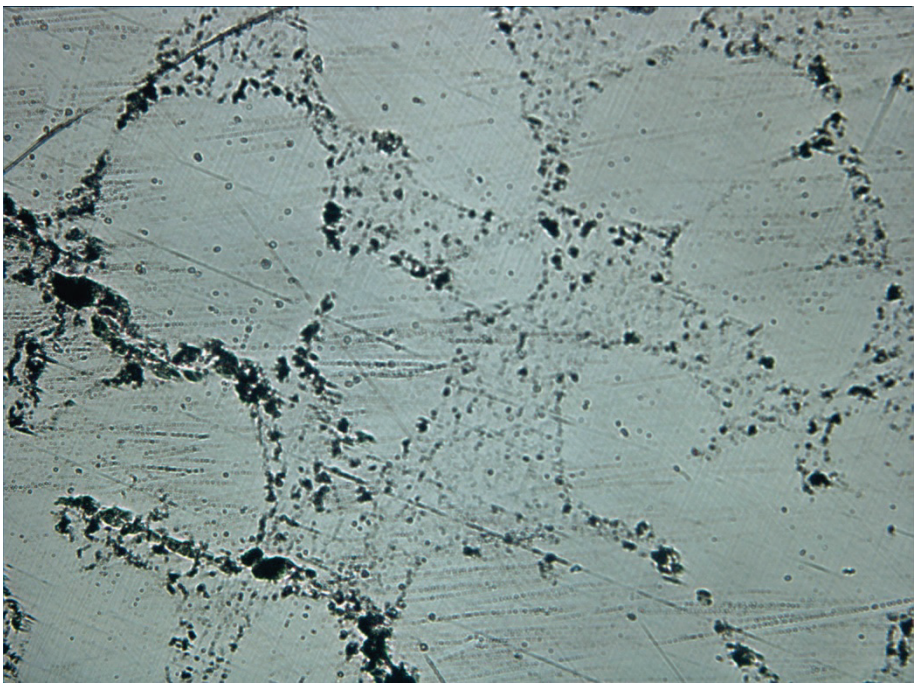

Fig 2. Microstructure of an alloy on the basis of the gray pig-iron containing 6% (weight) In (b), x500

CID: J21208-641

UDK 621.762

V.V. Malovik, V.V. Martynov, V.S. Panov,

L.V. Myakisheva, V.Y. Lopatin

THE INVESTIGATION OF INFLUENCE OF ALLOYING ADDITIONS ON STRUCTURE AND PROPERTIES OF UO_2-BASED FUEL PELLETS

Public Corporation "Engineering Plant", Elektrostal; National University of Science and Technology "MISiS", Moscow

The object of this investigation is study of influence of alloying additions $Al(OH)_3$ and TiO_2 on structure and properties of UO_2-based fuel pellets. It has been found that alloying addition incorporation enhances macro- and microstructure parameters of fuel pellets and influences positively on their properties, specifically, increases strength and thermal conductivity in lesser extent.

Key words: fuel pellets, uranium dioxide, aluminium hydroxide, titanium dioxide, properties, microstructure, porosity, strength, thermal conductivity, density.

In Russian Federation as well as in the majority of industrialized countries more and more attention is focused on problems of nuclear power engineering development as alternative to other power sources. The corresponding Federal Program provides achievement of 20 – 25 % of nuclear power in total power volume to 2020 year provided safe operation of power plants.

The important area of enhancing economic indicators for nuclear reactor is prolongation of operation period by increasing of burn-up level up to 80 – 100 MW·day/U kg. Achievement of such high burn-up is concerned with necessity of using of modified oxide nuclear fuel alloyed both burned down neutron absorbers and small amounts of alloyed additives [1, 2].

The analysis of patent information sources had revealed that currently interest to alloying additives to UO_2-based fuel is significantly great. Finely dispersed powders of Al_2O_3, $Al(OH)_3$, TiO_2, Cr_2O_3, Gd_2O_3, $Gd(OH)_3$, Nb_2O_5 etc, attract particular interest. However the amount of investigations aimed at determination of dependences "technology–structure–properties" on alloying additive content is limited.

In this connection the aim of investigation was enhancing of fuel pellet quality by means of incorporation of small amounts of $Al(OH)_3$ and TiO_2 which influence at pellet structure and properties.

RESULTS AND DISCUSSION

The following powders were used in this investigation: $Al(OH)_3$ with average size of 8 mm obtained by chemical deposition from aluminium nitrate solution by ammonia water; TiO_2 with average size of 11 mm obtained by chloric method; conventional $Al(OH)_3$ with average size of 45 – 70 mm and gas-flame UO_2 (10 – 40 mm). Powder grain-size composition was estimated by laser diffraction method using ANALIZETTE 22. The amount of alloying additives is given in table 1.

The analysis of structure of powders and sintered samples was carried out using scanning electron microscope EVO-40 and optical microscope MIM-9. The structure of powder mixtures was investigated using stereometrical metallography [3].

Fuel pellets was produced according to technology of Public Corporation

"Engineering Plant", which includes the following operations:

1. Preparation of press-powder by mixing of raw materials (UO_2, pore-former, alloying additives) in high-speed mixer "Labotex", densification, drying;
2. Fuel pellet pressing at 150 – 300 MPa (1.5 – 3.0 t/cm^2);
3. Pellet sintering in pusher-type furnace in dry hydrogen at 1730 ± 20 ^oC with 6-hour soaking in high-temperature zone.

The density of sintered pellets was determined by standard procedures of hydrostatic weighing and calculation.

The specific characteristic called "after-sinterabiluty" was estimated by the lever of density achieved.

The mechanical strength of sintered pellets was estimated by maximum load (kg) at fixed sample cross section.

Table 1

The amount of alloying additives incorporated in UO_2

Material	Additive incorporated	Amount, %
1	$Al(OH)_3$	0.05
2	$Al(OH)_3$	0.10
3	$Al(OH)_3$	0.50
4	$Al(OH)_3$	1.00
5	TiO_2	0.05
6	TiO_2	0.10
7	TiO_2	0.50
8	TiO_2	1.00
9	Without additive	0
10	Conventional $Al(OH)_3$	1.00

The structure and grain size were estimated using metallographic sections treated by specially developed etching agent containing 8 – 12 % H_2SO_4, 20 – 38 % H_2O_2, 50 – 60 % HNO_3, 4 – 8 % HF.

The thermal conductivity was measured by standard method using NETZSCH LFA 457 Micro Flash (laser flash method) [4].

It was revealed by grain-size composition analysis that $Al(OH)_3$ particles in initial state had non-exuiaxial form (figure 1 a), minimum size of 4 mm and

agglomerate size 25 – 50 mm. In turn TiO_2 particles had regular shape (figure 1 b),

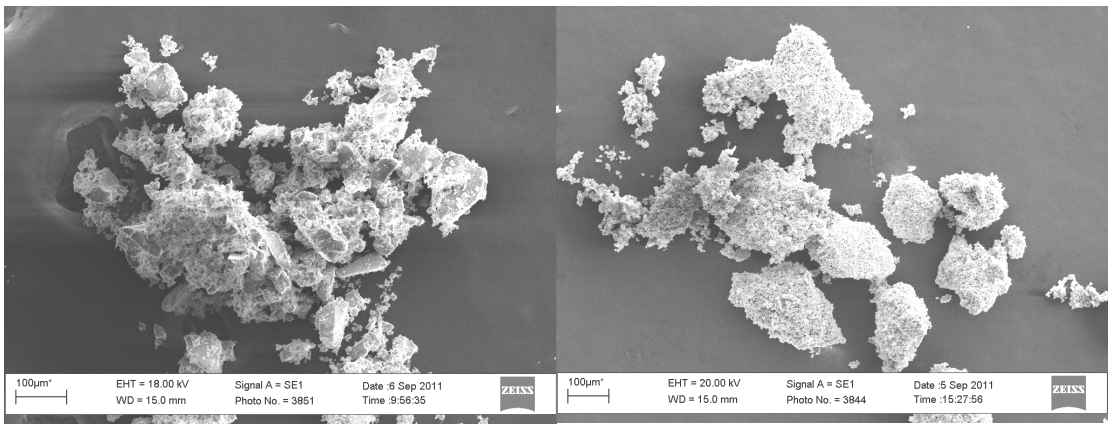

average size about 2 mm, agglomerate size up to 200 mm.

а) б)

Figure 1 The agglomerates of alloying additive particles: a – $Al(OH)_3$, b – TiO_2

It was revealed by fuel pellet pressing experiments that incorporation 0,05 – 1,00 % of alloying additives doesn't influence virtually on densification process. Linear dimensions and density of green pellets did not change actually. Small variations recorded are in metering error limit.

During sintering, which is one of the most significant process in fuel pellet production, alloying additives did not affect dimensions and density of sintered samples, although they being carriers of redundant oxygen may activate some processes of mass transfer.

Therewith it was shown by experiments carried out that incorporation of $Al(OH)_3$ and TiO_2 particles in UO_2-matrix allows significant increasing of grain size in fuel pellets up to 18 – 36 mm (conventional technology provides grain size 8 – 12 mm). It is necessary to mention also that there is evident maximum at 0.5 % for aluminium hydroxide, whereas titanium dioxide provides monotone decreasing after 18 mm at 0.05 %.

The dependence of average grain size on alloying additive amount is presented in figure 2.

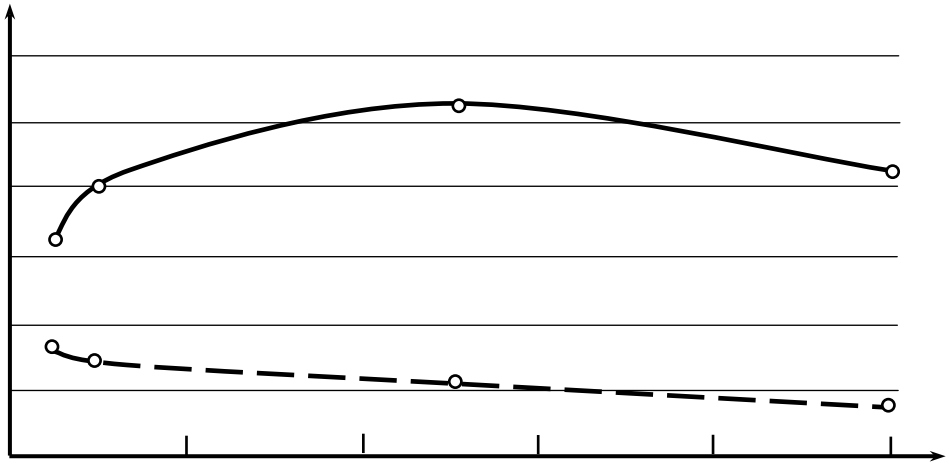

Fig. 2 The dependence of grain size on alloying additive amount

Metallographic investigations had shown also that alloying additive incorporation allowed decreasing of pore size from 4.8 mm to 4.3 – 4.5 mm. The average fraction of pores no more then 10 mm in material without additive is about 7 % (in section plane) and 4 – 5 % in material with additive. Using additives volume fraction of opened pores decreased from 0.5 % to less then 0.3 %.

The figure 3 shows the dependence of compression strength for fuel pellets on type and amount of additives incorporated. It is seen that increasing of additive amount strength rises from 198 up to 218 kg for TiO_2 and remains unchanged virtually for $Al(OH)_3$.

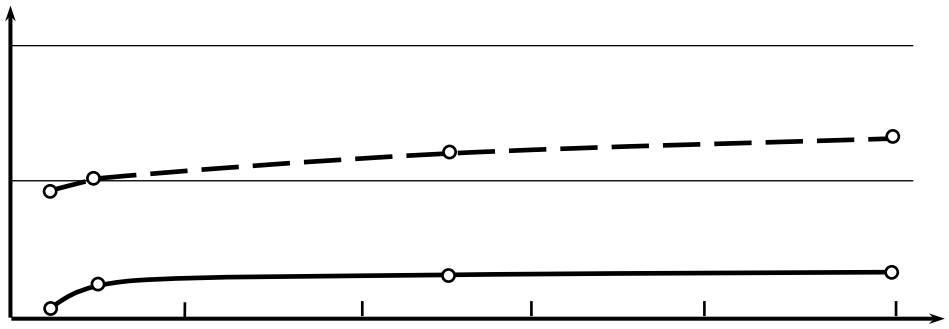

Figure 3 The dependence of compression strength on alloying additive amount

As was mentioned above, alloying additives don't affect overall porosity level

but decrease significantly the amount of large pores thereby increasing pellet strength and its homogeneity (the more average pore size, the less strength). Fuel pellet destruction at loading is going on by intercrystalline mechanism [4, 5]. The dependence of pellet strength on average grain size is described by the following empirical equation:

$$Y = 198{,}06 \times e^{-0{,}233x} \qquad (1)$$

where: Y – compression strength, kg, x – average grain size, mm.

The thermal conductivity is one of most significant characteristics of nuclear fuel because it affect fuel properties and processes in it during burn-up, as well as determines the design and specifications of fuel elements.

The figure 4 shows two curves for temperature dependence of pellet thermal conductivity (for initial material without additive and for one with 0.5 % $Al(OH)_3$). Curves for other materials are placed wholly in "tunnel" shown, and in most cases confidence intervals for corresponding temperatures overlap. This circumstance allows talking about small influence of additives on thermal conductivity. Coefficients of thermal expansion for samples without additives and alloyed ones differ no more then 8 %.

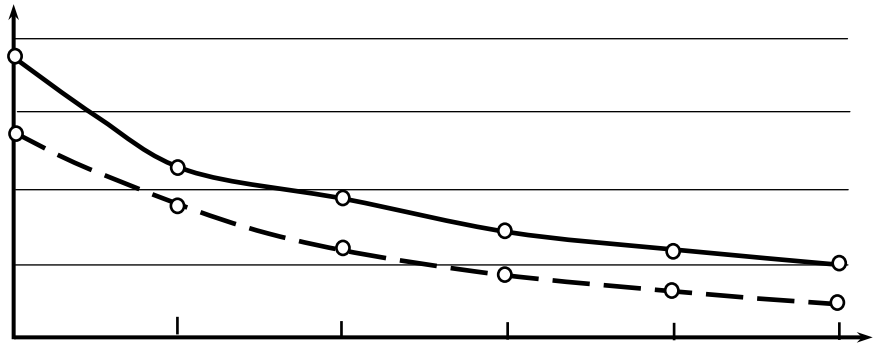

Figure 4 The temperature dependence of sintered pellet thermal conductivity

Thereby experiments carried out had shown that alloying additives incorporation can enhance macro- and microstructure parameters of fuel pellets and affects positively their specifications.

This investigation is carried out in the network of State Contract 16.513.11.3034 "The investigation of principles for creation of new fuel pellets generation based uranium dioxide for fuel elements modified by nanosized alloying compound".

CONCLUSIONS

1. The influence of small amounts of alloying additives $Al(OH)_3$ and TiO_2 on structure and properties of UO_2-based fuel pellets is investigated.

2. It was shown that incorporation of $Al(OH)_3$ and TiO_2 particles allows increasing of grain size (up to 35 mm) and mechanical strength as compared with material without additives with simultaneous enhancing of pore size distribution and small increasing of thermal conductivity.

REFERENCES

1. S.V. Khalatov //Nuclear Engineering abroad (in Russian), 2007. – №8. – P.32

2. Radford K., Pope J. //J. Nucl. Mater, 1983. – №2. – V.116. – P.305

3. S.A. Saltykov Stereometric metallography //Moscow: Metallurgy, 1976. – 270 p.

4. K.P. Dubrovin, P.N. Strazhov, V.N. Proselkov The investigation of operation capacity and safety of regular fuel elements VVER-440// The report of NPI named after Kurchatov. № 60/208. – Moscow, 1986. – 51 p.

5. K.P. Dubrovin, U.G Ivanov, N.L. Fotieva at all The experience of exploitation of fuel assembly with pelleted fuel in VVER-440 reactors.- Moscow, 1986. – 70 p.

CID: J21208-600

UDK 621.311.24

A.V. Golieva

DEVELOPMENT OF WIND ENERGY EFFICIENCY AND RELIABILITY INCREASING TECHNIQUES

Zaporizhzhya National Technical University

In this work various techniques of wind energy efficiency and reliability increasing are developed. The research takes into account installation conditions peculiarities as well as merits and demerits of each particular case.

Key words: efficiency, offshore wind farms, Genset, hybrid installations, reliability, maintenance, Power Management Strategies

Among the traditional and renewable energy sources wind energy is considered as a highly prospective one. Considerable investments are made into the research of this issue and great amount of specialists in this field are graduated every year.

Despite the fact, that capacity of wind power plants considerably increases every year, insufficient efficiency of wind power plants remain an urgent matter.

When possible, wind farms should be installed on the offshore areas. Better wind speeds are available offshore compared to on land, so offshore wind power's contribution in terms of electricity supplied is higher. [1] Waters of 20-80 meters deep are available for solid-base offshore installations. For deeper waters, floating wind farms are being developed.

The only demerit of this topology is that because of being less accessible for maintenance and repair, the reliability of those wind turbines should be considerably increased, that would result in capital investments costs increasing.

In rural areas, where constant wind farm maintenance cannot be guaranteed, the operation of wind plants can be supported by Genset generators, which are automatically turned on in case of emergency, as well as in cases when additional power source is required in order to increase the quality (sinusoidality) of electrical energy supplied.

The demerit of this method is that application of power converters, which are strongly required as it is conditioned by presence of both AC and DC components simultaneously, provide additional power losses and result in general efficiency decrease.

It can be concluded, that this method can be considered as a sufficient one for reliability increase purpose, but not for efficiency increase.

Different connecting topologies and configurations of power sources require application of hard Power Management Strategies. On the basis of research, carried out in The Netherlands it can be concluded, that the best efficiency can be reached by the mixed-coupling Hybrid Power System [2], thus it can be considered as demerit, because this system requires further development and additional investments.

For high power consumption industries a series of hybrid solar-wind energy plants can be adjusted in order to increase sustainability of the entire network (depending on cyclical changes in power consumption capacity the ones will compensate the impact on the load.) [3], thus yet they cannot be assumed as an independent energy source, because of insufficient capacity.

It can de concluded that among various topologies of wind energy efficiency and reliability increasing methods there is no one, which fully meets the common requirements, thus all of them need further development and optimization.

References:

1. Madsen & Krogsgaard. Offshore Wind Power 2010 - BTM Consult, 22 November 2010

2. L. E. Weldemariam Genset-solar-wind hybrid power system of off-grid power station for rural applications – TUDelft: 2010, - p. 44

3. Дзензерский В. А., Житник Н. Е., Плаксин С. В., Погорелая Л. М., Соколовский И. И. Принципы построения гибридных ветро-солнечных энергоустановок. – ЗНТУ: Електротехніка та електроенергетика. 2007, - 67 с.

CID: J21208-787

UDK 622.276

Lekomtsev A.V.

TECHNIQUE OF ELECTRICAL SUBMERSIBLE PUMPS SELECTION IN WELLS WITH THE HIGH GAS FACTOR ON THE UPPER KAMA OIL FIELDS

State National Research Politechnical University of Perm

Algorithm of electrical submersible pump selection in wells with the use of characteristics correcting calculations results by extraction of the gas-liquid mix. Given dependences could be used for pump exploitation efficiency estimation in wells with the high gas-oil ratio.

Key words: producing well, electrical submersible pump, inlet pump gas content.

Recently the steady negative tendency to deterioration of exploitation conditions of wells on oil deposits of Russia owing to the introduction of deposits with favorable geological parameters in a late stage of working out and increase in a relative share of oil extraction from deposits with recoverable reserves was outlined. As a result of decrease reservoir and bottom hole pressure, sealed processes in productive layers, especially in bottomhole zone, carrying out of geologo-technical actions are shown the complications leading to off-schedule repairs, time between failures decrease, pump failure. Thus work technical characteristics of the well equipment worsen that leads to its inefficient work. There is a necessity for change of a mode of operation (for example, transfer into a periodic mode pumping out) or in change of a standard size of the pump. Obviously, in these conditions the great value gets accuracy from which the technical service defines an installation standard size, its packaging arrangement and setting dept that, in turn, depends on quality of standard and methodical documents according to equipment selection to a chink is carried out.

However wide practical use of instructions on selection to oil wells electrical submersible pumps (ESP) is complicated by a lack of the initial information on oil

fields, its low reliability, the big labor input of calculations. For purposes of the further reduction of volume of calculations without essential decrease in accuracy of received results the variant of selection ESP to wells with use grapho-analytical method has been offered.

The technique consists of a number of consecutive steps, each of which, in turn, from separate operations. As the first step preparation of the initial data and an estimation of degree of their reliability is provided. The basic indicator for selection ESP is bottom hole pressure (P_{BHP}) at work of a well which is defined by direct measurements by means of deep manometers or carrying out of calculations on the basis of the data about annular space pressure, dynamic levels and density gas liquid mixes (GLM) in annular space.

Definition bottom hole pressure in the mechanized wells without deep devices and in wells with independent devices is carried out under the scheme

$$P_{BHP} = P_{input} + \Delta P_w \quad (1)$$

P_{input} – pressure input at pump; ΔP_w – pressure of a column of a liquid or GLM in a well in the range from reception of the pump to hole bottom.

Pressure R_{input} is defined on known annular space pressure (P_s), pressure of a column of gas (ΔP_g) between wellhead and dynamic head and to pressure of column GLM in annular space (ΔP_{GLM})

$$P_{input} = P_s + \Delta P_g + \Delta P_w \quad (2)$$

In the absence of the given deep researches for trustworthy information reception about pressure use the correlation dependences constructed by results of processing of measurements of pressure by means of manometers at level of their installation in a chink below the pump and definition of density GLM in annular space

$$\rho_{GLM} = \frac{\Delta P_w}{(L_p - H_h) \cdot g} \quad (3)$$

L_p – depth of ESP; H_h – dynamic head.

For the Shershnevsky oilfield (the Upper Kama oil fields) calculation ρ_{GLM}

according to 179 simultaneous measurements wellhead and deep manometers in 11 wells is executed. By the received results of definition of density GLM correlation dependences $\rho_{GLM} = f(H_h)$ [1] on which with sufficient accuracy for practice and efficiency it is possible to estimate pressure upon input at pump and on hole bottom are constructed. Reliability of the received values of pressure will define quality of selection of the pump and its technical characteristics in a well. Analyzed wells operation performances are revealed in table 2 and 3.

Table 2

ESP operation performances

ESP type	Pump rate Q_{ESP}, m^3/day		Head H_{ESP}, meter of water column	
	Change limits	Average value	Change limits	Average value
ESP5-18-1700	13,7…30,0	20,7	898…1114	1026
ESP5-30-1700	31,5…40,0	37,0	822…1078	1037
ESP5-60-1700	55,2…73,8	66,7	925…1234	1154

Table 3

Pump rate data grouping

ESP type	Quantity calculations	Average pump rate Q_{ESP}, m^3/day	Average head H_{ESP}, meter of water column
ESP5-18-1700	5	14,9	1105
	7	17,5	1063
	9	21,2	989
	6	25,3	903
ESP5-30-1700	13	33,0	1056
	15	34,9	1011
	18	38,6	914
	20	41,3	822
ESP5-60-1700	4	56,1	1224
	6	61,3	1144
	8	66,2	1026
	5	71,3	930

On the second step indicators of work of the pump are defined: pump rate according to measurement by a flowmeter on a wellhead Q_{ESP}; pressure P_{ESP} and pump head H_{ESP} in well

$$P_{ESP} = P_{output} - P_{input} \quad (4)$$

$$H_{ESP} = \frac{P_{ESP}}{\rho_w \cdot g} \quad (5)$$

P_{output} – pressure at pump output; ρ_{GLM} – water density.

As the third step recalculation of actual characteristics of the pump on bench, then on the certified value is carried out. Adjustment factors on a head, pump rate, efficiency (η_{ESP}) and capacity (N_{ESP}) have been defined for the Unvinsky deposit by results of processing of 144 measurements of characteristics of pumps [2].

Dependence of factors is revealed from specific gas content on reception of the pump and represents the nomogram (fig. 1).

Definition of bench characteristics of the pump is carried out under formulas [2]

$$K_Q = \frac{Q_{ESP}}{Q_b};\ K_H = \frac{H_{ESP}}{H_b};\ K_\eta = \frac{\eta_{ESP}}{\eta_b};\ K_N = \frac{N_{ESP}}{N_b}; \quad (6)$$

Q_b, H_b, η_b and N_b – pump rate, head, efficiency and consumed the capacity, corresponding to bench characteristic ESP. Then recalculation with bench on certified value is accepted.

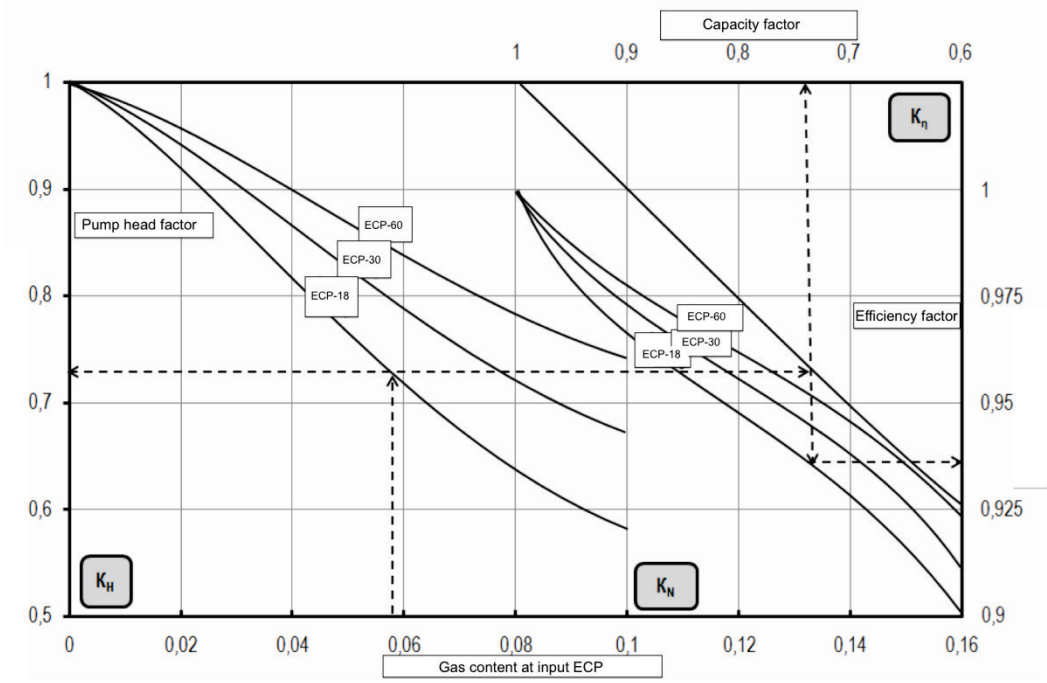

Fig. 1. Correcting factors assessment nomogram (ESP-18-1700, ESP-30-1700, ESP-60-1700)

The offered technique allows to select operatively the pump to a well or to optimize its work taking into account the negative factors, which shown at operation of extracting wells of deposits of the Upper Kama oil fields. For application of this

technique in other regions and service conditions construction of correlation dependences by definition of pressure on input at pump and at bottom hole taking into account physical and chemical properties of a pumped out liquid and its additional adaptation is necessary.

References:

1. Lekomtsev A.V., Mordvinov V.A., Turbakov M.S. Estimation of bottom-hole pressure in producing wells of Shershnevkoe oilfield // Oil indusry. – 2011. – №10. – p.30-31.
2. Mordvinov V.A., Turbakov M.S., Lekomtsev A.V. Characteristics of the submersible electrocentrifugal pumps at extraction of the gas-liquid blends from wells // Oil indusry. – 2010. – №8. – p.124-126.

CID: J21208-681

L.V.Bal-Prilipko

INNOVATION AS A VECTOR FOR FOOD INDUSTRY OF UKRAINE

National University of Life and Environmental Sciences of Ukraine

The paper analyzes the current state, the main tendencies and perspectives of innovation of the food industry of Ukraine and the world, the ways of strengthening innovation.

Key words, innovation, food products, strategy, development.

Accordingly, the basics of food safety Ukraine main purpose and priorities of food and processing industries associated with the production of safe and quality food. However, in order to ensure public health and sustainable development in all areas of the required deep understanding of community and various agro-food technologies, as the initial basis for the development of science and innovation priorities, especially related to guarantee safety and food quality . The existing system of state regulation of quality management and food safety does not provide a series of coordinated work of the ministries and departments, leading to duplication

of powers by some indicators and lack of control by some other, as well as the national system of non-compliance with the requirements of international practice. According to Ukrainian and European experts, the vast majority of food products do not meet quality requirements, and sometimes dangerous. For Ukraine as a country in transition, only an innovative development strategy can determine the path of socio-economic changes in the food industry. Innovative mechanisms of economic development should use scientific and technical potential and based on the relevant infrastructure. The role of innovation in the modern food industry is extremely important. Therefore, the time a "system of innovation", which involves the functioning of certain rules, laws and procedures of the legislative authority. It should be noted that innovation - innovation is introduced to ensure quality growth efficiency of processes or products required by the market and society. They are the end result of intellectual activity of man and his creative process, discoveries, inventions and rationalization.

CID: J21208-160

UDK: 664:635.655

A. Kuznetsova, L. Karavay, O. Nikolaenko

THE ENZYMATIC HYDROLYSIS INFLUENCE OF THE SOYA OKARA PHYSICAL-CHEMICAL AND ORGANOLEPTIC PROPERTIES

Far Eastern Federal University

Possibility of enzyme treatment soya okara by enzymes cellulolytic and proteolytic actions for the purpose of improvement of its processing properties and increase of comprehensibility of food production on its basis is considered.

Keywords: soya okara, enzymatic updating.

One of the main goals of scientific developments out in the field of processing of by-products of soya raw materials is the fullest utilization of the food, biological potential of soya that can be reached at the expense of enzymatic cleavage of cellular

walls of the soya raw materials which basis is made by a proteinaceous-carbohydrate complex.

The enzymatic biocatalysis makes it possible for the radical changes of the functional and manufacturing properties of the soya raw materials during all steps of the processing. This allows wide facilities for the creation of the new digestible food products for ordinary, prophylactic, dietotherapy and rehabilitation nutrition for the various social and age groups of the population.

Unconditional interest as an additional raw resource for manufacture of foodstuff represents soya okara - a by-product of processing of Chinese beans by manufacture soya emulsion.

In the modern food industry a perspective direction is manufacture of products from the nonconventional raw materials containing a wide spectrum valuable micronutrients, necessary for preservation or recovery of health of the person, and simultaneously fuller complex utilisation of natural resources.

Therefore one of paramount problems of scientific workings out in the field of processing of by-products of soya raw materials is the fullest utilisation of their food, biological potential that can be reached at the expense of enzymatic degradation of cellular walls of the soya raw materials which basis is made by a proteinaceous-carbohydrate complex.

Unconditional interest as an additional raw resource for manufacture of foodstuff represents soya okara - a by-product of processing of Chinese beans by manufacture soya emulsion.

By manufacture of soya products of dairy type there is non-extractable a firm part - soya okara. From each kg of the Chinese beans which have gone on preparation soya emulsion it turns out about 2 kg of the soya okara. Okara contains a significant amount of food filaments (8,4%±0,7) and a high-quality vegetable protein (6,9±0,8) which form difficult assimilable a proteinaceous-carbohydrate complex (Kuznetsova, Lyevochkina, 2007). To improve its processing properties and to raise comprehensibility of finished products with the soya okara it is necessary to destroy or leaven partially a proteinaceous-carbohydrate complex of the soya okara. In this

connection, the big practical interest processing of the soya okara enzymes cellulolytic and proleotytic represents actions.

For hydrolysis carrying out the enzyme preparations having high cellulolytic and proleotytic of activity have been chosen: Tsellolyuks F (Activity 2000±200 ed/g) and Protomegaterin Г20Х (Activity 800±200 ed/g)

For the purpose of optimisation of conditions of influence Tsellolyuks F were its three concentration are taken: 30 AU (active units) (0,015 % to weight of raw materials), 40 AU (0,02 % to weight of raw materials) and 50 AU (0.025 % to weight of raw materials) on 100 grms soya okara. According to literary data, the most part of the cellulases have an action optimum at pH 4 … 5,5 and temperature 40-600C (Kislukhina, Kyudulas, 1997), hydrolysis spent within 8 hours at natural pH mixes (okara: the distilled water, the hydromodule - 1:3) which makes 5.0. Hydrolysis soya okara spent at temperature 450 With which was optimum for the given technological process.

Efficiency of hydrolysis judged on maintenance reduction cellulose in soya okara. (Fig. 1)

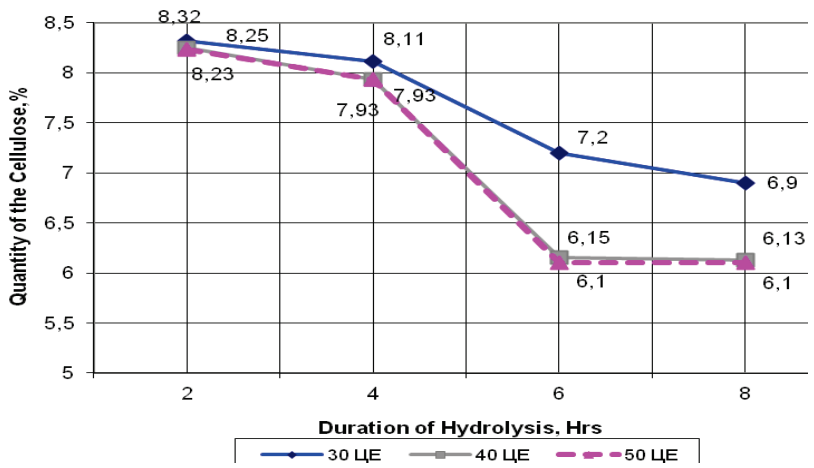

Fig 1 - Influence of concentration of enzyme on the maintenance cellulose

It is experimentally established, that optimum concentration Tsellolyuks F is the dose 40 AU on 100 г okara. At decrease in concentration of enzyme to 30 AU reduction cellulose goes less intensely. At entering into a substratum of enzyme in number of 50 AU also is inexpedient as the maintenance cellulose changes slightly in

comparison with the second sample.

By us it has been established, that temperature change in the big or smaller side, essentially influences a fermentolysis course. At temperature 37^0 With for 6 hours the maintenance cellulose has made 6,70 %, and at temperature 50^0 With - 6, 22 %, while at 45^0 With - 6,15 % (a Fig. 2).

Further, for influence on a protein complex okara, influenced on preliminary hydrolyzed soya okara enzyme proteolytic actions Protomegaterin Г20х. For this purpose, a substratum heated up to 80-90^0 With within 8-10 minutes for inactivation cellulose enzyme, cooled to 45^0 With and entered into it Protomegaterin Г20х also in three concentration: 30 AU (0,04 % to weight of raw materials), 40 AU (0,05 % to weight of raw materials) and 50 AU(0,006 % to weight of raw materials) at natural pH mixes (the distilled water: soya okara) - 5.0. Hydrolysis spent at a comfort temperature 45^0 With within 4 hours.

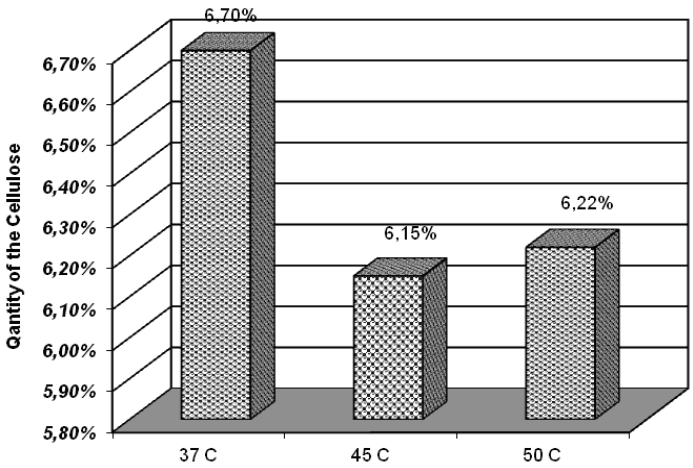

Fig 2 - Influence of temperature of hydrolysis on the maintenance cellulose in soya okara

Experimental researches have shown, that influence proteolytic enzyme, without dependence from its concentration, (Tab. 1) have led further, though also to protein content little change in the hydrolyzed product.

Table 1 - the Protein content in soya okara at hydrolysis proteolytic enzyme

Time of the Hydrolysis, hrs	Protein content, %
1	6.9

2	6.72
3	6.41
4	6.33

From the data presented in table 1 it is visible, that the protein content in okara changes slightly. But at its consecutive hydrolysis organoleptic indicators (table 2) change: okara becomes more friable and homogeneous, its colour and a smell improves.

The received results of organoleptic indicators hydrolyzed okara allow to assume, that application of enzymes Tsellolyuks F and Protomegaterin Г20х influences a proteinaceous-carbohydrate complex soya okara and cellulose under their influence breaks up to shorter polymeric chains.

Table 2 - Organoleptic indicators modified and unmodified soya okara

The name Product	Consistence, Appearance	Colour	Smell
Okara unmodified	Curdy consistency with insignificant inclusions of the soya bean coating	Light yellow	Bean, intensely expressed
Okara the modified	Friable, homogeneous, pastelike weight Without the visible Inclusions Soya bean coating	Cream, with a lung yellowish Tint	Bean smell it is not observed

The technology of reception biomodified soya okara has experimentally been developed. In fig 3 the flow sheet of its manufacture is presented

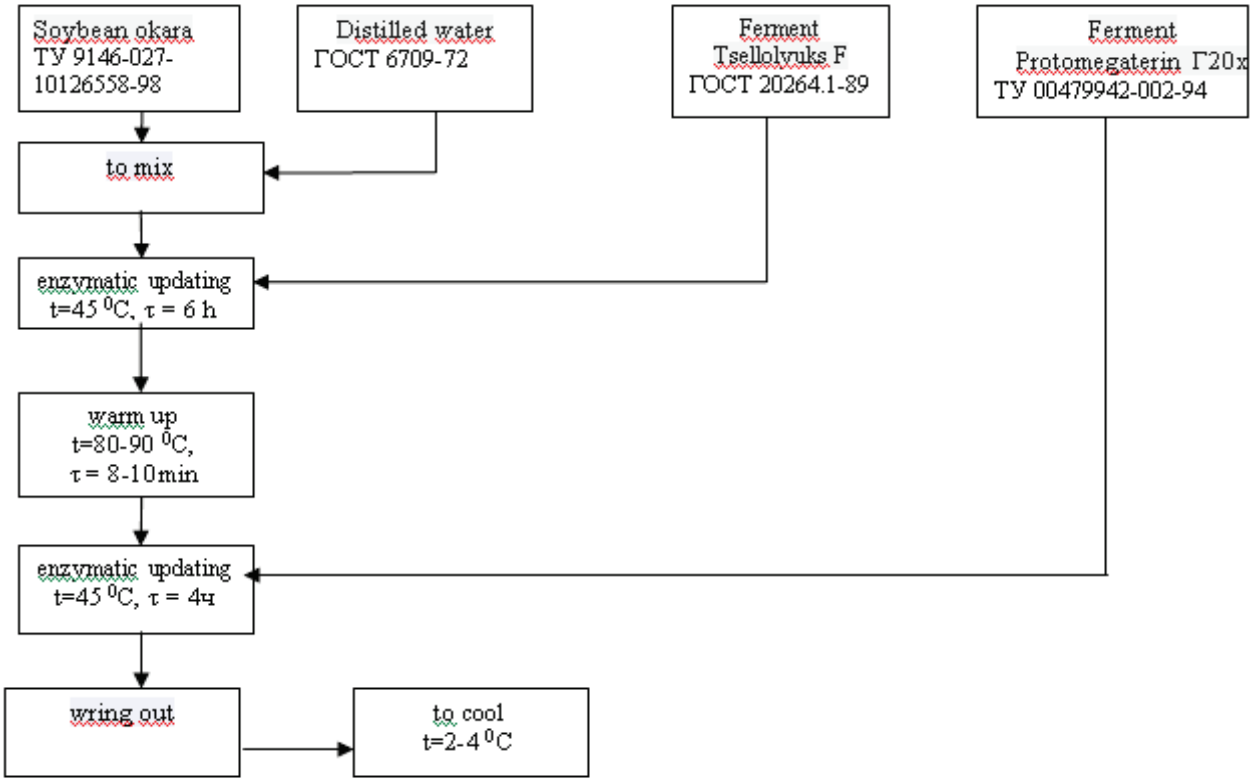

Fig 3 - The Scheme of manufacture biomodified soya okara

The received results testify that at enzymatic updating in soya okara there are structural changes in a proteinaceous-carbohydrate complex, improve its organoleptic and processing properties that allows to use the modified product as structuring by manufacture of wide assortment of foodstuff.

The literature:

1. Kislukhina O.V. Biotehnologicheskie of a basis of processing of a plant raw material / O.Kisluhina, I.Kjudulas. - Kaunas: Technology, 1997. - 183 pages.

2. Kuznetsova A.A. Ispolzovanie soya okara for manufacture of culinary products from invaluable fish raw materials / A.A.Kuznetsova, L.V.Levochkina//Bulletin ТГЭУ. - 2007. - i3 (43). - S.68-71.

CID: J21208-185

Anikeeva N.V.

WORKING OUT OF TECHNOLOGIES ON APPLICATION OF BIOLOGICAL PREPARATIONS FOR BAKING BRANCH

The Volgograd state technical university

In given article are shined fundamental biochemical to researches on application of the albuminous preparations developed from seeds nut in the baking industry. As a result of the spent researches it has been established about expediency of use of the albuminous preparations developed from seeds nut, in bakery. The analysis of the received given finished articles has shown that physical and chemical and органолептические indicators of bread "Nutovyj" surpass indicators of bread wheaten.

*Key words**:** albuminous ist fast, Fermental preparation, nut, albuminous preparations, vegetative fibers.*

One of ways of a solution of a problem of a lack of fiber is use of a fundamental natural-science reserve in such branches, as physical and biochemical chemistry, molecular biology, genetics and selection. Result were new technologies of reception of food fiber from the raw materials earlier not used and lost in the course of reception of foodstuff, but containing high-grade fiber. At traditional ways of manufacture only the part of fiber in the form of vegetative production is consumed directly in food, but the most part is exposed to processing in food the indirect methods including, at least, three stages: the plant growing - animal industries - foodstuff, each of which is accompanied by considerable losses. Perspectivity of those or other sources of food fiber is defined by resource reasons, for example, renewed character and in scales of manufacture of this food fiber and the scientific and technical level reached in the field of allocation from the given kind of raw materials of food fiber with high and varied functional properties [1, 2].

Seeds concern the most perspective sources of food fiber olive, yeast and bean, and also the secondary raw materials of the food-processing industry formed by

manufacture of vegetable oils, starch, at milk and meat processing. At comparison of expediency of use of animal protein it is necessary to consider continuously increasing cost of high-quality them, and also deficiency and labor input of reception. By manufacture of cattle-breeding production it is usually lost ¾ vegetative fiber, therefore fiber of beef costs at 30-50 time more expensively fiber, for example, a fat-free soya flour, and in 70 times – nut torments. Biochemical researches have shown that seeds нута are cheap высокополноценным albuminous raw materials for manufacture of albuminous preparations for the food-processing industry. At studying of a chemical compound of seeds нута and others, bean depending on a biological grade and growth conditions the first is favourably allocated with level of the maintenance of fiber (to 32 %), and also level of the maintenance of irreplaceable amino acids.

On level of the maintenance of irreplaceable amino acids of the squirrel нутовой torments favourably differ from wheat flour fibers. Calculation аминокислотного it is fast, has shown that on the sum of irreplaceable amino acids of the squirrel нута exceeds fibers of wheat flour, especially on a lysine and треонину, this indicator makes on nut 130,4 % and 100 % against 45,5 % and 75 % on wheat [3, 4].

Fibers nut favourably differ from fibers of others bean, for example string beans, peas, a soya level of the maintenance of antinutrients, that is inhibitors of proteolytic enzymes. Researches have shown that in seeds нута three units inhibited tripsin (EIT - IT) in number of 5-6 % from the general maintenance of fiber, whereas in string bean seeds-17 units contain. In a small amount in seeds нута contain lektin (400-800) genaglyutelinovyh units on 1 mg. The squirrel, in string bean seeds-3200-6400. As a whole fibers нута are characterized low трансингибирующей by the ability equal on the average of 1,3 mg/g, hence, it well and easily acquired. Нут on level of the maintenance of fiber in seeds concedes only a soya. Emulgirujushchaja ability is great enough (9,8-10,3 of oil on 100 mg. The squirrel). Thus, the expediency of application of a flour nut and albuminous preparations in manufacture of foodstuff is defined нетолько by biological value, but functional properties of its fibers [5,6].

The literature:

1. Anikeev, N.V.Scientific a theoretical and practical substantiation of treatment-and-prophylactic properties нута and the products created on its basis Volgograd: IPK "Tsaritsyn", 2002. – 230 with.

2. Anikeev, N.V.New of property of bread/N.V.Anikeeva// Vestnik.-2002.- № 4.-s.52-53.

3. Anikeev, N.V.Reception nut torments. An information leaflet 51-116-02 N.V.Anikeeva – Volgograd ZNTI, 2002.-3 with.

4. Anikeev, N.V.One from ways of reception нутового milk: an information leaflet №51-195-02/N.V.Anikeeva – Volgograd: ZNTI, 2002.-3 with.

5. Anikeev, N.V.Way of reception of biologically active additive from nut: an information leaflet №51-118-02/N.V.Anikeeva. - Volgograd: ZNTI, 2002.2 with.

6. Anikeeva, N.V. Characterization methods of production of bakery products with protein products: newsletter № 51-012-03 / N.V.Anikeeva. - Volgograd: CSTI, 2003.- 2.

CID: J21208-163

UDK: 664:663.854.793:635.073

N. Chesnokova, S. Bozhko,

T. Ershova, N. Masalova

The use of bio modified burdock root in pastry production

Far eastern federal university

This report focuses on different ways of bio modification of great burdock root and its use in custard gingerbread production.

Key words: burdock root, bio modification, hydrolysis, organoleptic estimation, custard gingerbread.

Analysis of health status of Russian population shows steady increase of people that suffer from or prone to different diseases because of lifestyle and diet are the main factors that define person’s health and theirworking capacity.

It's possible that health status of Russian population can be quickly improved only as a result of such events that play leading role in food patterns improving for example wide use of functional food products.

One of the sources of functional ingredients especially food fiber iswild plants. For that reason researches in this field should catch attention of specialists and scientists. One of the aims of such researches can be development of food products with the use of burdock root for increasing food value.

Great burdock root that was studied in this work was grown in Primorsky region with ripeness level from 1 to 2 years. Bio modification of burdock root was made by acid, fermentative and acid- fermentativehydrolysis. Tzellolyuks F was used as a ferment.

After bio modification burdock root fibers softened, colour of burdock root changed from dark brown and almost black to light peach and creamy. Taste and smell became more tenderafter bio modification.

Since products rich in fiber are used in dietetic therapy. Because they excretecholesterol from organism, the amount of fiber in burdock root was evaluated. In table 1 presented the amount of fiber in 4 samples (1 – fresh fine-cut burdock root, 2 - fine-cut burdock root, which has been exposed to acid hydrolysis, 3 - fine-cut burdock root, which has been exposed to fermentativehydrolysis, 4 - fine-cut burdock root, which has been exposed to acid-fermentativehydrolysis). The results of thedefining of fiber amount presented in table 1.

Table 1

Research data of the amount of fiber in burdock rootdepending on bio modification

№ of sample	Content of fiber, %
1	42,3
2	33,5
3	30,1
4	27,4

As it can be seen, the highest rate of fiber is in the first sample, where burdock root was exposed to mechanical treatment only. The lowest amount of fiber is in the fourth sample where burdock root was exposed to the hardest treatment of all the samples.

The next step was to define the presence of toxic elements in burdock root. The results presented in table 2.

While researching burdock root on safety there was the same tendency – in non-hydrolyzed burdock root were the highest indicators of heavy metals, in sample exposed to acid-fermentativehydrolysis the lowest indicators of heavy metals. It's clear, that bio modification reduces the amount of heavy metals in studied samples.

Table 2

Research data of the amount of toxic elements in different samples of burdock root

Toxic element	Sample № 1	Sample № 2	Sample № 3	Sample № 4
Cd	0,060	0,032	0,030	0,020
Pb	0,530	0,380	0,390	0,300
As	0,086	0,048	0,045	0,040
Hg	not detected	not detected	not detected	not detected

Bio modified burdock root was added in custard gingerbread, replacing 15%, 20 % and 30 % of flour. As a result of researches there was made a conclusion that

custard gingerbread sample with 20 % replacing of flour to bio modified burdock root has the bestorganoleptic qualities. Adding burdock root in custard gingerbread also showed that items with bio modified burdock rootin comparison with items without using burdock root bio modification improved significantly in the structure of crumb, consistence of gingerbread became softer,fibrestock became more tender than in untreated burdock root samples. In addition hardening of product was slower. Food value and caloric value of custard gingerbread with 20 % flour changed to burdock root were calculated. The amount of protein is 6,9 grams, fat is 5,9 grams, carbohydrates is 68,8, caloric value is 356,38 kilocalories. Consequently pastrieswith burdock root are rich in food fiber and can berecommended as a functional food product.

CID: J21208-162

UDK 664:637.521:637.54

O. Nikolaenko, A. Chernyshova,

A. Kuznetsova, L. Karavay

CULINARY PRODUCTS WITH MODIFIED SOYMEAL PRODUCT IN THERAPEUTIC FOOD

Far eastern federal university

Technology of soymeal product modification by papain is described. Soymeal products without anti-nutritional qualities were found.Effectivenessof developed products for metabolic lipid imbalance was shown.

Key words: soymeal product, soymeal okara, soymeal milk, enzymatic modification, papain.

It is well known that soymeal seeds have high amount of valuable food protein and are used for production of different kinds of protein concentrate - flour, okara, soymeal milk. Use of vegetable raw material rich in essential amino acid allows to eliminate the lack of animal proteinand soymeal protein among all the raw materials that stand on the first place. Therefore the role of soymeal combined products as a

source of nutrition for people and animals increased.

However not all the proteins entering person's organism can be assimilated because there are anti-alimentary factors such as antitrypsin and chymotrypsin in soymeal and soymeal products. They are represented by water-soluble inhibitor of Kunizt, alcohol-soluble inhibitor of Bauman-Birk and small amount of other proteins that are capable of reducing activity of proteoclastic ferment. Assimilability of soymeal proteins depends directly on the presence of these biologically active components therefore they should be removed by using different methods of soymeal raw products processing. One of the possible methods of increasing of soymeal assimilability is its fragmentary proteolysis under the effect of proteoclastic ferment. As a result of this process antitrypsin and chymotrypsin are split because they have protein nature and received peptides and amino acids are assimilated easily in the organism.

Soymeal milk received by traditional technology has specific "bean" smell, bitter taste and it slows down its use in person's diet. For improving nutritious and functional qualities of soymeal products we produced method of fermentative proteolysis.

As an object of research we used heat-treated soymeal homogenate that represents suspension consisted of 2 fractions, - hard and liquid okara – of soymeal milk.

Proteolytic ferment of natural origin papain was used as an instrument of modification.

Activation of papain was made by adding activator solution including 1 Mm disodium salt of ethylenediaminotetraacetic acid (trilon B) and in the presence of reducer cysteine-HC1 (activator solution 1) or sodium borohydride NaBH4 (activator solution 2)

Method of fermentative proteolysis based on pH-metrical evaluation of acidification of research sample, achieving as a result of peptide (amide) bonds hydrolysis in protein. Proteolysis was performed with initial pH 7,2 and during specific conditions.

Highly sensitive method of vertical protein electrophoresis in polyacrylamide gel (PAAG) in the presence of sodium dodecyl sulfate that allows to measure content of protein with different molecular mass was used in this research.

Proteolysis was performed in the ratio protein:papain – 1000:1. Degree of proteolysis was evaluated by changing degree of pH structure.

Time history of changing of pH structure in the process of ferment was point to the high degree of proteolysis.

As you can see from the picture 1 during protein proteolysis of homogenate by papain there was slow decrease of pH structure as a result of carboxyl group of amino acid remains release, that 2 hours later appeared on plato. As far as pH doesn't influence papain activity from 4 to 9, consequently it can be suggested that appearance on plato caused by decrease of concentrations of impact centers of ferment on protein. On the picture 2 there are homogenate electrophoregrams exposed to papain proteolysisat different time.

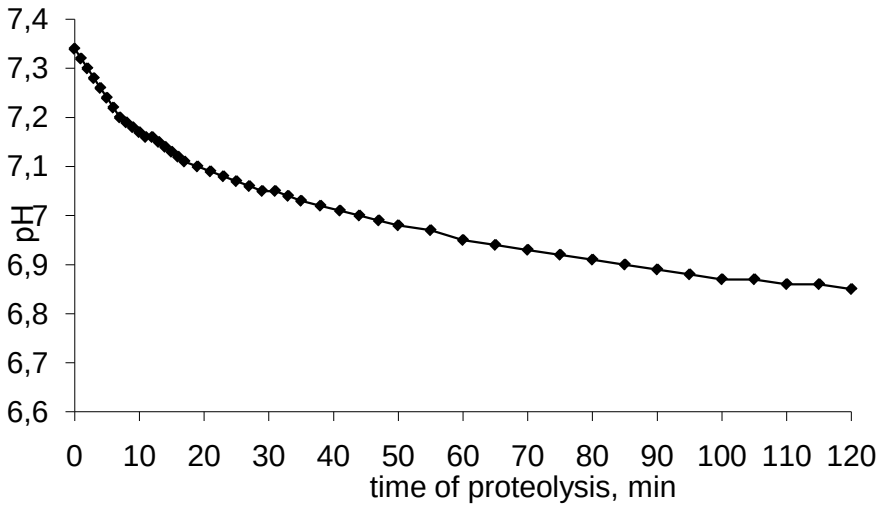

Fig 1 – Dynamics of changing of pH soymeal substrate effected on it by papain activated by solution №1

As a control for molecular weighing of soymeal proteins product myofibrilla from anti-striated part of adductor muscle with well-known molecular protein mass (heavy chain o myosin – 220 kilodaltons, paramyosin – 105 kilodaltons and actin – 45 kilodaltons) was taken.

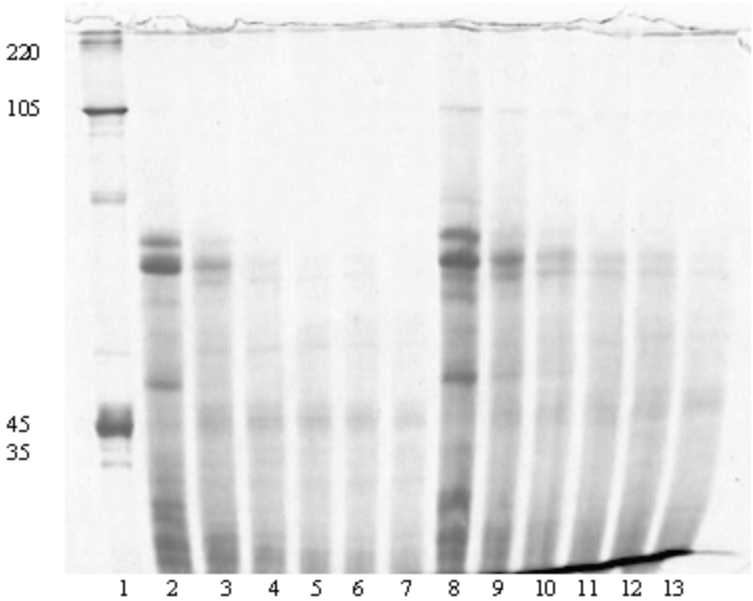

Fig 2 – electrophoregram of soymeal homogenate in 12 % in polyacrylamide gel

1-Myofibrilla from anti-striated part of adductor muscle of shell-fish, 2-7 soymeal homogenate exposed to papain proteolysis activated by solution №1, 8-13 – soymeal homogenate exposed to papain proteolysis activated by solution № 2

It can be seen that while increasing time of ferment exposition high-molecular proteins with mass 220, 80, 70 tones Dalton disappeared and appeared new low-molecular components with molecular mass less than 20 thousand Dalton. These data correspond to results of changing degree of pH structure. (pic 1)

Consequently proteolysis reduces molecular mass of protein components helps to improve assimilability of proteins by person organism on the one hand and on the other hand helps to reduce the amount of anti-nutritional soymeal components – products of protein nature, positively influence on organoleptic characteristic of soymeal products.

Use of fermentative modification allows to correct technological criteria of soymeal milk

Production: to reduce the temperature and to shorten the length of process and as a result amount of vitamins and phytoestrogen of finished product will increase.

Modified soymeal milk made according to suggested technology was used for producing combined products that have specific structure. One of the most important

aims is to develop food recipes with good organoleptic indicators.

We developed combined snack and dessert products that have raw material of animal and vegetable origin (carrot, beetroot, black currant and red currant, dried apricot, pumpkin) as flavor-active additives. Modified soymeal milk in combination with sodium alginate, that are part of food product “Laminal’” produced by laboratory FGUP TINRO-center served as the basis for combined and dessert products.

Modified soymeal okara made by suggested technology was used for preparation of “Syrniki with okara” and “olad’i with okara”. Adding modified okara to traditional products led to increase of nutrition and biological value of culinary food.

The opportunity of food correction of lipid exchange with the help of developed combined dairy products and developed syrniki and olad’i was added to sick-volunteer s diet and researched in hospital conditions.

Group of sick people included 20 people from 43 to 83 years old. 5 sick had hypertensive disease, 8 sick had stenocardia of 3rd functional class, 4 sick had stenocardia of 4th functional type. 3 sick had myocardial infarction.

Developed food products based on modified soymeal milk and modified okara were presented in the following list:

· Dessert “Solnyshko” (soymeal milk, pumpkin/dried apricot, soil-aggregate stabilizer)

· Dessert “Yagodka” (soymeal milk, black currant and red currant)

· Snack product “Bodrost’” (soymeal milk, carrot and beetroot mash, cottage cheese, soil-aggregate stabilizer)

· Snack product “Zdorov’e” (soymeal milk, Alaska Pollock, onion, carrot, soil-aggregate stabilizer)

· “Syrnik s okaroi” (soymeal okara, cottage cheese, egg, flour)

· “Olad’i s okaroi” (soymeal okara, soymeal milk, egg, flour, yeasts)

Developed products included in diet of patients during 21-30 days from the date of coming to hospital at the rate of 100 grams a day.

General state of the patient and influence of combined products on changing of lipid exchange were observed.

During taking soymeal products and refusal of it, no allergic reactions and other effects were noticed. Patients notices high organoleptic qualities of products, no racy bean flavor, identity of suggested products made according to traditional technologies.

On top of that there is a tendency of reducing of lipids in blood. The amount of ß-lipids reduced to 5.4 %; the amount of triglycerides to 18 %; the amount of cholesterol to 9 %.

We should notice that suggested products with modified soymeal milk and okara are not medical products but products with high taste and nutritional properties and with healthcare effect.

On the basis of undertaken researches we recommend to add developed products to old people diet, to people suffer from obesity, cardiovascular diseases and hypertension.

Literature:

1. Tolstoguzov V.B. New forms of protein food. – M.: Agropromizdat. 1981,- 303 p.

2. Kalenik T.K., Ol'hovaya L.P., Chernysgova A.N. Influence of biotechnological modification of soymeal on her protein components. – M.: Food industry.- keeping and processing of agricultural raw material. №2, 2009. – p.71.

3. Chernyshova A.N., Nikolaenko O.A., Kalenik L.V., Levochkina L.V., Korchagin V.P. Use of therapeutic diet of nano-bio-technological products on the milk basis. –Vladivostok.: Pacific medical magazine, 2009, №1.

CID: J21208-161

UDK: 664:637.521:637.54

S. Bozhko, T. Ershova, N. Chesnokova,

A. Chernyshova

DEVELOPMENT OF MEAT-VEGETABLE SEMI-FINISHED PRODUCT S TECHNOLOGY MADE OF POULTRY MINCED MEAT

Far Eastern Federal University

This report focuses the opportunity of using poultry minced meat for meat-vegetable semi-finished products production. Functionally-technological qualities of flow minced meat, species of vegetable additives and their technological qualities have been studied and optimal amount of contributed vegetable additives were developed.

Key words: meat-vegetable semi-finished products, production of semi-finished products made of poultry minced meat, vegetable additives, functionally-technological qualities of stuffing.

Recently the tendency of domestic poultry meat production has increased. Huge amount of poultry goes to semi-finished products production of different degree manufacturing. One of the promising directions in this area is high level processing of poultry, minced meat production and its semi-finished products.

Minced meat is a complicated system with different degree of dispersion, having exact functionally-technological qualities. Functionally-technological qualities of minced-meat is understood to be total amount of exponents such as water-binding ability (MBA), water-holding ability (WHA), fat-holding ability (FHA) and also emulsion stability. One of the most important minced meat quality factors is its water-binding ability. Organoleptical factors such as juiciness, softness and losses during thermal conditioning depend on that ability.

At present day there are two ways of deboning poultry meat during minced-meat production - manual and mechanical. Mechanical deboning of poultry meat evaluates having lower factors WHA, MBA and АРФ because of the mechanical influence on

muscular tissue structure and its high deformation degree during deboning. To improve functionally-technological qualities of minced meat, improve taste and increase nutrition value in recipe mixture it is necessary to add different components whichhelp to bind free water and improve thixotropic qualities of semi-finished products. These additives are protein products of vegetable origin (soymeal concentrate and isolates); egg products; fresh vegetable additives (in a powder form, mash form and raw pounding form); berries and fruits (in a powder form, mash form and homogenate); wheat and rice flour; dietary fibers (vegetable fiber); cereals. The amount of additives depends on its species and makes from 5 through 60 % (minced meat mass). Rice flour and potato flakes are added at the rate from 5 to 15 % and minced meat enriches itself with ballast and mineral substances and vitamins. Vegetable additive binds water and fat through adsorption and as a result keeps stability of semi-finished product form, loses during thermal conditioning are reduced, juiciness of product is improving and production is increasing, and that gives strong economic effect. The amount of vegetable additives isreally higher and makes about 40 % for grated carrot and 60 % for potato carrot and blanched carrot.

In our work we studied the opportunity to produce meat vegetable semi-finished products from chicken minced meat, produced in a Far East region. Chemical composition of chicken minced meat is different according to protein, fat, and energy value. Minced meat “Osoby” and “Dietichesky” producing by poultry farm “Michailovsky broiler” (Artem city) were chosen as an object of this research because they have a huge amount of protein. Recipe structure of minced meat was studied and functionally-technological qualities were defined. Researched samples of chicken minced meat have an extra moisture and low water-holding ability. That’s why while choosing vegetable additive species it is necessary to use such additives that not only enrich the structure of minced meat with minerals and vitamins but also help to reduce loses during thermal conditioning by binding free water and fat. On this basis the task to produce wide range of meat-vegetable semi-finished products made of presented minced meat was set and good value of components in recipes of these semi-finished products was defined. Rice flour, potato flakes, mashed potato,

finely divided raw carrot and blanched green head cabbage were used as a vegetable component. These kinds of minced meat vary in recipe and have different functional qualities and what defines different amount of additives. Raw vegetables and mashed potato were added in the amount from 5 to 50 % of minced meat mass, potato flakes and rice flour in the amount from 5 to 20 %. It was set that dry vegetable additives help to improve functionally-technological qualities of minced-meat more than vegetable mash. Optimal amount of potato flakes in “Osoby” minced meat is 5 % and in “Dietichesky” minced meat is 10 % (Pic. 1**).**

Distribution of this amount of additives improved functionally-technological qualities of minced meat reduced loses during thermal conditioning and increased organoleptic indicator of finished product.

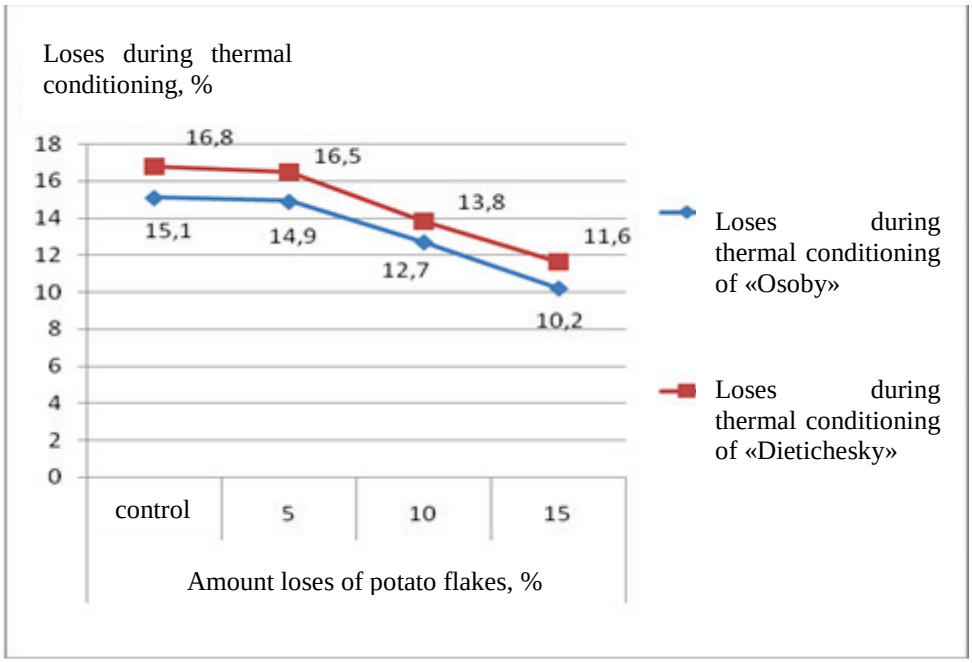

Fig. 1. Influence of potato flakes additives on the amount of loses during thermal conditioning of chicken meat balls

Dependence between the amount of additives and finished products was noticed. However increasing of the amount of additives more than recommended reduces organoleptic indicators of finished meat balls, they appeared to be dry and harsh.

Literature:

1. Baboilova L.K. About increasing of chopped meat products range // Meat

industry. – 2007, - №.-p. 80-81.

2. Mitrofanov N.S. Makoveev I.I. Poultry meat – basis for increasing of meat products range// Meat industry.-2006. №4.-p.26-27.

3. Bozhko S.D. Levochkina L.V., Ershova T.A. Production of meat vegetable semi-finished products made of poultry minced meat. // Keeping and recycling of agricultural raw material. – 2011. №3- p.19

CID: J21208-899

UDK 637.56.05

Sapetova T., Kucheruk MD

Quality chilled fish

National University of Life and Environmental Sciences of Ukraine

Chilled fish is a fish, the body temperature of which in the meat thickness varies from -1 to -5 °C and stays at this level, close to krioskopic point, but not below it. For the most of fish krioskopic temperature ranges from 0 to -2 ° C. In freshwater fish the freezing point of tissue juice is at the level of -0,5 to -0,9 ° C.

For cooling suitable live fish or is that at the beginning stages of post-mortem rigor.

The speed and duration of the fish cooling are directly dependent on the thermal conductivity of tissues. The higher fat content of fish, the longer the cooling process, since the thermal conductivity of fat at plus temperatures in halfless the thermal conductivity of muscle.

In addition to fatness the size and body shape, chemical composition of fish, the difference between the temperature of the environment and product are affected on the cooling rate.

It is increased density of tissues, tenacity of tissue juice and blood, reduced weight due to evaporation of moisture from the body surface of chilled fish. The higher the humidity of the environment and lower fatness content of the fish, the higher the mass loss, because subcutaneous fat prevents the evaporation of moisture.

Packaging materials and containers protect fish the from shrinkage.

While cooling in ice the shrinkage is less than the cooling in air. At cooling in liquid medium the shrinkage is not observed.

The temperature rises in the fish body after its death, as a chemical decomposition of muscle tissues takes place. This enzyme is not inactivated, but their activity is reduced. Life activity of microorganisms only slows down, so shelf life of chilled fish is limited.

The quality of chilled fish is estimated by the following parameters: surface clean, without damage, self-colored, shiny scales, gills from dark red to pink color, the consistence of meat is dense, eyes are not sunken, shiny, smell is tipical for fresh fish with no signs of damage. It is allowed slight sour smell in the gills, which easy removes after washing, and slightly loose, but not friable consistence of meat.

The main cause of chilled fish spoilage are microorganisms that are in the mucus and in intestines of fish. Penetrating into the muscle tissue of fish, they decompose its protein white, causing deterioration of taste and unpleasant smell.

Autolitic changes have a great influence at the chilled fish quality during storage. There are occurring under the influence of endogenous and proteolytic enzymes that are presented respectively in muscle tissue and internal organs of fish. The action of endogenous enzymes leads to post-mortem rigor that at around 0 °C temperatures in most species occurs during the first day of storage after fishing, and then fish meat softens gradually. These enzymes have the greatest influence on the change of the fish meat taste properties.

So, to get chilled fish of good quality it is essential to keep to the temperature and humidity regimes of storage, and sanitary standards at technological processing, to use only specially designed materials of high quality for packaging.

CID: J21208-196

Javorskiy V.T., Perekupko T.V.,
Perekupko A.V.

OBTAINING OF CONDITIONAL POTASSIUM-MAGNESIUM FERTILIZER FROM SOLUTION OF POTASH TAILINGS PRODUCTION

Lviv Polytechnic University

The results of studies of the process of obtaining conditional potassium-magnesium from potash tailings production solutions are given.

Keywords: waste; tailings; evaporation; crystallization; potassium-magnesium.

In our previous studies [1] it is shown that in the process of evaporation of the Stebnik tailing dump solution the sodium chloride is crystallized. In obtained solution after separation of the solid phase remains a significant amount of ions K^+, Mg^{2+} and SO_4^{2-}. In order to develop of new technology of complete processing of tailing dump solutions, the possibility and conditions for extraction of conditioned potassium-magnesium fertilizer from the evaporated solutions, depending on the degree of evaporation, it is necessary to determine. To this end, the obtained solutions were cooled to room temperature and the sediments, which were generated at the same time, have been separated. Yield and composition of obtained precipitations are given in the following table.

Yield and composition of sediments obtained from the evaporated solutions after their cooling

The degree of evapo-ration, %	Yield of sediment (on a dry substance)			Composition of sediment, wt. %						
	kilogram with 100 kilogram of initial solution	over sulphate ion, %	over potas-sium ion, %	leonite	Na Cl	KCl	schoenite	bloedite	epsomite	hygroscopic H_2O
23,47	3,22	4,22	4,98	-	74,46	-	11,73	5,95	-	7,86
31,30	4,57	28,68	38,04	68,02	20,10	-	-	5,41	0,45	6,02
40,00	6,50	38,79	65,52	55,	13,9	8,74	-	-	14,0	7,38

				94	0				4	
47,00	9,16	60,25	74,78	60,09	16,50	0,44	-	-	15,19	7,78

These data show that at relatively low degrees of evaporation of a initial solution (23,47 %) sodium chloride with admixtures of schoenite $K_2SO_4 \cdot MgSO_4 \cdot 6H_2O$ and bloedite $Na_2SO_4 \cdot MgSO_4 \cdot 4H_2O$ continues to crystallize, at the same time the salt yield is very low. Deeper evaporation leads to the sedimentation of the solid phase leonite $K_2SO_4 \cdot MgSO_4 \cdot 4H_2O$ in a mixture with sodium chloride, bloedite and epsomite $MgSO_4 \cdot 7H_2O$. Increasing of the evaporation degree of the initial solution for more than 40 % leads to the crystallization leonite, mixed with sodium chloride, potassium chloride and epsomite. The content of ion Cl^- in the obtained sediments with increasing degree of evaporation is reduced due to a more complete separation of sodium chloride in the solid phase on the previous stage (during the evaporation of the solution).

The filtered sediments were dried to constant weight at a temperature of (120 ± 0,2)0C. The obtained results of their chemical analysis are showed that the precipitate, which was separated from solution with the degree of evaporation of the 40 %, contains (wt. % on dry substance): K_2O 26,71; MgO 11,82; chloride ion 17,73, which corresponds to the requirements of technical specifications 6-05743160.002-94 to potassium-magnesium fertilizer grade B.

Thus, the possibility of conditional potassium-magnesium fertilizer obtaining from a tailings solution experimentally is proved that significantly will improve the technical and economic parameters of the process of its processing.

References:

1. Получение поваренной соли из растворов хвостохранилищ калийных производств /В.Т. Яворский, Т.В. Перекупко, К.И. Блаживский, И.Е. Максимович, А.В. Перекупко //Сборник научных трудов по материалам междун. научн.-практ. конф. «Современные проблемы и пути их решения в науке, транспорте, производстве и образовании'2011». – Т. 8. Технические

науки. – Одесса, 2011. - С.49-51.

CID: J21208-757

Kyrylchyk E.R.

COMPRESSION OF AUDIO SIGNAL

National Technical University of Ukraine "KPI"

This report focuses on the compression of audiosignals. principle of operation of the compressor is considered as the principle of operation of the device. the use of compression in the processing of music signals in the sound engineering is alsoinvestigated in this paper.

Keywords: compressor, modulation, audiocompression, effect of masking.

Computer processing of audio signals is a particularly urgent task for the engineer in modern acoustics. This is due to increased user demand for this task in the service sector. Often the music signal processing, you must first make its compression.

In order to implement the compression audio signal using a special device, called compressors. Compressor is a certain electronic device or a special computer program (subroutine), which is used to reduce the dynamic range of sound. This means that the compressor can be made more narrow the difference between the quietest and the loudest sound.

Thus, knowledge of the basic parameters of the compressor and its operation principle is especially important today.

Compression of audio signal based on the same principle as the modulation (the process of changing one or more parameters of high-frequency carrier signal according to the law of low-frequency information signal.). The total volume of the composition or a single party is increased by reducing the amplitude of the loudest parts of the composition and subsequent increase in the volume of the composition, due to space freed. As a result of more than loud sounds become quieter and quieter sounds louder, narrowing the dynamic range of compositions. Also, using the compression can be removed from the sound the so-called "peaks" - short bursts of

amplitude do not carry in itself any useful information, or aesthetics. Legibility and clarity is given to a number of instruments through a typical compression settings. For example, voice and speech after compression are becoming more selective because of artificially increasing the volume of quiet sounds that are otherwise masked by louder sounds (masking effect) [1].

The graph of the principle of operation of the compressor (Fig. 1) shows the dependence of the output signal from the compression and input level. Abscissa - the input signal, the vertical axis - the output. The gray line is inclined at an angle of 45 degrees - a line level signal (or compressed). Reaching the threshold, it is breaking and is somewhat lower. As can be seen from the graph, shows three variants of the broken line path. For the first option shows "2:1 compression". Continuation of the gray dotted line - is 1:1 compression. Hence, an increase in compression is a decrease in the output level to a specific value (1). This value can be calculated as:

$$out = threshold + (in - threshold) \times ratio, \quad (1)$$

where the threshold - a threshold,

in, out -, respectively, the input and output signals,

ratio - sootnoshenine compression (1:1, 1:2, ..., 1: infinity).

The horizontal broken line - a line of compression ratio (ratio), equal to 1: infinity. In this case, the signal will not be above the threshold level and, consequently, this line is limiting.

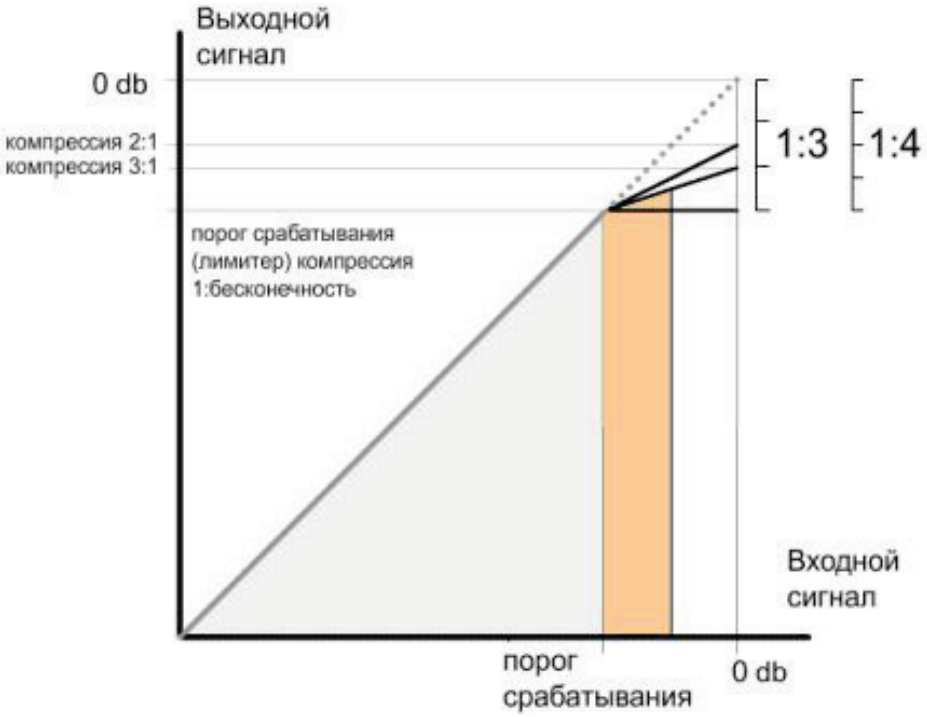

Fig 1. The principle of operation of the compressor sound

Compressors instruments constitute a class of dynamic signal processing. There are many different compressors - from simple to complex, from the universal to highly specialized, from single to multi-channel.

To date, no compressor is a part of the scope of professional audio equipment - especially the live sound reinforcement, as is often the behavior of any incoming audio signal to the "live" concert is unpredictable, whether it be voice or bass guitar. In the recording studio compressors as an integral part of sound processing. However, unlike the live sound, studio compressors are used with great care and only when necessary [2].

The task of research is complicated by compression of audio versatility of meaning in its application. However, to determine the principle of operation of the compressor in a variety of music editors (Audacity, Sound forge, Wave lab) will set up an experiment that would show what features of each of the compressors in the three programs. Then, a comparative analysis will be presented to the best principle of operation of the compressor. Thus, knowledge of the principle of operation of the compressor in the sound production is very relevant today.

References:

1. Leontiev V.P. Music and sound processing on the computer. - M.: OLMA-PRESS, 2005. - 192 p.

2. Meerzon B.J. Acoustic sound engineering basics, Part 2: A course of lectures at 1 and 2 courses, sound engineering department: the manual. - M.: Institute of Humanities and television broadcasting them. M.A. Litovchina, 2001. - 72.

CID: J21208-727

UDK 621.372.8:621.396:621.315

Bogachkov I. V.[1], Ovchinnikov S. V.[1],

Gorlov N. I.[2]

THE ANALYSIS OF SCATTERED OPTICAL SIGNAL IN OPTICAL FIBERS CONSIDERING NONLINEAR EFFECTS

[1]Omsk State Technical University

[2]Syberian State University of Telecommunications and Informatics

In this article the basic nonlinear effects in optical fiber are discussed.

Keywords: nonlinear effects, optical fiber, Brillouin scattering.

Increasing of the lightwave power and inculcation of WDM-technology brought to light the problems of nonlinear effects in optical fibers which limit length of regenerator section of optical fiber links and their transmission capacity. Thus it is necessary to determine top level of the optical power which in turn defines a limit of the signal-noise ratio. Nonlinearity of optical fibers is not a defect of manufacture or the fiber construction, it is a property of the medium itself if electromagnetic energy exceeding certain threshold propagates inside it.

Both elaborators and operators of fiber-optical communication networks should consider nonlinear effects because laser source used in these systems has high coherence of the radiation [1, 2]. At the set level of lightwave power the electric intensity increases with increasing of coherence degree of lightwaves. Nonlinearity of

the optical fiber becomes perceptible when laser radiation intensity (power density inside optical fiber) reaches threshold value. Besides nonlinearity influence is found out after passing by a signal of some way in the fiber depending on parameters, construction of the fiber and conditions of its work.

Nonlinear effects can be separated on two big groups: inelastic and elastic interactions [3].

It is known that refractive index (n) of the optical medium depends not only on frequency (this fact is considered within the limits of the linear theory), but also from intensity of light I or a quadrate of electric intensity E:

$$n\left(w,|E|^2\right)=n_1(w)+n_2\left(|E|^2\right), \quad (1)$$

where n_1 – the linear part featured by Sellmeier equation and depending on frequency, n_2 – the nonlinear component of the refractive index, depending on an electric field intensity.

The nonlinear component n_2 can be expressed by the following equation:

$$n_2=\frac{3x_1^{(3)}}{8n|E|^2}=k_n\times|E|^2, \quad (2)$$

where k_n – coefficient of the refractive index nonlinearity, $x_1^{(3)}$– a component of a nonlinear dielectric susceptibility of 3-rd order.

The phenomena depending on refractive index include [3]:

- Self-Phase Modulation (SPM) or action of a signal on its phase;
- Cross Phase Modulation (XPM) or action of a signal of one channel on the phase of a signal in other channel;
- Four Wave Mixing (FWM) or Mixing of some number of waves with occurrence of radiation on new lengths of waves.

Stimulated inelastic scattering unlike elastic interaction (studied in the linear theory) is caused by inelastic interaction at which part of the lightwave energy is transferred to nonlinear medium. There are two effects in this group:

- Stimulated Raman Scattering (SRS),
- Stimulated Mandelshtam – Brillouin Scattering (SBS).

The phenomenon SBS has become a subject of more steadfast studying recently

in connection with the significant improvement of transmission systems with one carrier and achievement of near limiting factors on length of regenerator section due to use of powerful laser radiation sources and also velocity factors of the transmitted signal, due to magnification of resolving ability (a monochromatically degree) laser signal. The density of a light energy flux in both cases is incremented and is observed the amplification of nonlinear effects which first of all are shown through SBS, considering, that it has the lowest level of occurrence. Having arisen SBS itself gives at the certain levels of power pump wave beam to occurrence of the threshold phenomena restricting power of the useful propagating signal.

It is also known [2, 4], that the spectral components caused by SBS have an important property for practical applications that their frequency is shifted on the quantity proportional to a tension of a fiber. Examples of the typical frequency shift dependences of a tension and temperature are given in [4, 6, 7].

Since the practice of last decades has shown, that the longevity of an optical fiber depends on its tension [4, 5, 6, 7] and receiving of a trustworthy information about physical state of fiber is the important problem of monitoring and diagnostics of fiber optic systems.

For detailed examination of the viewed effects and procedures of testing it is necessary to construct mathematical models of distribution of optical waves in strained fiber [5, 8]. For the analysis of the SBS effect the system of partial differential equations [5] is used:

$$\begin{aligned} \frac{n}{c}\frac{dIp(z,t)}{dt} + \frac{dIp(z,t)}{dz} &= (-a - g_B Ip(z,t))Is(z,t) \\ \frac{n}{c}\frac{dIs(z,t)}{dt} - \frac{dIs(z,t)}{dz} &= (-a + g_B Is(z,t))Ip(z,t) \end{aligned}, \qquad (3)$$

where *Ip (z), Is (z)* – the intensity of pump wave and Stokes wave respectively, a – the attenuation constant, *c* – the velocity of light in vacuum, g_B – the Brillouin gain coefficient (BGC):

$$g_B = g_B / \left(1 + \left(2\frac{\Delta f - f_Б}{\Delta f_Б}\right)^2\right), \qquad (4)$$

(g_B – the maximal BGC; Δf_B – the brillouin gain bandwidth usually equals 50…70 MHz; Δf – the difference between carrier frequency and frequency of measurements). The tensile load applied to optical fiber changes its parameters: refraction index and module of elongation which in turn changes the velocity of an ultrasonic wave [4, 6].

Complexity of the solution of system (1) with regard to optical fiber demands applying of numerical methods. For modeling the method of finite difference was used and the observation space was divided into a grid with a step on coordinate and time Δz and Δt and values of functions in knots of a grid further were calculated.

As a result of evaluations the pattern of allocation of intensity of a Stokes wave for fragments of fiber with a various degree of its tension (Fig. 1) was obtained.

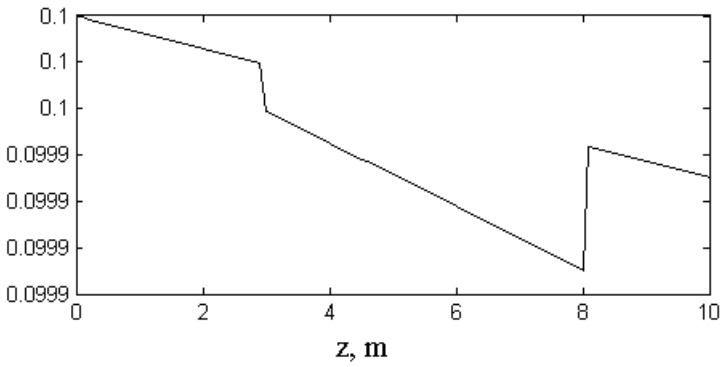

Fig. 1

Dip in the diagram corresponds to change of intensity of Stokes wave on the given frequency.

Let's see the case when instead of continuous emission there are short probe pulses [9]. In that case for the analysis of spontaneous Brillouin scattering (SPBS) spectrum in view of spectrum width of the light source caused by phase noise it is convenient to consider the expression [10, 11]:

$$S(f) = S_P(f) \text{Ä} S_B(f) \text{Ä} S_L(f), \qquad (5)$$

where $S_P(f)$ – the pulse spectrum; $S_B(f)$ – the Brillouin scattering spectrum; $S_L(f)$ – the light source spectrum. Symbol Ä means the convolution operation.

Based on expression (5) the view of spectrum of SPBS for fragments of fiber under mechanical stress at various quantity of tensile loads (on Fig. 2) was gained.

It is visible on the diagram that shift of a spectrum practically linearly depends on a tensile load.

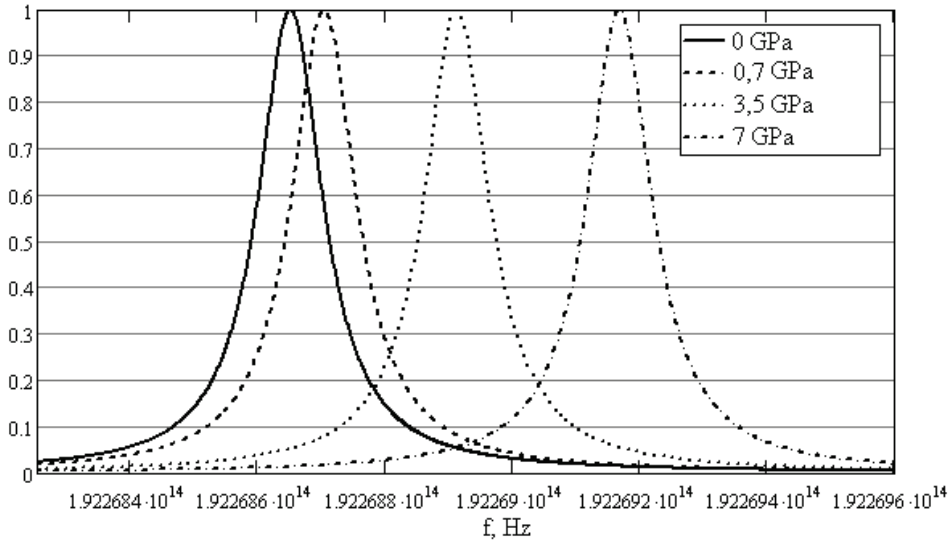

Fig. 2

On Fig. 3 Brillouin backscattering spectrum is given at various bandwidth of a light source.

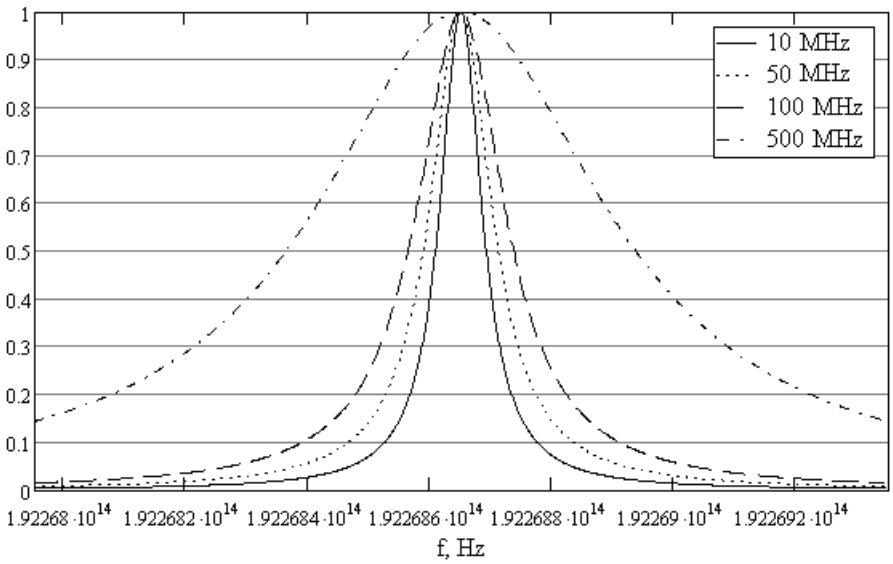

Fig. 3

On Fig. 3 it is visible that the brillouin scattering spectrum width depends on spectrum width of a light source.

The obtained results have allowed to allocate the basic kinds of nonlinear effects

influencing on signal propagation in fiber-optical line and to make an estimation of some effects characteristics.

References:

1. Peskov S. N., Barg A. I. Nonlinear distortions in fiber-optical cables. Part 2 // Telesputnik №11, 2005. – P. 58 – 61. (In Russian)

2. Gorlov N. I., Bogachkov I. V. Fiber optic communication lines. Methods and means of parameter measurement: monograph. – Moscow:: Radiotechnica, 2009. – 192 p. – ISBN 978-5-88070-234-3. (In Russian)

3. Agraval G. Nonlinear fiber optics. – Moscow.: Mir, 1996. – 323 p. (In Russian)

4. Bogachkov I. V., Gorlov N. I. Measurement of characteristics of fiber-optical communication lines by means of pulse-reflectometry methods: monograph. – Omsk: Publishing house OmSTU, 2008. – 160 p. (In Russian)

5. Bogachkov I. V., Gorlov N. I. Components of fiber optic communication systems and methods of parameters control: monograph. – Omsk: Publishing house OmSTU, 2011. – 200 p. – ISBN 978-5-8149-1193-3. (In Russian)

6. Bogachkov I. V., Maistrenko V. A., Gorlov N. I., Ovchinnikov S. V. New problems of monitoring and early diagnostics of the branched out fiber-optical networks: Methods and devices of transfer and processing of the information, V. 11. – Moscow: Radiotechnica, 2009. – P. 295 – 300 (In Russian)

7. Yanukovich T. P., Polyakov A. V. Using analysis method of the Brillouin optical frequency domain for registration of fiber-optical microbendings // Devices and systems. Management, control, diagnostics. – 2006. – V. 1. – P. 51 – 55. (In Russian)

8. Bogachkov I. V., Gorlov N. I. New problems of technical maintenance of ramified fiber optic networks // Omsky Nauchny Vestnik. – number 1 (77). – Omsk: Publishing house OmSTU, 2009. – P. 195 – 198. (In Russian)

9. Bogachkov I. V., Ovchinnikov S. V. Modeling of signal propagation in optical fibers considering nonlinear effects for applying in virtual laboratory works // Remote and virtual education: Scientific journal. – Moscow.: Publishing house SGU, 2011. – № 12 (53) December. – P. 108 – 115. – ISSN 1561-2449. (In Russian)

10. The Brillouin Backscattering Modeling for Analysis of Distributed Irregularities in Optical Fibers / I. V. Bogachkov, S. V. Ovchinnikov, N. I. Gorlov // IEEE 2010 10th

International Conference on Actual Problems of Electronic Instrument Engineering Proceedings. – V. 1, P. 30 – 31. ISBN 978-1-4244-8208-5, IEEE Catalog Number CFP10471-PRT

11. D. Iida, F. Ito. Detection sensitivity of Brillouin Scattering Near Fresnel Reflection in BOTDR Measurement // Journal of Lightwave Technology, V. 26, 2008. – P. 417–424.

[1] Chervony I. F., [2]Rekov Y. V., [1] Golovko O.P.,
[1]Egorov S.G., [1] Golovko Y. V., [1] Volyar R.N

PROCESS PLANNING OF POLYSILICON

[1] Zaporizhzhaya State Engineering Academy,
[2] Zaporizhzhaya Semiconductor Plant

The paper presents technology bases of polycrystalline silicon, properties of technological materials have been considered. The production processes of technical silicon and its hydrochlorination have been described. A thermodynamic analysis of reactions in the hydrochlorination of silicon has been done. It is shown that the usage of a closed cycle in the production of polycrystalline silicon provides efficiency upgrading of the chosen technology solutions.

Keywords: silicon, recreation, quartzite, chlorinating.

For the semiconductor industry as semiconductor electronics, and solar electrical energy industry, silicon is the basic material. Silicon of semiconductor quality is produced in accordance with technology, which provides processing of quartzites with producing of technical (metallurgical) silicon and its chlorination, treatment of silicon chlorides, hydrogen reduction of chlorides with producing of polycrystalline silicon of semiconductor grade, the subsequent growth of monocrystals, cutting them into plates and manufacturing of devices for different purposes (Figure . 1).

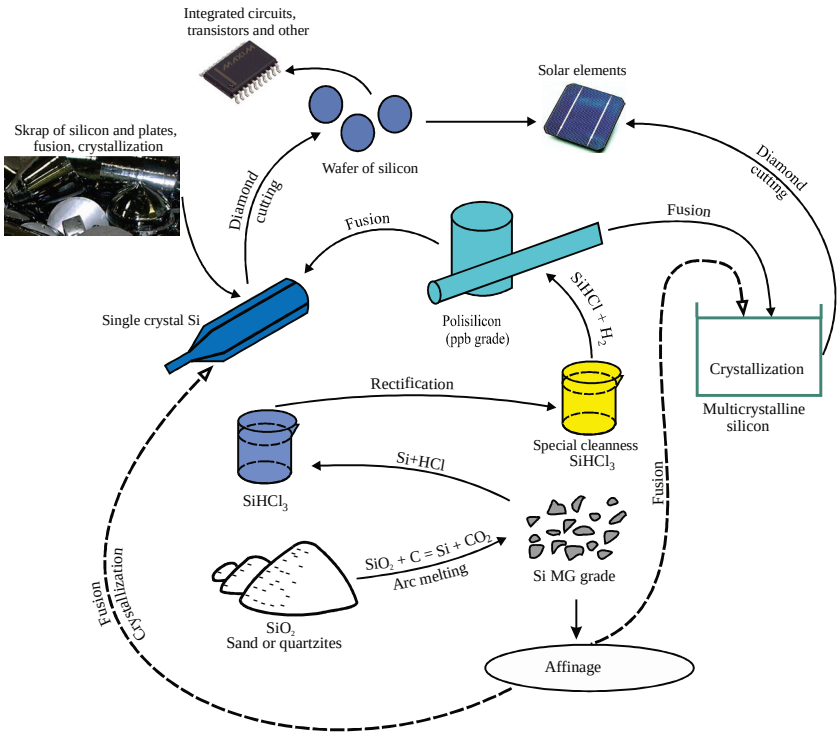

Fig. 1. Scheme of silicon production for electronics

The main (primary) process of polycrystalline silicon production is the silica processing (quartz - SiO_2). The most abundant mineral in the Earth's crust is quartz, which in some deposits forms large cluster of high-purity silica. Natural forms of silica may be represented by rocks, almost completely stacked quartz, quartzite and quartz sandstones. Quartzites may contain limonite, hematite, pyrite, feldspar, clay minerals, mica, rutile, zircon, etc. The content of impurity elements in raw materials significantly affects the quality of crystalline silicon, that’s why the choice of deposit mineral resource is very important.

The average chemical composition of quartz and quartzites which are suitable for crystalline silicon production, can be represented by the following data,%:

SiO_2	Al_2O_3	TiO_2	Fe_2O_3	CaO	MgO
98,62…99,55	0,02…1,00	0,001…0,1	0,04…0,87	0,03…0,3	0,001…0,1

Native quartz deposits in the Earth's crust occur as layers, inclusions, lenses and section bars of structural bodies consisting of unconsolidated quartz crystals, each of different size. The density of quartz is 2.59...2.65 g/cm^3, hardness on the Mohs scale - 7. However, different deposits of quartz contain a variety of mineral inclusions, and

that's why quartz of these deposits has different hardness and has a different color: white, red etc.

In Ukraine, the total stocks of basic raw material for production of silicon - Quartzite - exceed 180 million tons [1].

Their deposits are in Dnipropetrovsk, Zhytomyr, Kirovohrad regions (Ovruch, Tolkachevskoe, Belokorovitskoe, Vasilkovskoye and Ivanovskoe). In this regard, crystalline quartzite quality and supplies of the Ovruch quartzite deposit has no analogues in Europe. The content of SiO_2 makes 98.8%, known reserves - more than 150 million tons, probable reserves - 500 million tons. The scheme of raw material sources for silicon production [2] is shown in Figure 2.

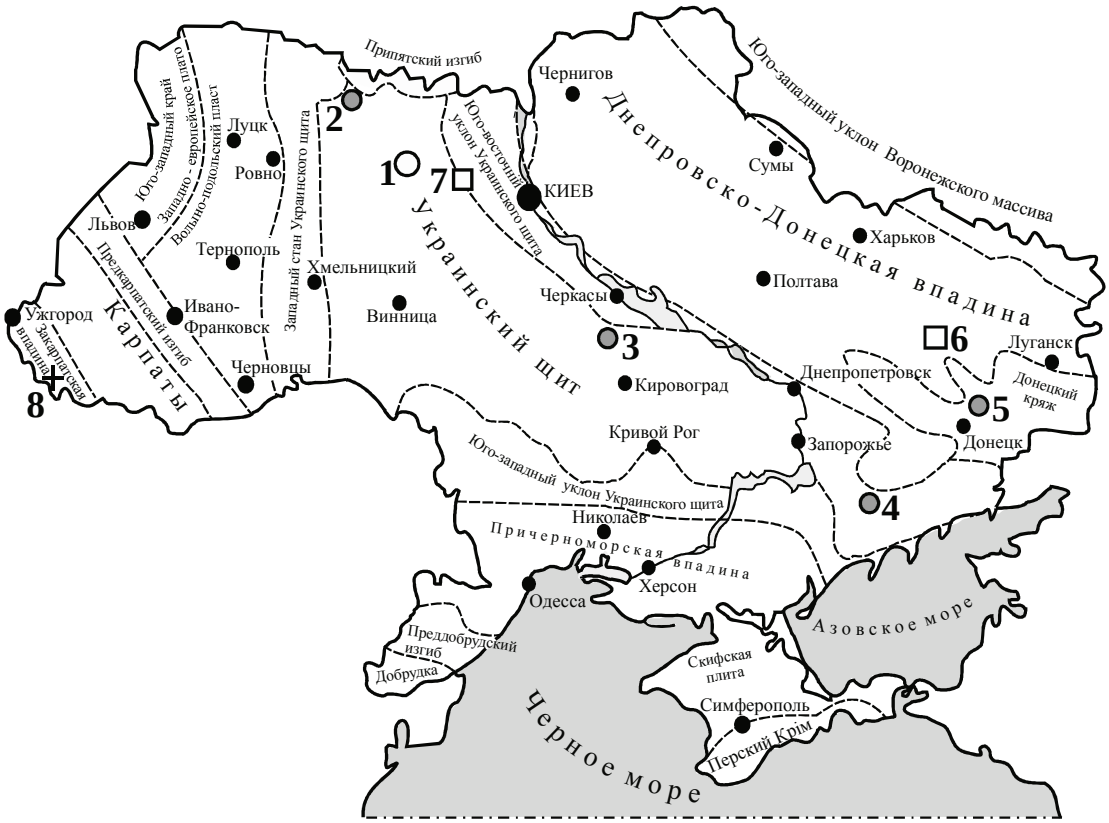

Quartz from chamber pegmatite (1 - Volyn deposit). Quartz veins (2 - Lenchinskoe exposure (occurrence) 3 - Arsenovskoe 4 - Glass Mountain, 5 - Donets basin exposure (occurrence). Quartz sand (6 – Gusarovskoe; 7 - Belokrinitskaya, kodrinskoe); Rhyolites (8 - Andreevskoe)

Figure 2 - Location of the primary sources of raw materials in the territory of Ukraine for silicon production.

Gangue quartz consists of twin crystal crystalline aggregates, has high hardness, low in impurities, differs from plane fracture. Quartzites, usually consist of tightly coupled quartz grains. Impurities of different minerals are between quartz grains, and sometimes as inclusions in quartz grains. They usually have a light-gray or gray color and uneven fracture.

Placer deposits of quartz are widespread in nature, which are products of the destruction of its original deposits, and also sands, consisting of separated quartz grains.

Quartzitic sandstones were formed from quartz grains (sand), cemented by silica. Silica sands and sandstones are not strong and are not applied in the production of crystalline silicon, as the fine grains of sand are sintered on the furnace mouth into a solid crust, which prevents descent of charge materials into the shaft furnace, hindering the release of resulting gases. Quartz and quartzite of different deposits have different degree of recoverability.

Quartz or quartzite, used for technical silicon production should contain as little as possible spreads (clay, soil, waste rock, etc.).

Quartzite for crystalline silicon melting is usually shipped in pieces of size 20...60 mm, while for large furnaces chunks of up to 80 mm are used

The mined quartzite is exposed to processing and enrichment, during which earth, clay and others are separated from it. In modern large quarries crushing and screening plants are installed, where the mined quartzite is preliminarily crushed into pieces <110 mm in diameter, then washed and exposed to screen separation. Often, selective ore extraction is carried out for improving of quartzite quality, thus it allows to reduce the amount of harmful impurities - shale, clay, rocks, etc.

After crushing the quartzite is subjected to wet screening with sifting of fractions <20 mm, which makes it possible to sharply reduce the content of clayed spreads, veined bodies, sand formations, the iron minerals, shales, etc. in the ore.

A generalized scheme of industrial production of silicon is shown in Fig. 3.

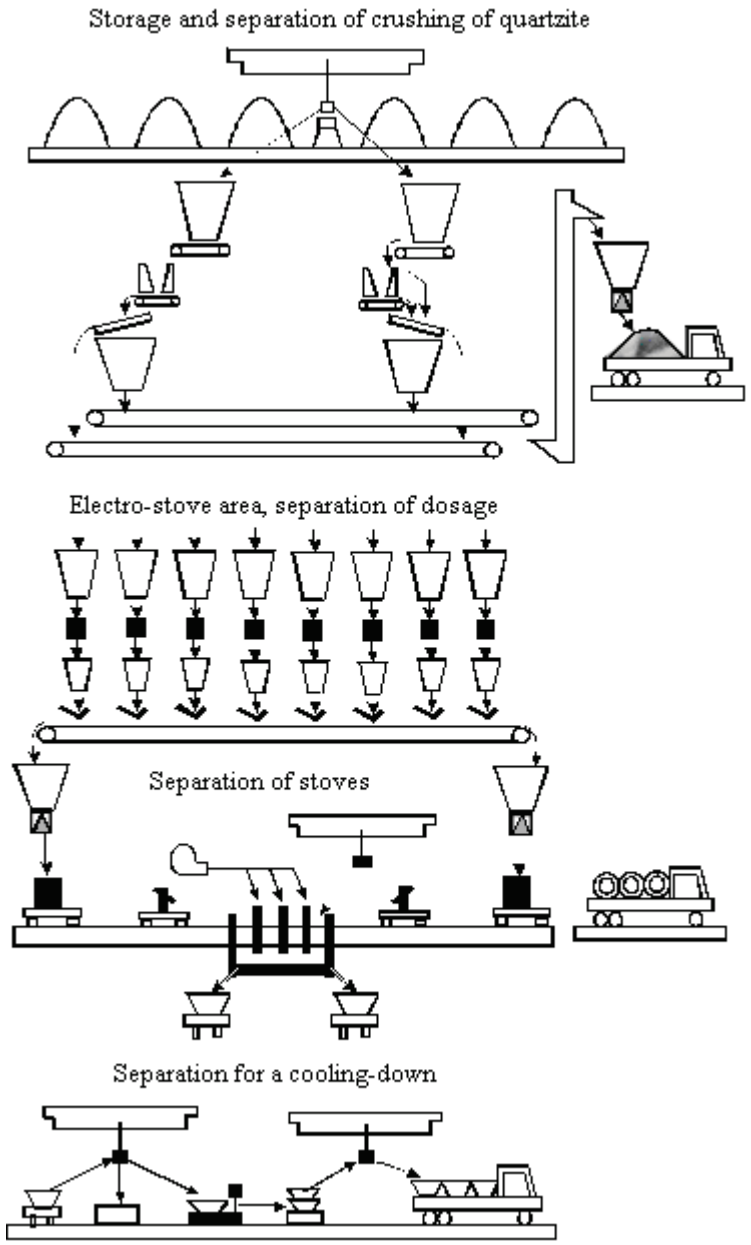

Fig. 3. Generalized scheme of industrial production of silicon

In Zhytomyr region on the basis of Ovruchsky deposit of quartzite the enterprise for the extraction, processing and enrichment of quartzite was established. Today it is - JSC "Ovruch GOK" Quartzite ". The company is specialized in development of open-cut mining using drilling and blasting operations. Now up to 2 million tons of crushed quartzite, up to 300 tons of crushed quartzite and 1 million tons of gravel per year have been extracted here.

The total reserves of quartzite sandstones in Ukraine are more than 9.5 million tons. The deposits are located in Sumy region (Banichskoe and Matskovskii).

Estimated reserves of Matskovskii silicon feedstock deposit are about 100 tons of rich quartziferous ore, the productive area is more than 7 hectares. Banichskoe quartzite deposit is larger, its reserves are more than 600 tons

Technological scheme of industrial silicon production is shown in Fig. 4.

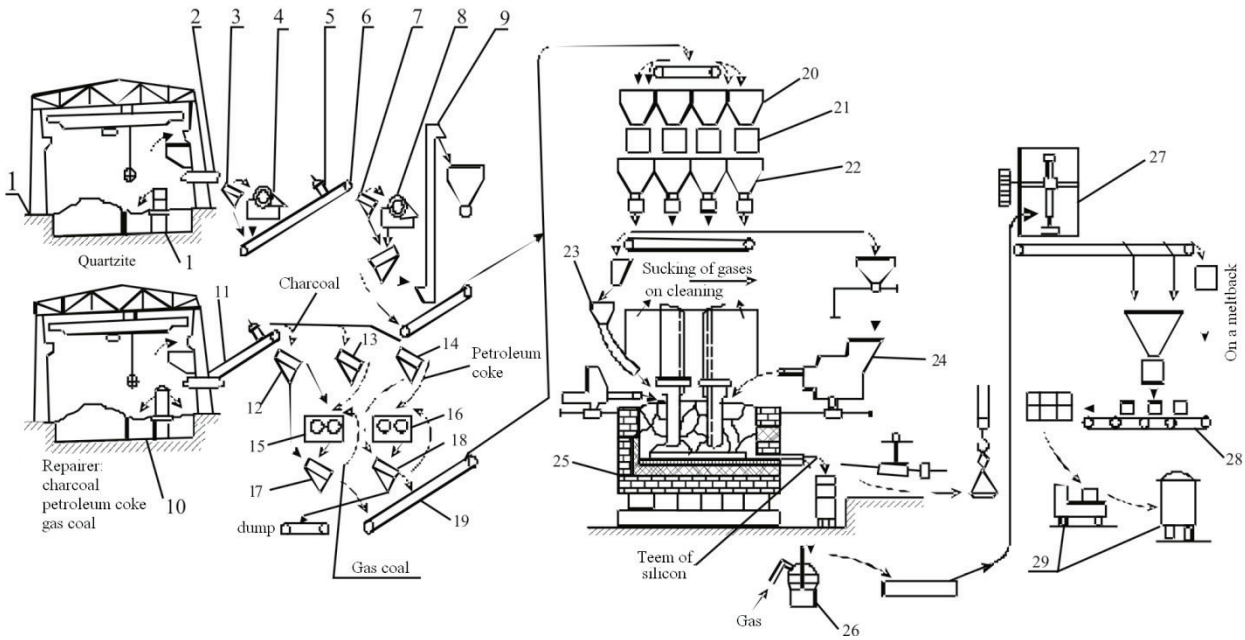

Fig. 4 - Technological scheme of industrial silicon production

1 - hopper with quartzite (fraction up to 300 mm), 2 - apron conveyor, 3 - grizzly grate , 4 - jaw crusher, 5 - magnetic separator, 6 - belt conveyor 7 - grizzly grate, 8 - jaw crusher, 9 - elevator , 10 - bunker with reducing agent, 11 - belt conveyor, 12 - grizzly (80 mm), 13 - grizzly (25 mm), 14 - grizzly (15mm), 15 - roller crusher, 16 - roll- hammer crusher, 17, 18 - double-deck screen, 19 - conveyor belt; 20 mobile reversible conveyor; 21 - batch-weighing scales; 22 - modular belt conveyor, 23 - mobile bunker, 21 - charging carriage, 25 - ore-smelting furnace; 26 - refined device; 27 - sorting unit, 28 - device for packing fastening, 29 - to the consumer

Silicon technology from quartzite is carried out by carbon reduction. Carbonaceous reducing agents contain a significant amount of impurity substances, and work experience of electrothermal plants shows that the transition of impurity

elements into the crystalline silicon from carbonaceous reducing agents during melting makes high value. For example, from charcoal ashes the iron oxides are restored almost completely, aluminum oxides till - 85%, calcium oxide – 45 %. That's exactly why for improving the quality of the crystalline silicon it is reasonably to use low-ash reducing material with siftings of fine fractions (up to 5 mm) containing as a rule, the inclusion of sand and clay, occurred in the carbonaceous reducing agent during the transportation and storage.

The carbon is introduced into the composition of carbonaceous reducing agents. They meet high requirements on purity. The higher content of solid carbon and lower ash content, the higher the quality of the reducing agent.

The main types of reducing agents include:

Charcoal (birch, pine). It contains on a dry weight (anhydrous) to 80 % of solid carbon, not more than 4 % ash and the rest is "volatile".

Petroleum coke - a solid residue of pyrolysis oil, which contains up to 96 % of solid carbon, not more than 0.6 % ash, the rest is "volatile."

Coal has a relatively high ash content (up to 6 %) and high content of volatile substances (40 %). These coals are called "long-flame" or "gas". They are highly reactive and show significant electrical resistance.

Wood chips. It is used in the charge containing 40 % of coal gas (to increase the gas permeability of the furnace).

Table 1

Summarized data on the chemical composition of the mineral part of reducing agents

charge material	The chemical composition of the mineral quartz, and reducing agents,%									
	SiO_2	Fe_2O_3	CaO	Al_2O_3	MgO	TiO_2	$C_{тв}$	W^p	A^c	$V^г$
quartzite	98,3	0,5	0,2	0,9	-	-	-	-	-	-
charcoal	17,3	1,5	57,0	4,4	6,3	-	70	9,5	1,5	19
oil coke	55,0	11,2	17,0	3,6	6,0	-	85	3,0	0,5	11,5
coal	40,9	15,9	1,8	32,3	0,44	-	55	4,5	4,22	36,3

wood chips	17,3	1,5	57,0	4,4	6,3	-	10	36,9	1,7	54,1

where Wp - moisture content in the working mass, Ac - ash on dry weight basis, Vr - the content of volatile components.

The most suitable reducing agents are considered retort charcoal, petroleum coke and recent low-ash coal.

Charcoal due to the high porosity with the equal mass of anthracite is 6 times more in volume. The pores of charcoal stimulate passing of vapor products formed in the reduction smelting of quartz that accelerates the reduction process.

Carbonaceous reducing agents should be low-ash, they should have low content of volatile components, have high reactivity, sufficient mechanical durability and high electrical resistivity.

Reactive capacity of the carbonaceous material is closely connected with its electrical resistance, it also depends on the size of the reductant crystals. Reactive capacity of the carbonaceous reducing agent describes its ability to react with carbon dioxide (CO_2) and restore the various oxides. It is determined by the reaction behavior

$$CO_2 + C = 2CO$$

during 30 min at 1223 K and is expressed by number (%) of the formed carbon monoxide (CO) as per 1 % of carbon dioxide (CO_2).

The high reactivity of charcoal accelerates the process of reduction reactions, and high electrical resistivity allows to work with deep-set electrodes in the mixture at a sufficiently high operating voltage. To reduce the total cost of the reducing agent in a mixture of charcoal the petroleum coke and low-ash coal is usually added.

Petroleum coke is the most low-ash reducing agent, because it contains 0.15...0.53 % of ash and carbon up to 95 % with small quantities of volatile products

(3.5...13.0 %). It is produced by coking of heavy cracking residues or residues after pyrolysis oil processing at 773...973 K in vertical reactors of delayed coking.

However, petroleum coke has a low reactivity and is not used for complete change of charcoal. It is usually loaded into the charge in an amount not exceeding 25 % of the charcoal, in order to reduce aluminum and calcium content in the smelted silicon

Recent low-ash coal is characterized by significantly high content of volatile components (30...37 %) and is called the gas coal. They are subjected to mechanical enrichment, which produces gas-coal concentrate containing approximately 5 times more than petroleum coke, and about 10 times compared with charcoal aluminum oxides. However, its addition to the charcoal reduces the calcium content in the crystalline silicon

The ash content of the wood without bark, usually in the 2...3 times lower than in coal, burnt from wood with bark. Usually charcoal has ash £ 3 %, and volatile components £20 %.

Processing quartzite is carried out in the electric arc furnaces using carbon reductants. The general scheme of the production cycle is shown in Figure 5 [3].

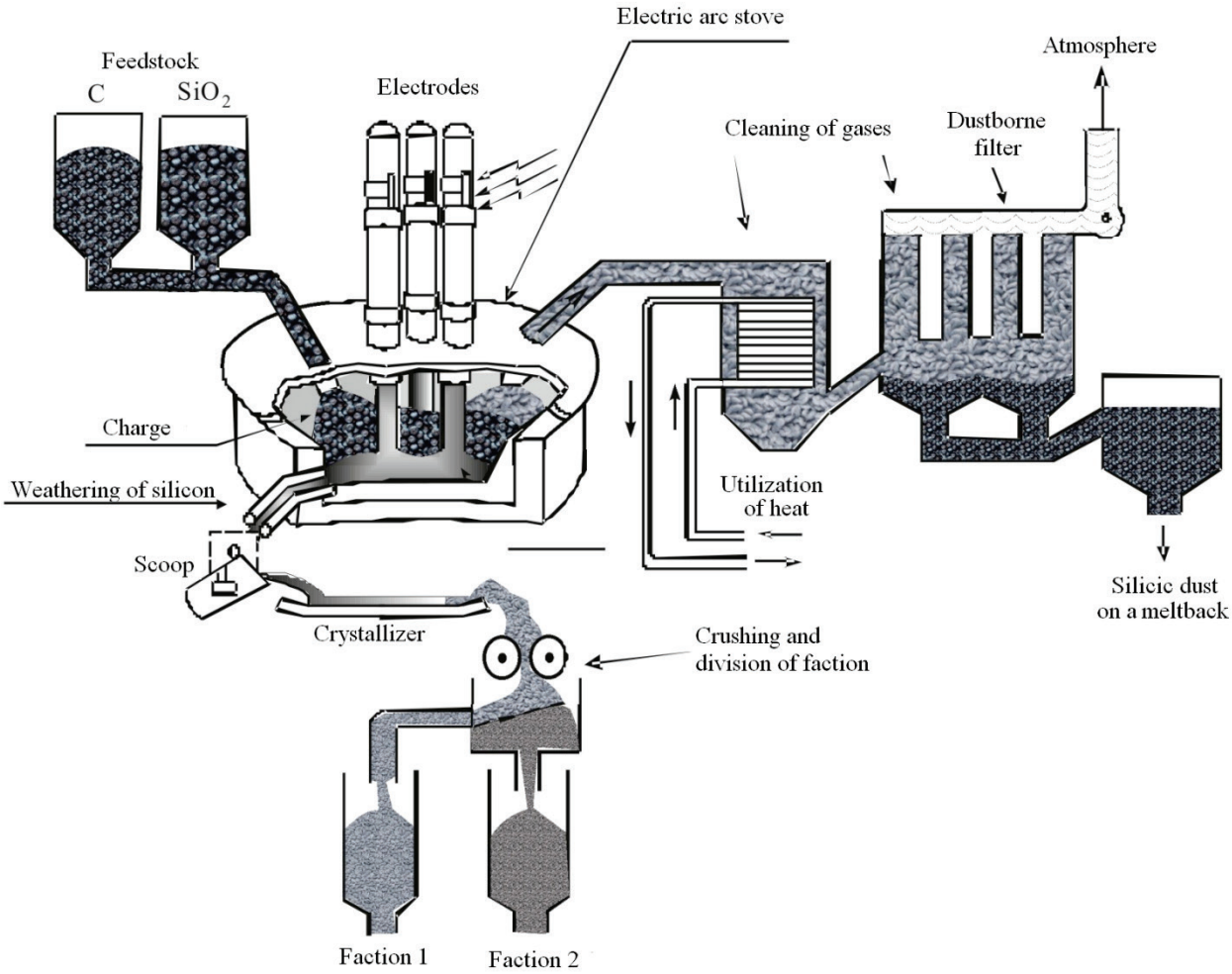

Fig. 5. The scheme of industrial silicon melting with the elements of waste gases recovery

The quartzite recovery process is described sufficiently in details in the works [4, 5] and is represented by the following reactions. Recovery of silica occurs in the ore-reduction electric furnaces at 2073...2673 K according to reaction

$$SiO_2 + 2C = Si + 2CO$$

with expenditure of heat 701.4 kJ / mol.

The participation of a reducing agent reduces the amount of heat due to its

release during combustion of carbon

$$2C + O_2 = 2CO + 221{,}6 \text{ кДж / моль},$$

$$C + O_2 = CO_2 + 394{,}1 \text{ кДж / моль}.$$

Analysis of reducing gases shows that the CO_2 content does not exceed than basis points of a percent, i.e. the last reaction role is small.

The temperature, at which a significant recovery of silicon dioxide begins, is 1933...1953 K.

When restoring silica by the carbon occurs a number of adverse reactions resulting in formation of volatile silicon compounds (carbon monoxide)

$$SiO_{2(ж)} + C = SiO_г + CO,$$

$$2SiO_2 + SiC ® \ 3SiO + CO,$$

$$SiO_{2(газ)} + C_{тв} = SiO_г + CO,$$

$$SiO_{2(ж)} + Si_{(ж)} = 2SiO_г$$

$$SiO_г + SiC ® \ 2Si_ж + CO.$$

The equilibrium gas phase over liquid silica at 2001 K contains: SiO - 45,9 %; O2 - 42,4 %; SiO2 - 5,1 %; CO - 6,6 %.

Silicon monoxide is removed from the mixture of gases and helps the incomplete extraction of silicon from the charge into a finished product. Partially the silicon monoxide can be dissolved also in slags. In addition, getting on the cold side of the furnace and the electrode-holder it is deposited in the gas ducts, which leads to

serious complications in the work of the closed furnaces.

In addition to volatile oxides, carbides are formed. For example, even at 1878 K the reactions proceed

$$SiO_2 + 3C = SiC + 2CO,$$

$$SiO_г + 2C = SiC + CO.$$

The formation of silicon carbide in the furnace baths makes the smelting process difficult, because of the formation of scull, aprons on the furnace base, resulting in decreasing the electrode reaction zone, the conductivity of the charge is increased, etc.

At the same time, silicon carbide can be destroyed by the reactions:

at temperature > 2025 K

$$SiC + SiO_г = 2Si_ж + CO,$$

and at temperature > 2490 K

$$SiC + 2SiO_2 = 3SiO + CO.$$

When melting the silicon the excess of carbon introduces, 20 % more than the stoichiometric amount and it promotes increasing the concentration of CO in the furnace gases and formation of a reducing atmosphere in the furnace.

The interaction of silicon with CO makes possible to form the silicon carbide

$$Si + 2CO ® SiC + CO_2.$$

It is especially important to take into account the processes of carbide formation during the so-called slagless processes.

In this case, the molten silicon is not separated from the zone of solid and gaseous materials with slag and the interaction of carbon monoxide with silicon gets

considerable development. It is confirmed by the research of the phase composition of crust formed in the furnace.

Practically, to slow the process of carbide formation, especially in the areas of discharge from the furnace, can be measures for putting the neutral gas into the furnace, the rapid discharge, and the slag-melt silicon of fluid slag formation on the border, which reliably separate silicon from contact with the gas phase.

For crystalline silicon melting the single-phase one-and two-electrode furnaces, as well as three-phase furnaces are used.

The disadvantages of single-phase furnaces, which limit their application, include a large phase distortion in the energy supply during the shutdown for repair works or furnaces shutdown. Typically, these furnaces have small capacity. In practice, single-phase two-electrode furnaces with capacity of 6500 kW are used. This is relatively low power, and therefore there are high specific heat losses, over-power and labor costs for 1 ton of a finished product.

The most promising are three-phase furnaces with carbon extruded electrodes of large diameter by capacity 16,500 kW.

A single-phase two-electrode ore-reduction furnace by capacity of 6500 kW consists of a bath formed by a furnace shell and a lining-up, electrodes, displacement mechanism and electrode slipping. The furnace is also provided with a cooling system, a device for burning notch, and the exhaust and blasting ventilation, electrical equipment (short-chain, furnace transformers, protective and control and measuring equipment). A furnace shell, lined with a lining-up, has a notch device.

The form of the furnace is determined by the arrangement of the electrodes. Single-phase furnaces with a single electrode and three-furnaces with equilateral-triangle arrangement have a cylindrical shape bath. Single-bath furnaces with two electrodes are oval in shape, and three-phase furnaces, where the electrodes are arranged in a line have a rectangular shape. Lining is made from highly refractory materials of great thickness, which reduces heat losses and creates a large thermal inertia. In addition, during the smelting process the scull is formed - a layer of melted solid charge, and not restored fusion products.

The thermocouples are placed in the fireclay brick hearth. The part of the coal brick hearth is lined from two or three coal-fired blocks. The welds between blocks in width < 50 mm are left, which are stuffed with a hot carbon paste. Sometimes the paste of graphite and silicate is used. The inner walls of the baths are spread with coal-fired units, tightly fitting them to each other. Between the blocks and the fireclay brick hearth a gap is left that is filled with grit, or fireclay hearth mass. The lining of the upper walls above the top of the coal blocks is lined with large fireclay bricks.

The working bath of silicon furnace according processes occurring in it can be divided nominally into four zones: the preparation of the charge for melting, reactions, solid charge materials and the olten melting products.

Preparation of the charge zone occupies the upper part of the furnace and consists of a layer of loaded charge (throat). Preparatory processes and physico-chemical transformation of materials take place in this zone. After charging of batch load the temperature is gradually increased. Upon reaching 373...473 K the removal of hygroscopic water from the middle of the pieces runs out, and at 673 K it happens with chemically bound water. The released water vapors in the flow of hot gases are decomposed to form hydrogen, carbon monoxide and carbon dioxide.

The reaction zone consists of the space around the electrode at the height of its burial in the charge and subelectrode area below the butt of the electrode (Fig. 6).

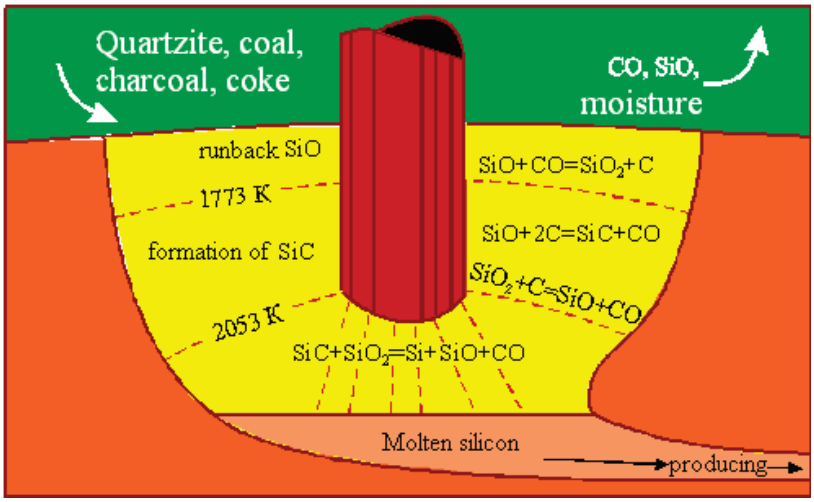

Fig. 6. Scheme of the reaction zone at the carbothermic reduction of quartzite

On each side it is limited by the solid mixture, forming as it were, a melting pot. Towards to the electrode the melting pot constitutes the softened charge, and near the electrode - fused layer of the charge, descending into subelectrode area which is filled with silicon vapors, silicon monoxide, and carbon monoxide. The combustion zone of electric arcs is here, and the temperature reaches 4273...6273 K. The produced gaseous substances go out from the furnace through the throat, and the slag falls on the bottom. There is a sharp decrease in the amount of material in the subelectrode area and a free space is formed which is filled with successive portions of the original charge.

The area of solid charge materials takes a fairly large space in the volume of the furnace between the electrodes in the center of the bath, deeply enters to the bottom of the bath, while the lining of the walls forms a scull.

The zone of molten products is at the lower part of the sub-electrode space on the bottom, silicon and slag and carbidic mixture is concentrated in it.

In the continuous production the amount of accumulated molten silicon in the furnace is small. The amount of slag produced per 1 ton of silicon is in average of 20...30 kg. The slag has viscosity close to the viscosity of silicon, so they are difficult to separate.

Extraction of silicon up to 80...85 %. A significant part of it (20 %) is lost in the form of mono- and silicon dioxide, silicon dust, carried away by the gases, ~ 0.5 % is lost with the slag and 0.2...0.3 % with the waste during making-up of finished product. A large amount of silica in the form of dust is carried away from the furnace with blast furnace gas (1.4...1.8 g/m^3). Silicon and slag make up only 25 % of the weight given to the melting of materials. The remaining share is the top gas. For a tonne of crystalline silicon 2.5...2.6 tonnes of quartzite is consumed, 1.2...1.35 tons of charcoal, 0.14...0.16 tons of petroleum coke and 0.2...0.25 tonnes of the concentration of the gas coal.

The silicon from the furnace is produced into the mold, lined with carbon blocks. After a silicon ingot has cooled down, it is sent to the crushing and cleaning.

Splintered on a lattice with a pneumatic hammer up to pieces of 250...290 mm silicon passes through the grate and enters into the reception hopper of the vibratory feeder, which delivers it to the strand of the make-up conveyor. Pieces of silicon on the assembly line are sorted by the number of visible inclusions of slag and weld spatters from the melt during casting, and are thrown into the ball charging container (Kibble)

To evaluate the quality during the production of silicon, samples are removed from the exhaust stream of the melt. The samples are averaged and subjected to spectral analysis on the content of iron, aluminum and calcium. According to the analysis the brand of silicon is set up from each melting of silicon. From silicon melting of a single brand the parties for the shipment to the consumer are formed.

Recently, the demand for crystalline silicon with low impurity content (especially calcium and aluminum), which in turn requires the usage of high-quality source of raw materials.

It’s possible to improve the performance of crystalline silicon using pelletized or briquetted batch, consisting of quartz sand, petroleum coke and carbon black. Recovery in the briquette (pellet) occurs mainly in the solid phase.

In the semiconductor industry the following specific requirements are made on to the crystalline silicon related to the fact that, for example, iron and copper contribute to processing of target chemical reactions; it’s very difficult to separate phosphorus, boron, carbon during chemical and metallurgical treatment at all stages of the process, and aluminum and calcium in large quantities deteriorate the performance on the processing, where chlorosilanes are got. At the same time at a certain relation iron and aluminum the conditions of purification are improved.

The obtained technical (metallurgical) silicon is sent for further processing, for the manufacture of semiconductor devices for various purposes.

The technology of silicon solar grade (UMG-Si SoG - Upgraded metallurgical-grade silicon Solar-grade) is currently being intensively studied and industrial production of cheap versions of polycrystalline silicon are being developed. Studies include a variety of methods of silicon refining: vacuum, gas, electron beam, plasma,

and special refinement techniques in the process of carbothermic reduction of quartzite.

Currently, the major part of polycrystalline silicon of electronic and solar-grade quality obtained in the global industry (80...90 %), is produced by hydrogen reduction of trichlorosilane, and (10...20 %) silicon - from tetrahlorsilana and monosilane. The share of solar grade silicon, which is produced from commercial silicon using special cleaning methods has been increased (Fig. 7) [6].

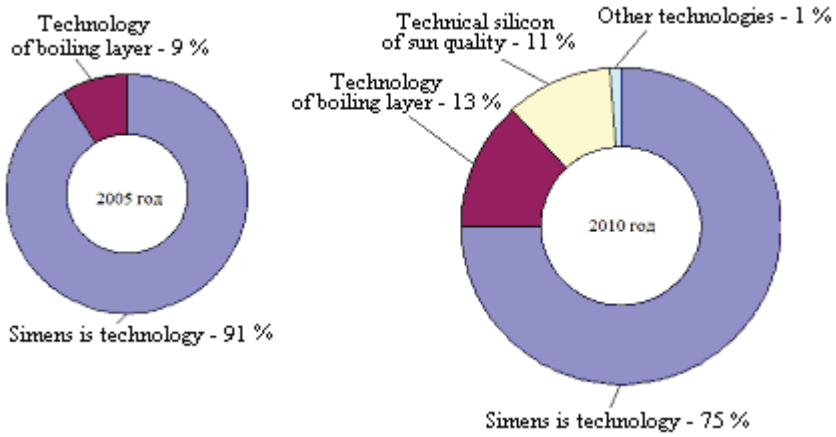

Fig. 7 - The ratio of production technologies for polycrystalline silicon

The technological cycle of polycrystalline silicon production consists of a series of successive operations, which provide the necessary degree of purity of the material [1-7]. The well-known and used for many decades technology involves carbothermic reduction of quartzite in obtaining of commercial silicon (Overseas classification - metallurgical silicon, Metallugical grade-silicon - MG-SI), chlorination of silicon, rectifying purification of obtained silanes, hydrogen reduction of silanes to elemental silicon in the form of polycrystalline silicon rods and monocrystalline silicon growth by Czochralski method or floating zone melting (Fig. 8).

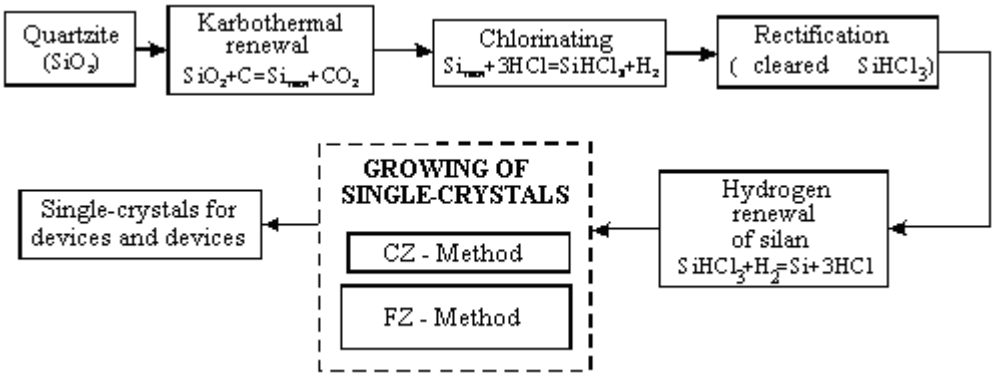

Fig. 8 - Technological scheme of silicon production

Such technological scheme is energy intensive, and its main element is the chloride technology. At the same time, the chloride part of the technology has insufficient output of the finished product due to the formation and the need for products processing of the intermediate chlorination reactions. It makes difficult to saturate the market by polycrystalline silicon of specified quality. According to the data from the work [2-8] by 2012 for the production of 20 GWh / year it will be necessary to increase the production of polycrystalline silicon up to 200 tonnes / year.

Industrial production of trichlorosilane ($SiHCl_3$) is based on the hydrochlorination process (HCl) of technical silicon in special reactors of pseudoliquid fluidized bed [1-7]. The process of hydrochlorination is carried out in three directions with getting by-products

$$Si + 2HCl = SiH_2Cl_2; \quad (1)$$

$$Si + 3HCl = SiHCl_3 + 2H_2; \quad (2)$$

$$Si + 4HCl = SiCl_4 + 2H_2. \quad (3)$$

Getting reaction by-products in the form of dichlorosilane (SiH_2Cl_2) and silicon tetrachloride ($SiCl_4$) creates the need for performing additional technological

operations for trichlorosilane emission and further by-products processing.

To create a closed production line by «Siliken» company [3-9] it is proposed after the rectification the separated hydrogen and silicon tetrachloride to return to the hydrochlorination redistribution, providing increased utilization of initial products and given end product – TCS (trichlorosilane) (Fig. 9).

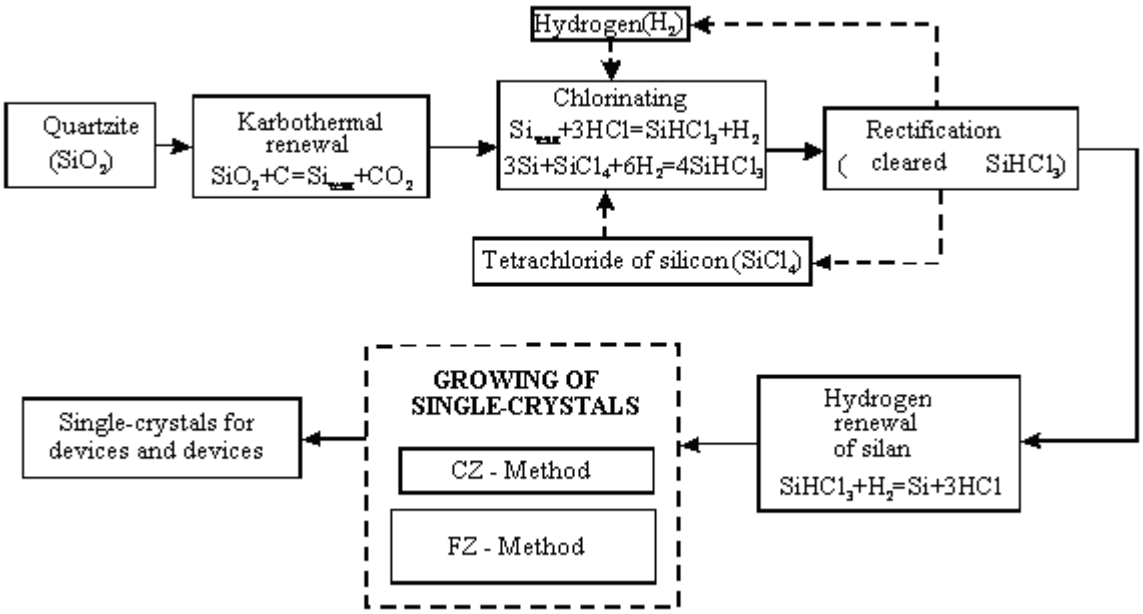

Fig. 9 - Scheme of silicon production with recycling of hydrochlorination products

Return of rectification products provides, according to the authors opinion, the efficiency increasing of the hydrochlorination process with possible reactions process

$$Si + 3SiCl_4 + 2H_2 = 4SiHCl_3, \quad (4)$$

$$Si + HCl + 2SiCl_4 + 2H_2 = 3SiHCl_3 + H_2. \quad (5)$$

In the work [4-10] it is offered to convert the hydrochlorination reaction by-products - silicon tetrachloride and the dichlorosilane ($SiCl_4$ and SiH_2Cl_2) to trichlorosilane by the reaction (Fig. 10)

$$SiCl_4 + SiH_2Cl_2 \text{ ®} \ 2HSiCl_3. \quad (6)$$

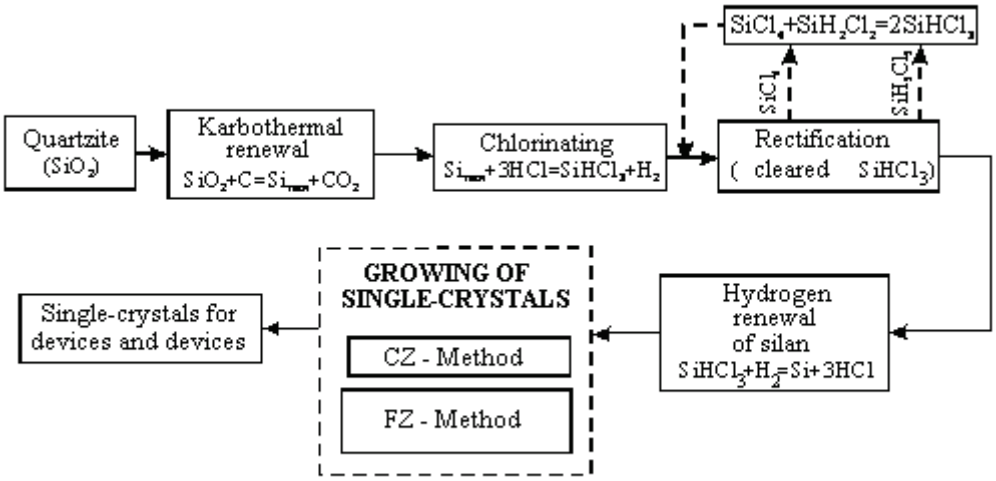

Fig. 10 - Scheme of silicon production with additional processing by-products of hydrochlorination

According to the authors of this paper, this reaction is possible at ambient temperature in a closed cycle of trichlorosilane production and it is quite easily kept under control

The aim of this study was to analyze the thermodynamic performance during hydrochlorination of technical silicon reactions and also reactions at the return of adverse reactions to hydrochlorination redistribution with the closed loop in the production of trichlorosilane.

Implementation of research and discussion of results. To perform the thermodynamic analysis a specialized program has been used [5-11]. The calculations were performed for the components, taken stoichiometric ratio. Changing of Gibbs energy has been measured in the temperature range from 273 to 1000 K. The dependence of the Gibbs energy change for reactions (1) - (3) is shown in Fig. 11.

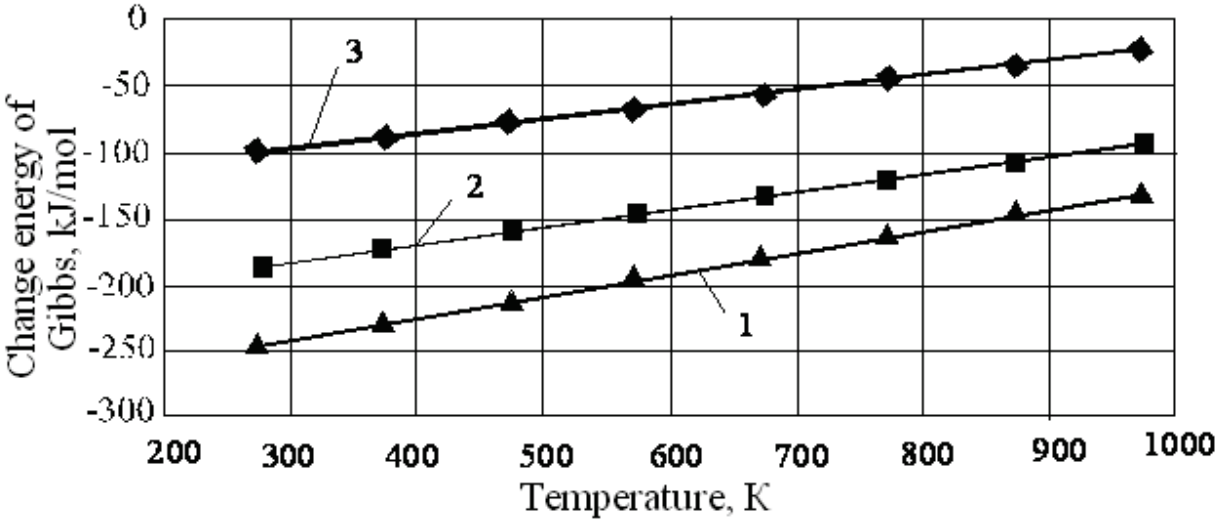

1 – $SiCl_4$; 2 – $SiHCl_3$; 3 – SiH_2Cl_2

Fig. 11 - Dependence of the change in Gibbs energy from temperature for hydrochlorination reaction of silicon

Figure 11 shows that for all the reactions of the Gibbs energy change has negative meaning, *and it means;* the possibility of hydrochlorination reactions of technical silicon with the formation of three reaction products. Thus reaction of silicon tetrachloride ($SiCl_4$) has a higher priority in the considered conditions.

In the works [3-9, 4-10] technological options for the return of hydrochlorination closed cycle products of rectification on the hydrochlorination redistribution (equation (4) and (5), Fig. 9) or tetrachloride silicon selection and dichlorosilane and transformation them into trichlorosilane have been reviewed and offered (equation (6), Fig. 10). The results of thermodynamic calculations for reactions (4) - (6) are shown in 11.

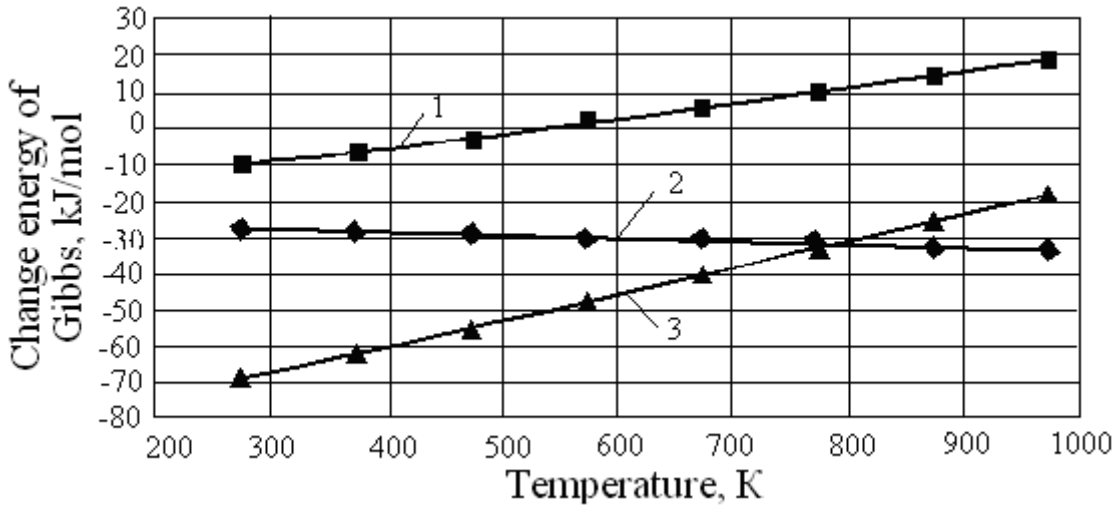

1 - results by reaction of (4) 2 - by reaction (6) 3 - by reaction (5)

Fig. 11 (5) - Dependence of the Gibbs energy change from temperature for reactions (4) - (6)

In accordance with the data presented in Figure 11, the most preferred is the reaction (5), curve line 4, which is carried out under the scheme of a closed cycle with the return of distillation products in the form of silicon tetrachloride and hydrogen in the process of hydrochlorination. The organization of the process of additional processing of rectification products in the form of silicon tetrachloride and dichlorosilane (curve line 2 in Figure 11) with the aim of obtaining trichlorosilane, is not sufficiently energetically reliable and, apparently, requires special techniques, the authors [4] do not give information about this[1].

The given above thermodynamic analysis of reactions (1) - (6) was based on the usage of elemental (pure) silicon. At the same time, in the studies of the hydrochlorination process [6-12, 7-13] it is noted about improvement in the chlorination process when not pure silicon is used, but silicon with some impurities.

Such kind of silicon is the technical silicon of lower grades, with silicon content ~ 98 %. It is noted about the catalytic effect of impurities such as copper on the

1

According to work [6], the temperature of the beginning of the reaction and activation energy decreases with increasing concentration of impurities in silicon in a row, pure silicon (99.9999%)> purified (99.8%)> technical (98%).

process of silicon hydrochlorination. The effect of the catalytic effect is explained in the final stage by dissociation of molecules of hydrogen chloride (HCl), with the formation of intermediate complexes with activated S-Cl bonds and Si-H and subsequent formation of trichlorosilane.

We carried out an approximate thermodynamic analysis of the estimated hydrochlorination process, by taking into account the effect of catalytic action of impurities in the formation of intermediate complexes. The approximate model of chemical reactions is as follows

$$Si + 2H + 2Cl = SiH_2Cl_2, \quad (7)$$

$$Si + 3H + 3Cl = SiHCl_3 + H_2, \quad (8)$$

$$Si + 2H + 4Cl = SiCl_4 + H_2. \quad (9)$$

The change of Gibbs energy, as in the previous reactions was calculated for temperatures ranging from 273 to 1000 K. The results of evaluation are shown in Fig. 12.

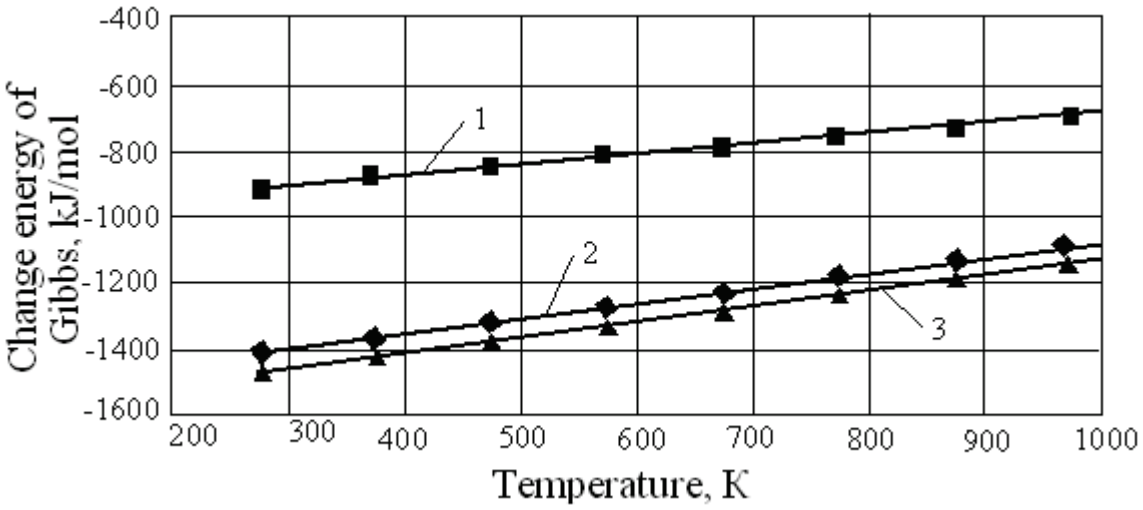

1 - Results according to reaction (7) 2 - according to reaction (8), 3 - according to reaction (9)

Fig. 12 (6) - Dependence of the Gibbs energy change from the temperature for reactions (7) - (9)

As you can see from the figure, all the reactions have a significant negative value, and provide the possibility of getting chlorosilanes in the form of dichlorosilane (curve line 1), TCS (trichlorosilane) (curve line 2) and silicon

tetrachloride (curve line 3) even at the room temperature. At the same time reactions (8) and (9) are more probable. The given calculations and the results obtained indirectly confirm the catalytic effect of impurities on the efficiency of the hydrochlorination of technical silicon. For descriptive reasons, the efficiency of the catalytic effect of impurities on the hydrochlorination of silicon in Fig. 13 is shown a comparative dependence graph of the change in Gibbs energy from the temperature for reactions (1) - (3) and (7) - (9).

A comparative analysis (Figure 13) of hydrochlorination processes of technical silicon shows that for efficiency improvement it is appropriate to use a catalytic effect of some impurities presented in technical silicon.

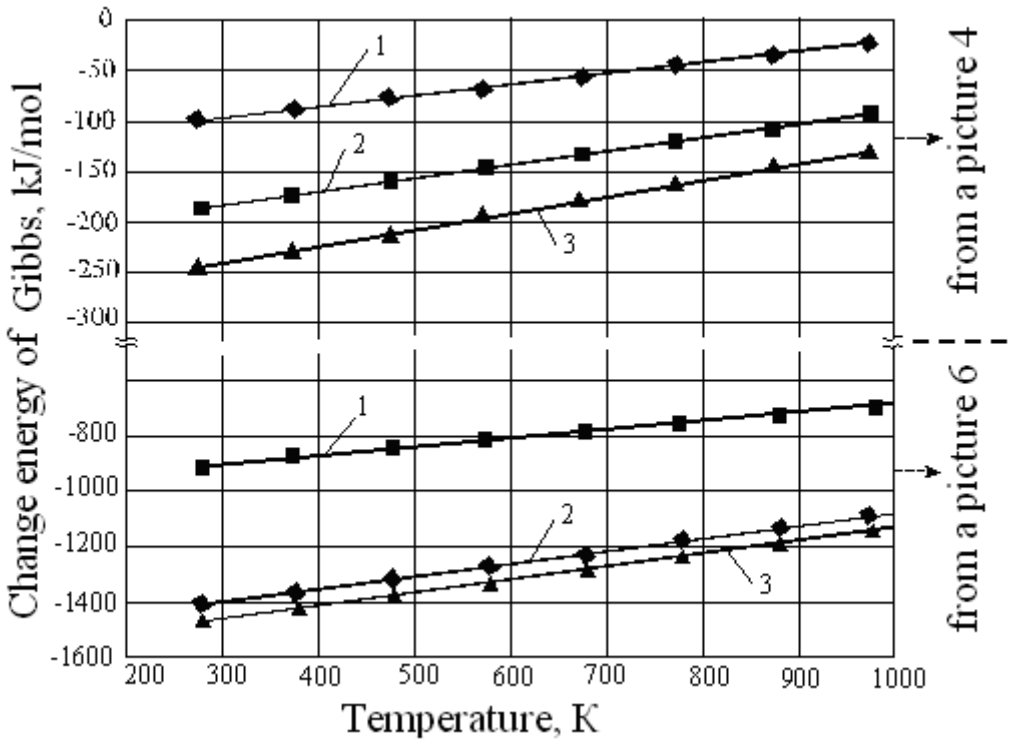

The Number of curve lines has been taken from the corresponding figures

Fig. 13 (7) - Dependence of the Gibbs energy change from the temperature for reactions (1) - (3) and (7) - (9)

In that way the usage of a closed cycle in the polycrystalline production of polycrystalline silicon provides efficiency improvement of technological process. The

usage of catalytic reactions that can significantly improve not only the hydrochlorination of technical silicon and, consequently, but the whole technological cycle of raw materials processing is of special interest.

References:

1. Фомина, О. Перспективы производства кремния в Украине. [Электронный ресурс] / Режим доступа http://news.bau.ua/20110426/perspektivy-proizvodstva-kremnija-v]. Выборка 12.01.2012 г. - Загл. с экрана.

2. САВИЦКИЙ А. Кремниевый «козырь» [Электронный ресурс] / Режим доступа : http://www.day.kiev.ua/292980/ Выборка 03.010.2012 г. - Загл. с экрана.

3. Metallugical grade-silicon (MG-Si) manufacturing technique [Электронный ресурс] / Режим доступа : http://www.displaybank.com/_eng/research/print_contents_m.html?cate=column&id=3808 / Выборка 12.12.2011 г. - Загл. с экрана.

4. Гасик, М. И. Электротермия кремния [Текст] / М. И. Гасик, М. М. Гасик . – Днепропетровск: Национальная металлургическая академия Украины, 2011. - 487 с. Библиогр.: с. 475-479. – 300 экз. – ISBN 978 966 2596-00-7

5. Фалькевич, Э. С. Технология полупроводникового кремния [Текст] / Э. С. Фалькевич, Э. О. Пульнер, И. Ф. Червоный, Л. Я. Шварцман, В. И. Яркий, И. В. Салли. – М. : Металлургия, 1992. - 408 с. – Библиогр.: с. 399-407. – 1170 экз. – ISBN 5-229-00749-0.

6. Hilary Flynn, Travis Bradford. Polysilicon. Supply, Demand, et Implication for the PV Industry [Электронный ресурс] / Режим доступа : http://pdfbest.com/09/0935c0f1e7576bb7-download.pdf / Выборка 26.10.2011 г. - Загл. с экрана.

7. Червоній, І. Ф. Напівпровідниковий кремній: теорія і технологія виробництва [Текст] : монографія / І. Ф. Червоний, В. З. Куцова, В. І. Пожуев, Є. Я. Швець, О. А. Носко, С. Г. Єгоров, Р. М. Воляр ; під. заг. ред. І. Ф. Червоного. – Вид. 2-е, допр. і перер. – Запоріжжя: Видавництво ЗДІА, 2009. – 488 с. – Бібліогр. : 446-484. – 300 прим. – ISBN 978-966-8462-24-5.

8. Чернюк, А. Кремний поликристаллический – производство [Электронный ресурс] / Режим доступа : http://www.newbiz.com.ua/Partner/kremnij-polikristallicheskij-proizvodstvo.html / Выборка 29.10.2011 г. - Загл. с экрана.

9. Siliken chemicals. Technology [Электронный ресурс] / Режим доступа : http://www.siliken-chemicals.com/technology / Выборка 26.10.2011 г. - Загл. с экрана.

10. Carl Merkh and Xiaojing Sun. Polysilicon plant waste recycling [Электронный ресурс] / Режим доступа :

http://www.electroiq.com/articles/pvw/2011/10/polysilicon-plant-waste-recycling.html / Выборка 26.10.2011 г. - Загл. с экрана.

11. Outotec.Технологии. HSC Chemistry [Электронный ресурс] / Режим доступа : http://www.outotec.com/pages/Page_21783.aspx?epslanguage=RU / Выборка 26.10.2011 г. - Загл. с экрана.

12. Горбунов, А. И. Реакции кремния и германия с галогенами, гидрид- и органогалогенами. [Текст] / А. И. Горбунов, А. П. Белый, Г. Г. Филиппов // Успехи химии. – 1974. – Т. 43, вып. 4. – С. 683-706. : библиогр. С. 703-706.

13. Аркадьев, А. А. Разработка способов синтеза трихлорсилана при повышенном давлении давлении [Электронный ресурс] / Полный текст : http://diss.rsl.ru/diss/05/0776/050776033.pdf / дисс. … канд. техн. наук : 05.17-01 / Назаров Ю.Н. – М.: РГБ. 2005 (Из фондов Российской Государственной Библиотеки). – 139 с. – Библиогр. : С. 115-123.

AUTHOR INDEX

Yashkov VA Silin LV	lecturer	Candidate of Technical Sciences	Murom Murom district Vladimir region. 602264
Turgenev D.V.		master	Tomsk Tomsk Region 634034
Grigoryev A.V.		Candidate of Technical Sciences	Kemerovo, Kemerovo region. 650055
Moskalev A. Y., Vetlova S. A., Gushchina I. O.		graduate student	Moscow 111116
Danenko V.F., Ponkratova G.V., Tsyutsyura V.YU.	senior Lecturer	Candidate of Technical Sciences	Volgograd Volgograd Region. 400131
Lvova J.S.	lecturer	Candidate of Technical Sciences	Volgograd 400048
Zaitseva T., Igrunova S., Nesterova E., Pusnaya O., Putivzeva N.	lecturer	Candidate of Technical Sciences	village Belomestnov 308570
Reyzlin V.I., Tartakovsky E.A.	lecturer	Candidate of Physical and Mathematical Sciences	Tomsk Tomsk region. 634034
Zaitseva N.O.		graduate student	Belgorod 308015
Saenko I.B., Nizhegorodov A.V., Kabanov A.S.	professor	Doctor of Technical Sciences	St. Petersburg 195256
Uryvskiy E., Smirnov U.		graduate student	Mr. Ukhta Komi Republic 169309
Sukhenko V.J.	lecturer	Candidate of Technical Sciences	Kiev 03134
O.V. Lomakina, V.I Galaev	lecturer	candidate of pedagogical sciences	Tambov Tambov region. 392018
Balakin P.D., Shamutdinov A.H.	professor		Omsk 644080
Krasovskij S.S., Borisenko A.V., Kovalyova N.I.	lecturer	Candidate of Technical Sciences	Kramatorsk Donetsk region. 84301
Visogorets Y.V.			Miass Chelyabinsk region. 456304
Reshetnikova O.P., Korolev A.V.	professor	Doctor of Technical Sciences	Saratov, October district, Saratov region. 410054
S. Krasovskii, V.	lecturer	Candidate of	Kramatorsk

Khoroshailo, V. Kovaljova, E. Ladyga		Technical Sciences	Donetsk region. 84313
Mikhalina E.S., Petelin A.L.			Moscow 129110
V.V. Malovik, V.V. Martynov, V.S. Panov, L.V. Myakisheva, V.Y. Lopatin	professor	Doctor of Technical Sciences	Moscow 121353
A.V. Golieva		student	Zaporozhye 69104
Lekomtsev A.V.		graduate student	Perm Permskiy krai 614022
L.V.Bal-Prilipko		Candidate of Technical Sciences	Kiev 03041.
A. Kuznetsova, L. Karavay, O. Nikolaenko		Candidate of Technical Sciences	Vladivostok Leninsky district Primorsky Krai 690013
Anikeeva N.V.	lecturer	Candidate of Agricultural Sciences	Volgograd Volgograd Region. 400120
N. Chesnokova, S. Bozhko, T. Ershova, N. Masalova	lecturer	Candidate of Biological Sciences	Vladivostok Leninsky district Primorsky Krai 690013
O. Nikolaenko, A. Chernyshova, A. Kuznetsova, L. Karavay	lecturer	Candidate of Technical Sciences	Vladivostok Leninsky district Primorsky Krai 690013
S. Bozhko, T. Ershova, N. Chesnokova, A. Chernyshova	lecturer	Candidate of Technical Sciences	Vladivostok Leninsky district Primorsky Krai 690013
Sapetova T., Kucheruk MD		student	Kiev 03040
Javorskiy V.T., Perekupko T.V., Perekupko A.V.	professor	Doctor of Technical Sciences	Lviv 79059
Kyrylchyk E.R.		student	Kiev 03148
Bogachkov I. V, Ovchinnikov S. V., Gorlov N. I.			Omsk, 644050
Chervony I. F., Rekov Y. V.,Golovko O.P., Egorov S.G., Golovko Y. V., Volyar R.N			